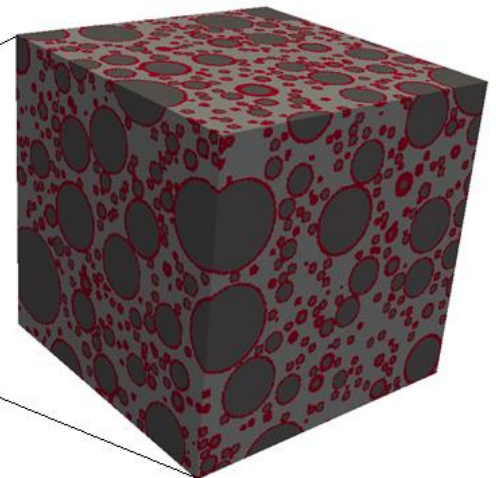


# CHALMERS



## Calibration of a 3D mesoscale FE model for chloride transport in concrete

A case study of the Bakkasund Bridge

*Master of Science Thesis in the Master's Programme Structural Engineering and  
Building Technology*

**ALEXANDER GUTIERREZ**  
**JOHN HALLBERG**

Department of Civil and Environmental Engineering  
*Division of Structural Engineering*  
*Concrete Structures*  
CHALMERS UNIVERSITY OF TECHNOLOGY  
Göteborg, Sweden 2014  
Master's Thesis 2014:97



MASTER'S THESIS 2014:97

# Calibration of a 3D mesoscale FE model for chloride transport in concrete

A case study of the Bakkasund Bridge

*Master of Science Thesis in the Master's Programme Structural Engineering and  
Building Technology*

ALEXANDER GUTIERREZ

JOHN HALLBERG

Department of Civil and Environmental Engineering  
*Division of Structural Engineering  
Concrete Structures*

CHALMERS UNIVERSITY OF TECHNOLOGY

Göteborg, Sweden 2014

Calibration of a 3D mesoscale FE model for chloride transport in concrete

A case study of the Bakkasund Bridge

*Master of Science Thesis in the Master's Programme Structural Engineering and Building Technology*

ALEXANDER GUTIERREZ

JOHN HALLBERG

© ALEXANDER GUTIERREZ, JOHN HALLBERG, 2014

Examensarbete / Institutionen för bygg- och miljöteknik,  
Chalmers tekniska högskola 2014:97

Department of Civil and Environmental Engineering

Division of Structural Engineering

Concrete Structures

Chalmers University of Technology

SE-412 96 Göteborg

Sweden

Telephone: + 46 (0)31-772 1000

Cover:

The Bakkasund Bridge (photo: Claus K Larsen, NPRA) and an SVE, which resembles the concrete in the Bakkasund Bridge, see Chapter 5.

Chalmers Reproservice / Department of Civil and Environmental Engineering  
Göteborg, Sweden 2014

Calibration of a 3D mesoscale FE model for chloride transport in concrete  
A case study of the Bakkasund Bridge

*Master of Science Thesis in the Master's Programme Structural Engineering and Building Technology*

ALEXANDER GUTIERREZ

JOHN HALLBERG

Department of Civil and Environmental Engineering  
Division of Structural Engineering  
Concrete Structures  
Chalmers University of Technology

ABSTRACT

Measurements of chloride ingress were made during 2013 at the Bakkasund Bridge which is located close to Bergen at the West coast of Norway with the aim of study the chloride ingress closer. This was a part of the project Durable Structures at the Norwegian Public Roads Administration. Narrow cracks were found on the lower parts of the columns, however no essential chloride ingress could be found in the cracks. In a recently finished PhD project at Chalmers University of Technology, a three-dimensional finite element (3D FE) model has been developed with the purpose to more accurately model mass transport in concrete. The aim of this thesis was to calibrate this model with the measurements taken at the Bakkasund Bridge and then estimate the chloride ingress at the service life of 100 years. Furthermore, the aim was also to study strengths and weaknesses of the FE model in comparison to analytical models. The concrete in the FE model evaluated on the mesoscale level, treated as a two phase material. The influence of cracks was out of the scope for this thesis work. Statistical volume elements were made from sieve curves from the concrete used at the Bakkasund Bridge. Thereafter transient analyses were carried out, in which different input parameters needed to be specified; the ambient chloride concentration, the convective coefficient, the diffusion coefficient of the cement paste and the interfacial transition zone (ITZ), the chloride binding capacity and the time. Since the measurements were taken in the “splash” and the “atmospheric” zones, the ambient chloride concentration in reality varied a lot, which made it difficult to specify an exact value. The convective coefficient of chlorides needed to be specified for the type of boundary conditions used. The diffusion coefficient of the ITZ was found in the literature to be approximately 10-15 times the diffusion coefficient of cement paste, which was calibrated to fit the measurements. The binding capacity has a non-linear relationship to the free chloride concentration, but could in the model only be specified as a constant. Some work was done trying to introduce the non-linearity in the model, but it was found that the effort needed was too large for this thesis project; i.e. this would require further work. Instead a reasonable constant value was used. At the moment the FE model is not necessarily more accurate than the analytical models, because non-linear effects are not included. However, there are possibilities to include these effects, but there are still uncertainties about these non-linearities. The results indicated that the concrete cover at the Bakkasund Bridge seemed to be sufficient; i.e. no corrosion is expected to take place during the service life of 100 years.

Key words: chloride, concrete, mesoscale, interfacial transition zone, finite element, calibration, chloride binding capacity, diffusion coefficient, E39

Kalibrering av en 3D mesoskal FE modell för kloridtransport i betong  
En fallstudie av Bakkasundsbron  
Examensarbete inom Structural Engineering and Building Technology  
ALEXANDER GUTIERREZ  
JOHN HALLBERG  
Institutionen för bygg- och miljöteknik  
Avdelningen för Konstruktionsteknik  
Betongkonstruktioner  
Chalmers tekniska högskola

## SAMMANFATTNING

Mätningar av kloridinträngning gjordes under 2013 vid Bakkasundsbron som är placerad nära Bergen vid den Norska västkusten med syftet att studera kloridinträngning närmre. Det var en del av projektet Varige konstruksjoner vid det Norska vägverket. Smala sprickor hittades i de nedre delarna av pelarna, dock upptäcktes ingen väsentlig kloridinträngning i sprickorna. I ett nyligen avslutat doktorandprojekt vid Chalmers Tekniska Högskola har en tre-dimensionell finita element-modell (3D FE) utvecklats med målet att studera masstransport i betong noggrannare. Syftet med denna avhandling var att kalibrera denna modell med mätningar taget vid Bakkasundsbron och sedan uppskatta kloridinträngningen vid livslängden 100 år. Inom syftet var också att studera styrkor och svagheter med FE-modellen i jämförelse med analytiska modeller. Betongen är i FE-modellen utvärderad på mesoskal-nivå, behandlad som ett trefas-material. Påverkan från sprickor var utanför omfattningen av denna avhandling. Statistiska volymentelement skapades från siktcurvor från betongen som användes i Bakkasundsbron. Därefter genomfördes tidsberoende analyser, där olika parametrar behövdes specificeras; den omgivande kloridkoncentrationen, konvektionskoefficienten, diffusionskoefficienterna för cementpastan och ITZ (den mellanliggande genomgångszonen), kloridbindningskapaciteten och tiden. På grund av att mätningarna var tagna i ”skvätt” och ”atmosfär” zonerna varierar den, i verkligheten omgivande kloridkoncentrationen mycket, vilket gör den svår att ange som ett exakt värde. Konvektionskoefficienten för klorider behöver specificeras för den typen av randvillkor som användes. Diffusionskoefficienten för ITZ hittades i litteraturen som approximativt 10-15 gånger diffusionskoefficienten för cementpastan, som kalibrerades för att passa mätdatat. Bindningskapaciteten har ett icke-linjärt förhållande till den fria kloridkoncentrationen, men kunde i modellen bara anges som konstant. Ansträngningar gjordes med försök att introducera icke-linjäriteten i modellen, men ansträngningarna som krävdes var för stora för denna avhandling, så det behöver studeras vidare. Istället användes ett rimligt konstant värde. För tillfället är FE-modellen nödvändigtvis inte mer noggrann än de analytiska modellerna, eftersom icke-linjära effekter inte är inkluderade. Men det finns möjligheter att inkludera dessa effekter, dock råder osäkerhet kring dessa icke-linjäriteter. Resultaten indikerar på att betong-täckskiktet för Bakkasundsbron verkade vara tillräckligt och ingen korrosion är förväntad under livslängden 100 år.

Nyckelord: klorider, betong, mesoskala, mellanliggande genomgångszon, finita element, kalibrering, kloridbindningskapacitet, diffusionskoefficient, E39

# Contents

ABSTRACT	I
SAMMANFATTNING	II
CONTENTS	III
PREFACE	VI
NOTATIONS	VII
1 INTRODUCTION	1
1.1 Background	1
1.2 Purpose and objectives	1
1.3 Method	1
1.4 Limitations	2
2 CHLORIDES AND CORROSION	3
2.1 Transport of chlorides in concrete	3
2.2 The corrosion process	4
2.3 Chloride binding capacity	5
2.4 Chloride surface concentration	11
2.4.1 Summary	16
2.5 Diffusion coefficient of cement paste	17
2.6 Diffusion coefficient of ITZ	18
2.7 Chloride threshold value	21
2.7.1 Summary	23
3 THE BAKKASUND BRIDGE	24
3.1 The concrete composition	25
3.2 Data from measurements at the Bakkasund Bridge	26
3.2.1 Chloride content	26
3.2.2 Cement content from calciumoxide	28
4 ANALYTICAL MODELS	29
4.1 The Simple error function model	29
4.2 The DuraCrete model	30
4.3 The ClinConc model	31
4.4 Results from analytical models	33
4.5 Comments on the analytical models	36
5 3D MESOSCALE FE MODEL	38

5.1	Generation of statistical volume elements, SVEs	39
5.2	Transient analysis in the FE model	40
6	CALIBRATION OF THE MODEL	42
6.1	Aggregates, size and amount	42
6.2	Influence of the mesh size	43
6.3	Influence of the size of the SVE	52
6.4	Boundary conditions	53
6.4.1	Influence of the ambient chloride concentration	54
6.4.2	Influence of the convective coefficient and tolerance in calculations	55
6.4.3	Influence of the chloride binding capacity	58
6.4.4	Comments on the chloride binding capacity	61
6.4.5	Influence of the time	62
6.5	Diffusion coefficients	63
6.6	Comparison between homogeneous and heterogeneous modelled concrete	65
6.7	Constants in the FE model	66
6.8	Comparison between FE model and analytical models	67
7	ESTIMATION OF THE CORROSION RISK	70
8	DISCUSSION	75
9	CONCLUSIONS AND OUTLOOK	79
10	REFERENCES	82
	APPENDICES	85
A.	Changes in the MATLAB code	86
B.	Hand calculations	87
C.	Measurement locations	88
D.	Diagrams for the convective coefficient, Section 6.4.2	90
E.	Sieve curves	92
F.	Table for mesh size study	95
G.	Input data in analytical models	97





## Preface

In this thesis was a 3D mesoscale FE model calibrated by measurements from the Bakkasund Bridge. The project was carried out from January to June during 2014, at the Department of Structural Engineering, Concrete Structures, Chalmers University of Technology, Sweden and it was a part of the cooperation with the Norwegian Public Roads Administration regarding the project “E39”.

Regarding the authors contributions to the thesis, it should be mentioned that a brilliant cooperation was performed through the whole project. An almost equal contribution to all the chapters was made.

We would like to send grateful thanks to our excellent supervisors; Professor Karin Lundgren who was the examiner, PhD Filip Nilenius and PhD student Carlos Gil Berrocal at Chalmers University of Technology for their support and valuable comments during the project. We would also like to express our premier appreciation to Claus K Larsen at the Norwegian Public Roads Administration, who made this project possible to perform. Grateful thanks to Claus and the Norwegian Public Roads Administration for given us the opportunity to visit the bridge in real.

Göteborg June 2014

Alexander Gutierrez, John Hallberg

# Notations

## Roman upper case letters

$A_{c_s,cl}$	Constant given in DuraCrete model, (Regression factor)
$B_c$	Cementitious binder content
$C$	Storage matrix in FE-formulation
$C_\infty$	Ambient chloride concentration
$C_b$	Bound chloride concentration
$C_c$	Cement content
$C_f$	Free chloride concentration
$C_f$	Free chloride concentration, vector
$\dot{C}_f$	Time derivative of free chloride concentration, vector
$C_s$	Chloride surface concentration
$C_{tot}$	Total chloride concentration
$C_{tot}$	Total chloride concentration, vector
$\dot{C}_{tot}$	Time derivative of total chloride concentration, vector
$D$	Diffusion coefficient
$D_0$	Diffusion coefficient measured by diffusion coefficient test
$D_{0c}$	Initial apparent diffusion coefficient
$D_{0w}$	Diffusion coefficient of the ion of interest in water
$D_{433}$	Diffusion coefficient measured through NTB443
$D_{6m}$	Diffusion coefficient measured through RCM test (NTB492), at 6 months
$D_{App}$	Apparent diffusion coefficient
$D_e$	Effective diffusion coefficient
$D_{ITZ}$	Diffusion coefficient of the ITZ
$D_{RCM}$	Diffusion coefficient measured through RCM test (NTB492)
$E_b$	Activation energy of diffusion coefficients
$E_D$	Activation energy of diffusion coefficients
$H$	Heaviside function
$J_{cl}$	Flux of chlorides
$K$	Resistance matrix in FE-formulation
$K_{b6m}$	Constant depending on gel content and water accessible porosity
$L_{box}$	Size of one side of the statistical volume element
$N$	Shape function matrix

$\mathbb{N}^T$	Transpose of shape function matrix
$OH_{6m}$	Hydroxide concentration at 6 months
$R$	Gas constant
$S$	Specific surface area
$T$	Temperature environmental conditions
$T_0$	Temperature laboratory conditions
Tol	Tolerance in FE-calculations
$V_p$	Porosity
$V_p^c$	Critical porosity
$W_{gel6m}$	Gel content of the concrete

### **Roman lower case letters**

$\dot{\mathbf{a}}$	Time derivative of the free chlorides (solution vector)
$a_t$	Factor for chloride binding capacity
$c$	Chloride concentration
$c_\infty$	Ambient chloride concentration
$c_s$	Chloride surface concentration
$erf$	Error function
$f$	Constant
$\mathbf{f}$	Force vector in FE-formulation
$f_b$	Chloride binding coefficient
$f_t$	Time dependent factor
$k_{c,cl}^c$	Curing factor
$k_{e,cl}^c$	Environmental factor
$k_{OH6m}$	Factor describing the effect of alkalinity
$k_{Tb}$	Temperature factor for chloride binding
$n$	Age factor
$n_{cl}^c$	Age factor
$n_x$	Number of elements in x-direction
$n_y$	Number of elements in y-direction
$n_z$	Number of elements in z-direction
$q_n$	Flux through the boundary with normal vector, $\mathbf{n}$
$t$	Time
$t_0$	The age of the concrete when the compliance is performed

$t_{6m}$	Age of concrete 6 months of exposure
$t_{cl}$	Time since that part of concrete was reached by the chloride front
$t_{ex}$	Age of concrete at the start of exposure
$\frac{w}{b}$	Water binder ratio
$x$	Depth

### **Greek upper case letters**

$\Phi$	Chloride binding capacity
$\Phi_s$	Chloride binding capacity, secant

### **Greek lower case letters**

$\alpha$	Convective coefficient for chloride ions
$\alpha_h$	Degree of hydration
$\beta_b$	Chloride binding exponent
$\varepsilon$	Water accessible porosity
$\varepsilon_{6m}$	Water accessible porosity at 6 months
$\varphi$	Porosity
$\varphi_{cri}$	Critical porosity
$\varphi_{ITZ}$	Porosity of the ITZ (interfacial transition zone)

### **Mathematical notations**

$\partial$	Partial derivative
$\nabla$	Nabla operator



# 1 Introduction

In this thesis it is described how a 3D, (three dimensional), mesoscale FE, (finite element) model was calibrated with measurements from the Bakkasund Bridge in Norway and numerical simulations of chloride ingress were carried out for that bridge. This was made in order to increase the knowledge of the chloride ingress at the bridge's service life of 100 years. The thesis should also point out how the model can be used and be improved to perform more accurate analysis of chloride ingress in concrete bridges in similar conditions.

## 1.1 Background

Along the west coast of Norway a major infrastructural project will be built in the coming years, the new E39, involving several bridges exposed to chlorides from sea water. Therefore it is of interest to know how current and future concrete structures will withstand the deterioration from chloride ingress. One concrete structure in that region is the Bakkasund Bridge, which is a balanced cantilever bridge built in 1999. The Norwegian Public Roads Administration, NPRA, wants to predict the chloride ingress in the concrete based on test samples taken from the bridge during 2013. This was a part of the RnD, (Research and Development), Project Durable Structures at the NPRA. If the prediction of chloride ingress gets more accurate, estimations of when reinforcement corrosion will initiate and, consequently, if bridge repair is needed in the expected service life of 100 years will be more trustworthy.

In a recently finished PhD project at Chalmers University of Technology, Nilenius (2014), a 3D mesoscale FE model that treats chloride ingress in concrete has been developed. With mesoscale meaning the scale where concrete can be considered as a three phase material of cement paste, aggregates and an interfacial transition zone (ITZ). The ITZ is a highly porous zone with high diffusivity, which therefore is important to account for in transport analyses in concrete. Six of the more important input parameters that need to be specified in the mesoscale model are the ambient chloride concentration, the convective coefficient for chlorides at the boundary, the diffusion coefficients of the cement paste and the ITZ, the chloride binding capacity and time.

## 1.2 Purpose and objectives

The purpose of this project was to calibrate the 3D mesoscale FE model with test samples from the Bakkasund Bridge. After the calibration, the model should be used to give estimations of the chloride ingress at the service life of 100 years. Within the aim of this master thesis was also to identify and study strengths and weaknesses of the mesoscale model in comparison to analytical models and to give guidelines for how future predictions of chloride ingress can be made with this model.

## 1.3 Method

The first step of the thesis work was to study some analytical models of chloride ingress in concrete described in literature. The chosen models were the Simple error function model, the DuraCrete model and the ClinConc model.

Then, several material structures of concrete which should resemble the concrete mixture in the Bakkasund Bridge as far as possible were generated.

After that, transient FE analyses were made and the input parameters were calibrated with existing measurement data from the bridge.

After the calibration, transient analyses were made to simulate the chloride ingress at the service life of 100 years. The results from the transient analyses were also compared with the results from the analytical models for verification.

## 1.4 Limitations

The calibration was made for the data with the highest chloride content, i.e. the splash zone, which represents the worst case. This should be conservative although there might be a location on the bridge where the chloride content is higher.

The diffusion coefficients for the cement paste and the ITZ, the chloride binding capacity, the ambient chloride concentration and the convective coefficient were all taken as constants over time in the transient analyses, i.e. only linear FE analyses were performed in the FE model. However, various constants were used in calibration.

The essential influence of potential cracks was not accounted for in the models. Smaller cracks were discovered in the splash zone, and even if investigations showed that one of the cracks did not contain any chlorides, it could potentially do that in the future.



## 2 Chlorides and Corrosion

Chloride ingress in concrete structures is one of the major causes for corrosion of reinforcement. For structures in marine environment the chlorides come both from sea water and de-icing salts during winter time. For the bridge considered in this thesis, the chlorides coming from sea water are dominant. In the past, also chlorides were added to the fresh concrete mix as an accelerator, but this is nowadays prohibited because of the high risk of corrosion cf. Bertolini et al (2004)

### 2.1 Transport of chlorides in concrete

The transport of chlorides into concrete is usually divided into the following categories:

- Diffusion – due to concentration gradients.
- Permeation – due hydraulic pressure gradients.
- Migration – due electrical potential gradients.
- Absorption/capillary suction and convection – due to moisture content gradients.

The transport of chlorides occurs mainly through diffusion and absorption/capillary suction. Absorption, due to surface tensioning in the capillary pores, is of great importance when the pore system is dry and empty of water, i.e. it influences the chloride ingress in zones where wet and dry cycles are common cf. Bertolini et al (2004). When concrete is saturated with water, diffusion is the main process. In saturated concrete, free chlorides may create a concentration difference between the surface and the inner part and can thereafter, by diffusion, be transported into the concrete. The presence of cracks affect the transportation as well, as it leads to a locally higher diffusivity. It is only free chloride ions that can initiate corrosion and be transported in the concrete, although the binding of chlorides is important and further described in Section 2.3.

The analytical models: the Simple error function model, the DuraCrete model and the ClinConc model, see Chapter 4, as well as the 3D mesoscale FE model, described in Chapter 5, are all based on transport by diffusion. In reality the transporting mechanisms mentioned above often act simultaneously and are hard to distinguish, therefore it is common to represent them together with an effective diffusion coefficient cf. Bertolini et al (2004).

In one dimension, Fick's second law describes diffusion through a material with regard to time as follows:

$$\frac{\partial C_{tot}}{\partial t} = D \frac{\partial^2 C_f}{\partial x^2} \quad (2-1)$$

where

$C_{tot}, C_f$	Total and free chloride concentrations, [ $kg/m^3$ ]
$x$	Depth, [ $cm$ ]
$t$	Time, [ $s$ ]
$D$	Diffusion coefficient, [ $cm^2/s$ ]

As mentioned, the analytical chloride ingress models only explicitly take into consideration the effect of diffusion, but absorption and smaller cracks are influencing the diffusion coefficient and are therefore indirectly considered. However greater cracks lead to a locally higher diffusion coefficient, which is not treated in the analytical models but is possible to include in the FE model.

## 2.2 The corrosion process

Corrosion of reinforcement is an electrochemical process, where cathodic and anodic reactions occur at the reinforcement bar. At the stage when there is no remarkable concentration of chloride ions and the concrete is of good quality, the pH value is high, about 12.5-13.5. Solid iron from the reinforcement bars dissolves to iron ions and two negatively charged electrons are released. A balance reaction due to cathodic reduction of oxygen which produces hydroxyl ions occurs at the same time. The products from these reactions will further react with each other, and create a thin and stable passive film on the reinforcement bars, which prevents further dissolution of iron ions.

At the presence of sufficiently high concentration of chloride ions, often called the chloride threshold value, this passive film appears to break down and corrosion will start. The pit that will initiate, acts as anode and areas where there is still a passivation layer act as cathode in the following reactions. This usually occurs locally, due to that the front of chlorides in the concrete is not uniform. When the corrosion has initiated, a very aggressive environment will arise inside the pits, where pH levels below 3 can be reached at the anode, see Montemor et al. (2003). The corrosion penetration may exceed 1 mm per year in the most severe situations cf. Bertolini et al. (2004). In Figure 2.1 the basics of the process of pitting corrosion are shown.

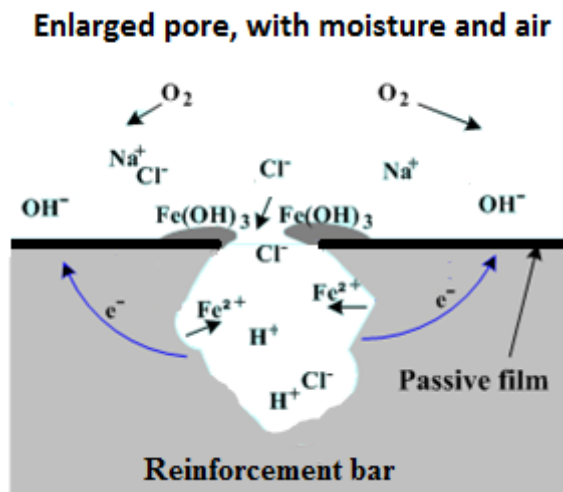


Figure 2.1 Process of pitting corrosion ([www.substech.com](http://www.substech.com)).

Corrosion of the reinforcement will as mentioned start when the chloride concentration in contact with the steel surface reaches a critical threshold value. This chloride threshold value is, together with other factors, controlled by the availability of oxygen, which is needed for corrosion to take place. Submerged structures will have large chloride content, but high water content in the pores, especially the outermost layer which is fully saturated will obstruct oxygen from reaching the steel surface. Atmospherically exposed structures will have lower chloride content but pores will be filled with more air and oxygen than in submerged condition. It is when the concrete is exposed to cyclic wetting and drying that corrosion is of greatest risk, because both chlorides and oxygen can reach the steel surface in large amounts. Tests show that a precise threshold value is not easy to determine, Ann and Song (2007), but it could be seen as the probability for corrosion to start at some range of chloride concentration.

### 2.3 Chloride binding capacity

As chlorides penetrate into the concrete some of the ions will be bound to the hydrated binder by adsorption or through chemical binding. Factors that influence the chloride binding capacity are the cement composition, temperature, degree of carbonation and pH value. Adding silica fume to the cement, as was done in the Bakkasund Bridge, will decrease the chloride binding capacity, Justnes (1998). The binding through adsorption depends on C-S-H (Calcium-Silicate-Hydrate) molecules in the binder. Binding through chemical reaction depends on the AFm phase (alumina, ferric oxide, monosulfate phase) in the binder where so called Friedel's salt is formed. The AFm phase is a group of minerals that occur in cement, Fagerlund (2011).

Even if the relationship between free and bound chlorides is non-linear it is sometimes assumed to be linear for simplicity, Liang et al. (2010). In equation ( 2-2 ) and equation ( 2-3 ) two expressions of the total amount of chlorides are shown.

$$C_{tot} = \Phi_s(C_f) \cdot C_f \quad (2-2)$$

$$C_{tot} = C_b + C_f \quad (2-3)$$

where

$\Phi_s$	Chloride binding capacity (secant), [-]
$C_{tot}$	Total chloride concentration, [ $kg/m^3$ ]
$C_b$	Bound chloride concentration, [ $kg/m^3$ ]
$C_f$	Free chloride concentration, [ $kg/m^3$ ]

Liang et al. (2010) analyzed measurements and found that the amount of bound chlorides can be roughly considered to be twice as much as the amount of free chlorides. That means that the total amount of chlorides is three times the amount of free chlorides.

But since the chloride binding capacity is actually non-linear it should be defined as equation ( 2-4 ), Xi and Bazant (1999).

$$\Phi(C_f) = \frac{dC_{tot}}{dC_f} \quad (2-4)$$

The influence of chloride binding capacity on chloride ingress is important because it is only the free chlorides that are transported into the concrete. The bound chlorides will not contribute to the concentration difference that causes the driving potential for the diffusion of chlorides. Consequently a high chloride binding capacity slows down the transport of chloride ions since much will be stored and will not be able to move further into the concrete. The relationship between free and bound chlorides is often modeled by the Freundlich isotherm or the Langmuir isotherm, Tang and Nilsson (1992). In the ClinConc model by Tang (2008), a modification of the Freundlich isotherm is used and he suggested to relate free chlorides to bound chlorides with time as equation ( 2-5 ). It is important to notice that calculations according to Appendix B are needed for transferring concentrations from the unit % chloride by concrete weight to grams per liter solution in pore system.

$$C_b = f_t(t_{cl}) \cdot k_{OH6m} \cdot K_{b6m} \cdot k_{Tb} \cdot f_b \cdot C_f^{\beta_b} \quad (2-5)$$

$$f_t(t_{cl}) = a_t \cdot \ln(t_{cl} + 0.5) + 1 \quad (2-6)$$

where

$f_t(t_{cl})$	Time dependent factor, [-]
$t_{cl}$	Time since that part of the concrete was reached by the chloride front, [years]

In the FE model, further described in Chapter 5, the chloride concentration quickly reaches values different from zero deep into the concrete, and in reality it is also usually a low background chloride concentration. That means that if the time,  $t_{cl}$ , starts counting from when the concentration differs from zero it would in almost the whole concrete start from the first time step. This implies that  $t_{cl}$  should start when the concentrations slightly higher than zero are reached. In Figure 2.2 the depths at which a certain chloride concentration is reached at different times at different depths is shown. Figure 2.2 gives an indication of what range of values are reasonable when such a number is given in the FE model in order to calculate  $t_{cl}$ . Studying the depth of 7 cm in Figure 2.2, a concentration of  $1e^{-6}$  is reached after about 5 years, a concentration of  $1e^{-4}$  is reached after about 10 years and a concentration of  $1e^{-2}$  is reached after about 30 years with concentrations in the unit [%  $Cl^-$  of concrete weight].

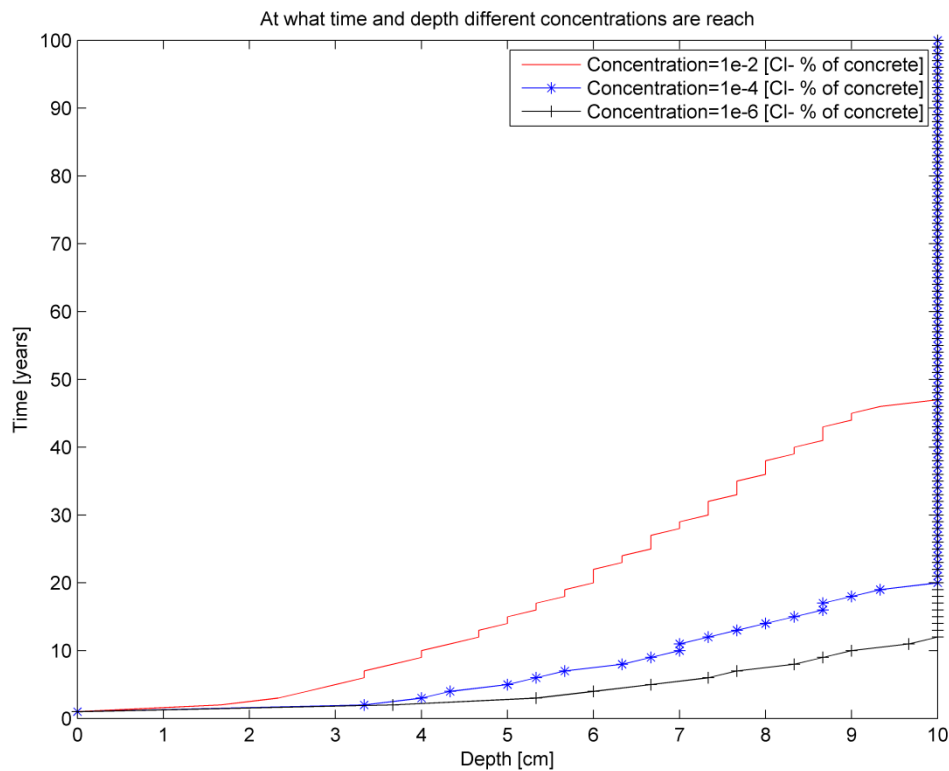


Figure 2.2 Plot of when different chloride concentrations are reached at different depths.

$t_{cl}$  is equal to the total exposure time,  $t$ , at the surface and  $t_{cl}$  is equal to zero where the chloride concentration is zero. The other input parameters in equation ( 2-5 ) are shown below.

$a_t$	Factor for chloride binding capacity, [-]
$k_{OH6m} = e^{0.59 \cdot (1 - \frac{0.043}{OH_{6m}})}$	Factor describing the effect of alkalinity, [-]
$OH_{6m}$	Hydroxide concentration at 6 months, [mol/l]
$K_{b6m} = \frac{W_{gel6m}}{1000 \cdot \epsilon_{6m}}$	Constant depending on gel content and water accessible porosity, [kg/m <sup>3</sup> ]
$W_{gel6m}$	Gel content, [kg/m <sup>3</sup> ]
$\epsilon_{6m}$	Water accessible porosity, [-]
$k_{Tb} = e^{\frac{E_b}{R} \cdot (\frac{1}{T} - \frac{1}{T_0})}$	Temperature factor for chloride binding, [-]
$E_b$	Activation energy of diffusion coefficients, [J/mol]
$E_D$	Activation energy of diffusion coefficients, [J/mol]
$R$	Gas constant, [J/(K · mol)]
$T_0$	Temperature laboratory conditions, [K]
$T$	Temperature environmental conditions, [K]
$f_b$	Chloride binding coefficient, [-]
$\beta_b$	Chloride binding exponent, [-]

Except from the temperatures the values chosen in equation ( 2-5 ) are recommendations from Tang (2008) and have been validated with submerged concrete at the Swedish west coast. Thus it should be noticed that the environmental conditions are not the same as for the measured locations at the Bakkasund Bridge and no consideration of this fact was taken in the calculations. In order to get more accurate values for concrete in splash zones, validation should be done also for that type of environment. The composition of the binder used for validation by Tang (2008), was 95% Ordinary Portland Cement and 5% silica fume, corresponding to the concrete in the Bakkasund Bridge.

The environmental temperature,  $T$ , comes from the mean air temperature which is about 9 °C, YR.no (2014), and the mean sea water temperature which is approximately 10 °C, Global Sea Temperature (2014). Thus the environmental temperature was chosen to 9 °C, assuming that it is the mean temperature the concrete

will have each year. The laboratory temperature is about 23 °C and comes from the measurement report from the Bakkasund Bridge, Jensen (2013).

A suggestion from Tang<sup>1</sup> was that the time dependence stops at around 5 years, meaning that  $t_{cl}$  can reach at maximum value of 5 years. In Figure 2.3 the time factor,  $f_t(t_{cl})$  in equation ( 2-5 ) is plotted against a time of zero to 5 years with  $a_t = 0.36$ . The free chloride concentration is multiplied by the time factor to get the bound chloride concentration. As can be seen in Figure 2.3 the time factor about doubles from  $t_{cl} = 0$  to  $t_{cl} = 5$ , which means that there are twice as many bound chlorides for every free one at about 5 years than when  $t_{cl} = 0$ , for that part of the concrete.

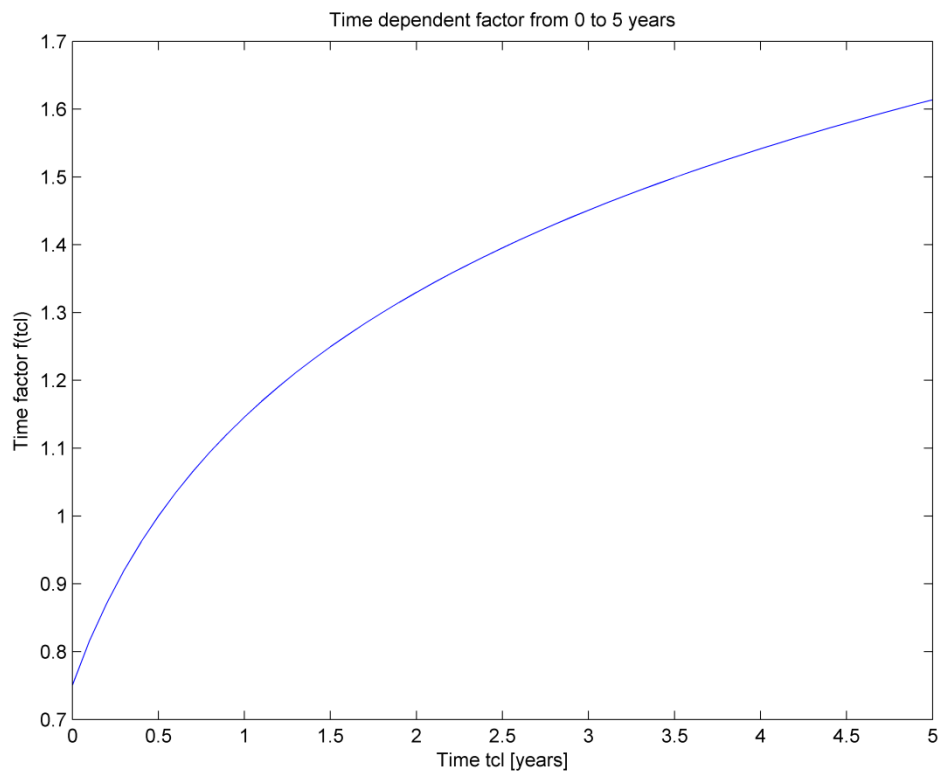


Figure 2.3 Plot showing how the time factor,  $f_t(t_{cl})$  varies with time,  $t_{cl}$ , from zero to five years.

From equation ( 2-5 ) calculations where done with a constant time factor at 5 years and the free and total amount of chlorides where plotted in Figure 2.4. The range of free chlorides on the x-axis can be compared to the chloride concentration in salt water which is about 18 g/l. Figure 2.4 shows that the bound chloride concentration increases fast in the beginning when the free chloride concentration is small. One can think of a system with large, smaller and even smaller pores where large pores are quickly saturated while it takes longer time to fill smaller pores. The concrete will continue to bind more chlorides as more pores are being saturated.

<sup>1</sup> Luping Tang, Professor in building technology at Chalmers, personal communication, 2014.

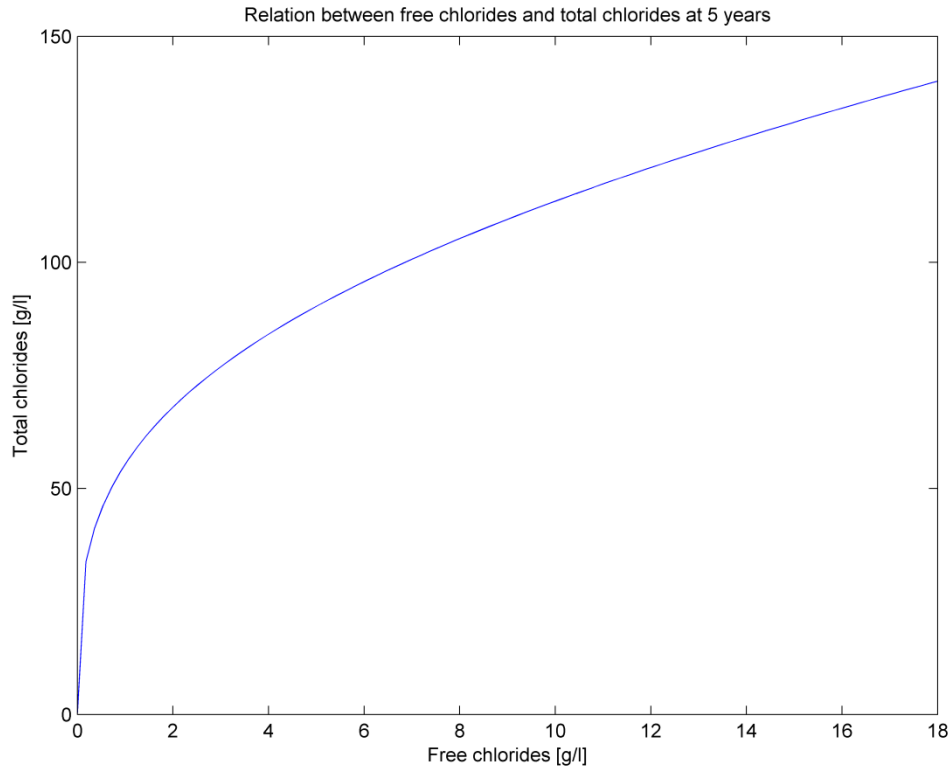


Figure 2.4 Relationship between free and total amount of chlorides at  $t_{cl} = 5$  years.

From Figure 2.4 the chloride binding capacity is calculated according to:

$$\Phi = \frac{dC_{tot}}{dC_f} \quad (2-7)$$

It corresponds to the tangent of the profile for the particular free chloride concentration and describes how much of the free chlorides that will be bound. The relationship between chloride binding capacity and free chlorides is then plotted in Figure 2.5. The same conclusion can be drawn as in Figure 2.4, the chloride binding capacity is higher for lower free chloride concentration and lower at larger free chloride concentrations.



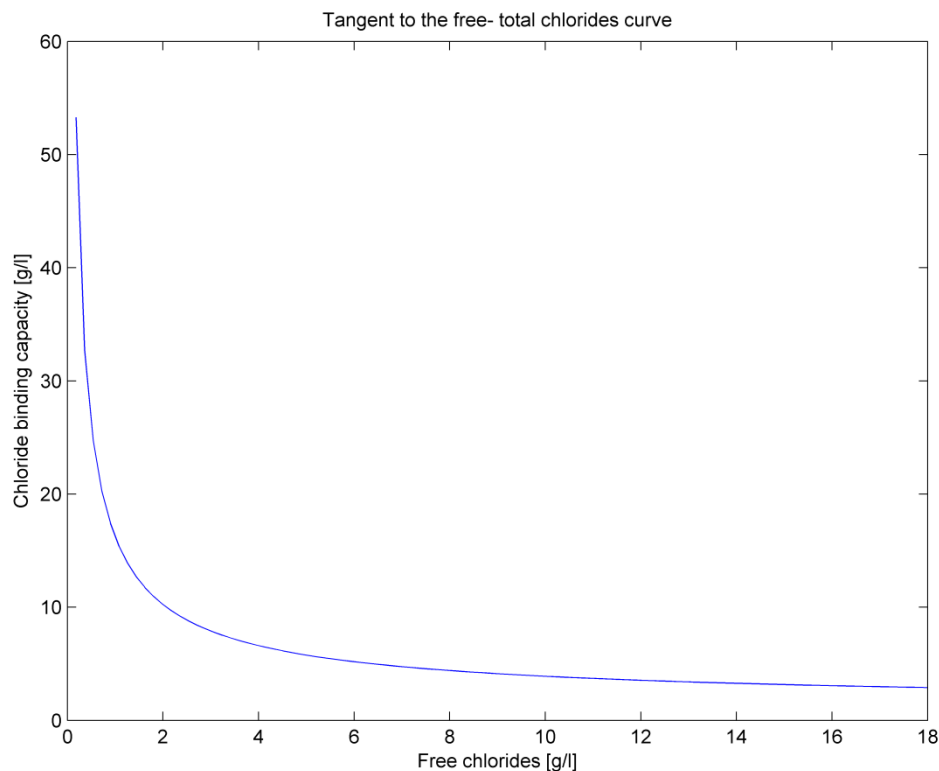


Figure 2.5 Tangent to the curve of free and total chlorides.

Chloride binding capacity is also of importance for the threshold value, see Section 2.7, since it is often given in terms of total chloride concentration but only the free chlorides take part in the reactions that cause corrosion in the steel cf. Bertolini et al. (2004). However studies by Bertolini et al. (2004) show that a large part of the bound chlorides are released when the pH value drops below 12. The pH value is often decreased to a value significantly lower than 12 in the part of the steel where pitting corrosion is taking place.

The process of carbonation influences the amount of free and bound chlorides as well since it reduces the pH value. But analyses on the Bakkasund Bridge show that carbonation only have occurred in the first couple of millimeters and cannot therefore be responsible for the drop in chloride concentration in the first 10 mm, as some of the measurements at the Bakkasund Bridge indicates, more explained in next Section 2.4.

The relation of free and bound chloride concentration in equation ( 2-5 ) holds after a certain time when they are in equilibrium which takes about 7 days, Tang (1996). Compared to the time for analysis regarding chloride ingress which is in years the equilibrium is established quickly and should not essentially affect the results. Tang and Nilsson (1992) also conclude that some of the bound chlorides are irreversibly bound.

## 2.4 Chloride surface concentration

The chloride surface concentration,  $C_s$ , is a factor which is important to consider in analyses of chloride ingress in concrete since it determines the potential difference of

chloride concentration between the surface and the inner part of the concrete. The chloride surface concentration is in most cases difficult to measure and shows a big variation due to weather conditions and height over sea level in marine environment. There is usually a significant variation in chloride surface concentration in the first meters over the sea level and the highest concentrations are also commonly noticed in this region. High values are also observed at a height of approximate 10 meters above the sea level, Bioubakhsh (2011).

When concrete is positioned under seawater and being constantly submerged, the chloride surface concentration is almost constant, around 18 g/l at the location of the Bakkasund Bridge. But when concrete is in the splash zone or atmospheric zone, the prediction of the chloride surface concentration gets more complicated.

How large the variations between different heights are in one location is individual and depends among others on wind speed, wind direction and also on the tidal water. Figure 2.6 shows the variation in tidal water level during one month at the Bakkasund Bridge and the difference in water level is approximate 1 meter. This variation is annually almost the same and comparing it with the height of the measurements at the Bakkasund Bridge, it is reasonable to assume that the lower measurements are in the splash zone, which is further described in Chapter 3.

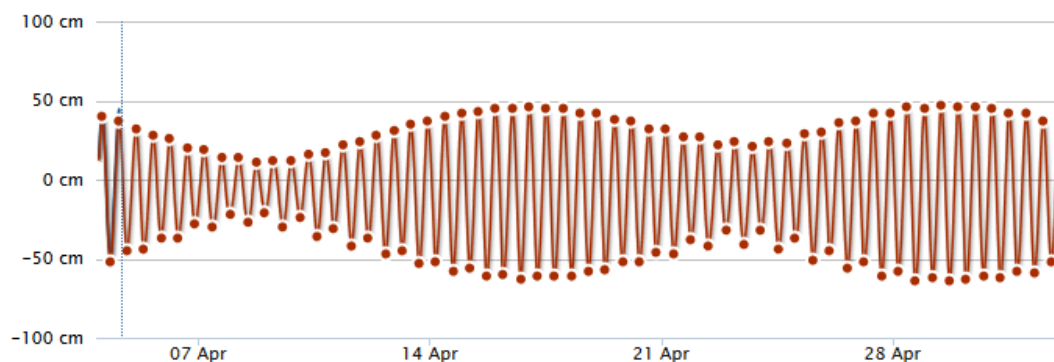


Figure 2.6 Change in tidal water at the Bakkasund Bridge, seHavnivå (2014).

It is reasonable to assume that the variations of the tidal water in some sense should affect the chloride surface concentration, but to take into consideration the daily variations which are shown in Figure 2.6 is both time consuming and probably not rewarding with respect to accuracy.

In the report by Fluge (2003) a figure is shown that illustrates the effect of wind and the difference between windward and leeward side, where the chloride surface concentrations comes from measurements at the Gimsøystraumen Bridge in Norway during 1992. Figure 2.7 below summarize what was found by Fluge (2003).

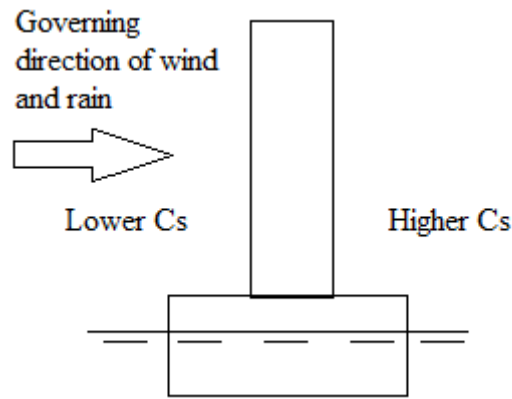


Figure 2.7 How wind direction influence the chloride surface concentration.

Figure 2.7 shows that the leeward side has higher chloride surface concentration than the windward side. The reason for this is that the wind makes it possible for rainwater which contains basically no chlorides to hit vertical surfaces. Depending on how much chloride that already was on the dry surface, as salt crystals, and how much it rains the chloride surface concentration may either increase or decrease. From Fluge (2003) it was found that the surface concentration usually decreases due to the wash out of chlorides, more than it increases due to the dissolving of salt crystals at a location with similar environment condition as at the Bakkasund Bridge.

The chloride surface concentration is difficult to rely on totally when measured and is therefore usually determined by curve fitting a model to measured chloride profiles according to Fick's second law, as can be seen in Figure 2.8. It can be seen that the chloride surface concentration from a model generally shows poor agreement near the surface. Therefore, the chloride surface concentration is taken as the value that best fits the data points at greater depths when using a model.

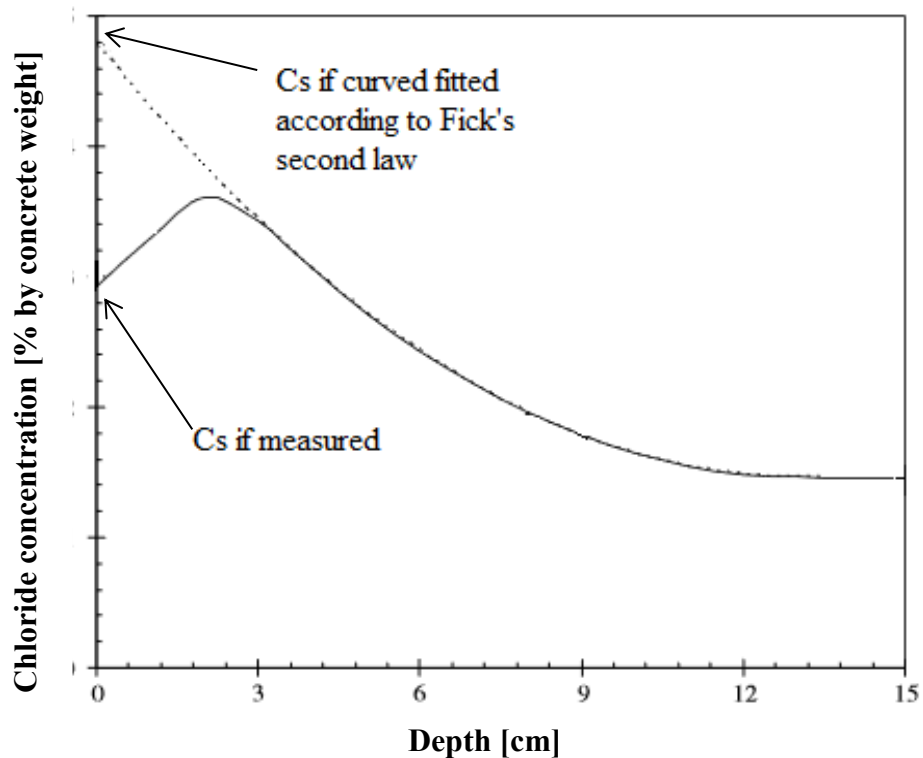


Figure 2.8 Showing how chloride surface concentration is usually measured from curve fitting and from real concrete in a structure, Song et al. (2007).

In Figure 2.9 and Figure 2.10 some of the measurements from the Bakkasund Bridge are shown. The large variation in the outer layer can be observed in these figures and it can be seen that the shape of the chloride profile, as mentioned above, does not correspond to diffusion theory completely.

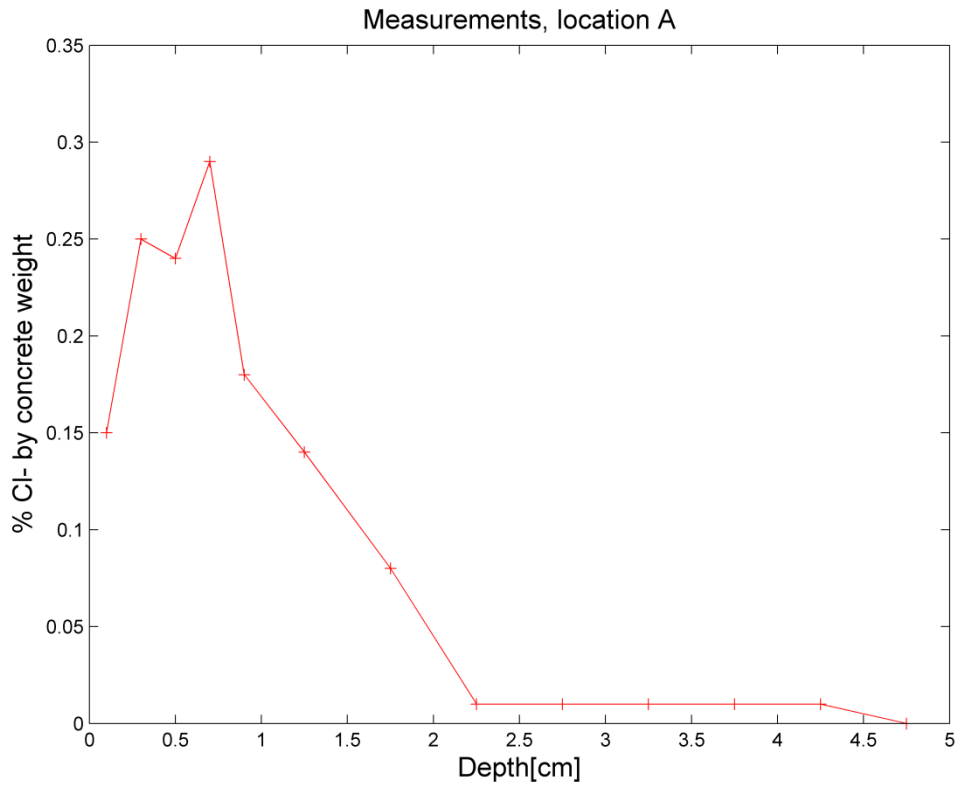


Figure 2.9 Measurements from the Bakkasund Bridge with a drop close to the surface.

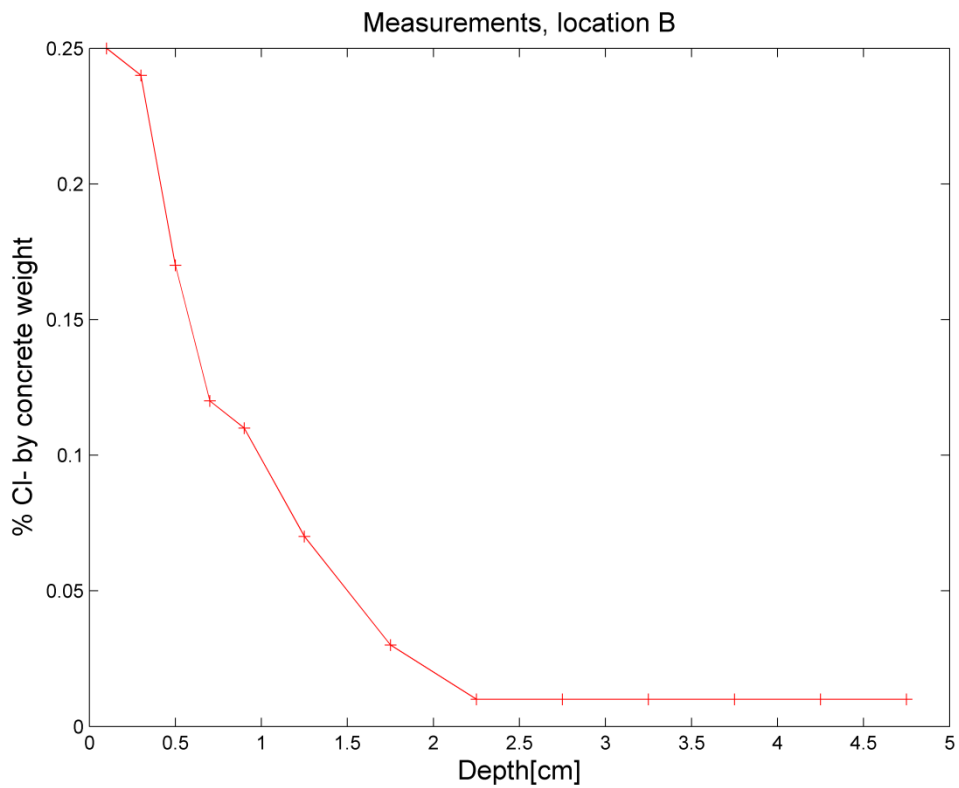


Figure 2.10 Measurements from the Bakkasund Bridge with continuously increasing concentration closer to the surface.

A process that influences the chloride concentration in the outer layer is carbonation, which releases bound chlorides into a free form. When carbon dioxide penetrates the concrete and reacts with the cement paste, hydroxide ions will be consumed and the pH value drops. The result is that the concrete no longer have the same ability to bind chlorides and they will be set free. When these bound chlorides have been released, they can much easier be washed out by driving rain. This wash out-/leaching effect influences the shape of the profile the first millimeters even though no significant carbonation has occurred. This is because when free chlorides have been reduced, the equilibrium between free and bound chlorides is not stable and therefore bound chlorides will be released to balance the equilibrium. This process may then continue as long as the free chlorides are leached out. Ann et al. (2009) also suggest the influence of the segmenting process when obtaining dust samples as a factor for this decrease at the outer layers. Contact with moulds, segregation of aggregates and dielectric reaction are other possible factors mentioned in Ann et al. (2009).

Several suggestions on how to model the chloride surface concentration have been presented in the literature. One study of chloride surface concentration has been made in the south eastern part of UK in marine environment. It was found that the highest values of  $C_s$  were obtained in splash zones, due to accumulation of chlorides during dry periods. The study also showed that chloride surface concentration depends on the concrete composition, where higher values were found for blended cement mixtures, Bertolini et al. (2004). Also the report by Bioubakhsh (2011) shows that concrete composition influences the  $C_s$  value. It states that the relation can simply be described as a more porous concrete will have a higher chloride surface concentration and the porosity of concrete is related to the water/cement ratio, where a higher water/cement ratio gives higher porosity.

Suggestions that the chloride surface concentration should increase linearly or with the square root of time for structures in marine environment were also made by Ann et al. (2007). Further development would be to also include an initial surface concentration. Recommendations on that the chloride surface concentration should vary linearly the first approximate five years and then be taken as constant have been made as well.

In the report by Fluge (2003) values for  $C_s$  are calculated using Fick's second law and fitting the measured chloride profiles from the Gimsøystraumen Bridge (at an age of 11 years of the bridge). Calculations were made for profiles at 920 locations, also measurements from other coastal bridges in Norway were included in these calculations, with different heights above sea level and summarized in four different zones, 0-3 m, 3-12 m, 12-24 m and above 24 m. Mean values of  $C_s$  together with standard deviations resulted in design values of 0.81, 0.67, 0.47 and 0.3 (% chlorides of concrete weight) i.e. these values are taken as constants.

## 2.4.1 Summary

As a summarization it can be said that the chloride surface concentration is a complex variable which depends on many factors such as environment, season, time of exposure, concrete composition, position related to the chloride source and curing time. The common way of modeling the chloride surface concentration is by curve fitting the measured chloride profile according to Fick's second law.

## 2.5 Diffusion coefficient of cement paste

Usually, laboratory experiments are needed to determine the diffusion coefficient of a porous medium. Avoiding this and instead be able to only use analytical formulas would save both time and resources. In Xi and Bazant (1999) there are suggestions on how to model the chloride diffusivity in concrete. They also give an expression for how to model the diffusion coefficient of the cement paste/mortar,

$$D = \frac{2[1 - (V_p - V_p^c)]}{S^2} (V_p - V_p^c)^f \quad (2-8)$$

where  $V_p$  is the porosity,  $V_p^c$  is the critical porosity,  $S$  is the specific surface area and  $f$  is a constant. Martys et al. (1994) suggest values of  $V_p^c$  to around 3%. Equation (2-8) might be useful to determine the diffusion coefficient of the cement/mortar paste but there still exist a lot of uncertainties regarding the variables. The porosity and the surface area have to be measured and in Thomas et al. (1999) it is explained that the measured surface area of cement paste gives a wide spread in results, due to different measurement techniques. The surface area also varies due to cement type, age and w/c ratio cf. Thomas et al (1999). Although, it was stated an approximate range between 80 m<sup>2</sup>/g to 280 m<sup>2</sup>/g for the surface area of hydrated cement paste. The porosity of the concrete used at the Bakkasund Bridge was measured to approximate 15 % and the porosity for the cement paste should be slightly higher.

Halamickova et al. (1995) made chloride diffusion tests on specimens with cement paste containing sand. Portland cement was used and the different sand volume fractions were 35 percent, 45 percent and 55 percent. The diffusion coefficient reached from 0.74·10<sup>-11</sup> up to 2.8·10<sup>-11</sup> m<sup>2</sup>/s. The mortars with more aggregate fraction showed the higher diffusion coefficients, but the most influencing factor was the degree of hydration. For 10 percent higher degree of hydration, the diffusion coefficient decreased with a factor of approximate 2 to 3. The measured values were also compared to an analytical formula, equation (2-9) cf. Halamickova et al. (1995).

$$D = D_{0w}(0.001 + 0.07\varphi^2 + 1.8 \cdot H(\varphi - \varphi_{cri}) \cdot (\varphi - \varphi_{cri})^2) \quad (2-9)$$

where  $D_{0w}$  is the diffusion coefficient of the ion of interest in water,  $\varphi$  is the porosity of the mortar,  $\varphi_{cri}$  is the critical porosity equal to 0.18, below which the capillary pores are disconnected,  $H$  is the Heaviside function which is equal to 1 for  $(\varphi - \varphi_{cri}) > 0$  and equal to zero otherwise cf. Halamickova et al (1995). The value used for  $D_{0w}$  was 1.5·10<sup>-9</sup> m<sup>2</sup>/s. In the report by Jin-yang et al. (2012) a value of 2.03·10<sup>-9</sup> m<sup>2</sup>/s was used for  $D_{0w}$ . From the comparison it was found that the measured and the calculated diffusion coefficient according to equation (2-9) corresponded very well for the mixes with water cement ratio of 0.4, less than 10 percent difference. The mixes with water cement ratio of 0.5 showed larger difference, the calculated were

approximate twice as large as the measured, which although were in acceptable agreement according to the authors.

The porosity in equation ( 2-9 ) can be estimated as,

$$\varphi = 1 - \frac{1 + 1.31\alpha_h}{1 + 3.2\frac{w}{c}} \quad ( 2-10 )$$

Where  $\alpha_h$  is the degree of hydration and  $w/c$  is the water cement ratio for the paste/mortar. This formula is very sensitive for change of degree of hydration.

Another proposal of how to calculate the porosity is given by Burström (2007) as equation ( 2-11 )

$$\varphi = \frac{C_c}{1000} \left( \frac{w}{c} - 0.19\alpha_h \right) \quad ( 2-11 )$$

Where  $C_c$  is the cement content in  $[\text{kg}/\text{m}^3]$  and the other variables as defined previously. This formula is much less sensitive to a change in degree of hydration. This formula gives the porosity for the concrete and can be modified to cement paste/mortar by

$$\varphi = \frac{C_c}{1000 \cdot (1 - \text{aggfrac})} \left( \frac{w}{c} - 0.19\alpha_h \right) \quad ( 2-12 )$$

With aggregate fraction, *aggfrac*, as the input value in the FE model. This modification gives a higher porosity for the paste than in the concrete, which is reasonable.

As a summarization, formula ( 2-8 ) gives a diffusion coefficient for the cement paste/mortar of approximate  $1.6 \cdot 10^{-8} \text{ cm}^2/\text{s}$  and ( 2-9 ) gives a value of approximate  $4.7 \cdot 10^{-8} \text{ cm}^2/\text{s}$ . This with the assumption of 17.4 % porosity of the paste/mortar from formula ( 2-12 ) with assumption of 80 % degree of hydration.

## 2.6 Diffusion coefficient of ITZ

The interfacial transition zone, ITZ, see Figure 2.11, is a highly porous zone of cement that forms around the aggregates in the concrete. Since the aggregates are much larger than the cement particles, the aggregates will appear like walls in the bulk cement paste. These walls cause the cement particles to pack differently than in the rest of the bulk cement paste and will result in an area with much higher porosity, which further results in higher diffusivity. One should be aware of that the ITZ is not



a discrete zone with higher porosity, but instead a gradually varying microstructure. Due to this the diffusivity of the ITZ increases gradually towards the aggregate, Garboczi and Bentz (1996). When studying the scale of cement particles even the smallest aggregates become large. The larger cement particles is not as common close to the surface of the aggregate (up to about 15  $\mu\text{m}$  from the surface) as smaller ones and the paste close to the aggregate consists of higher amount of water than other parts of the cement paste. That means that the w/c ratio usually is lower than the overall ratio in what would be regarded as the “pure” cement paste (the part of the paste that is not ITZ) of the concrete, Scrivener et al. (2004). By adding fine coarse particles to the concrete, for example silica fume, the size of the ITZ can be reduced. This was made for the concrete in the Bakkasund Bridge, why it might be reasonable to assume that the ITZ has been reduced in comparison to suggestions of thickness and diffusion coefficient in the literature. In Figure 2.11, an aggregate with its ITZ layer is shown.

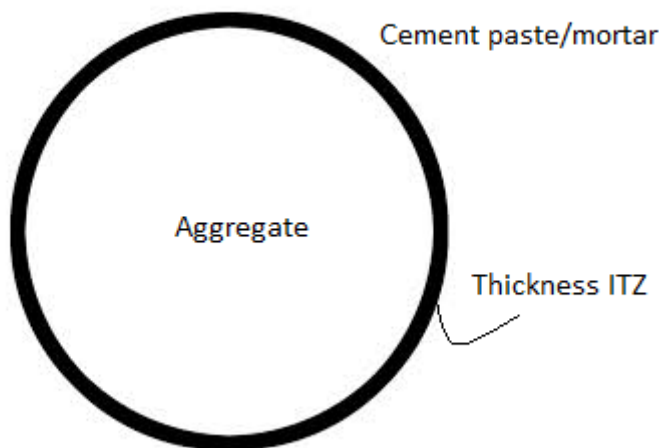


Figure 2.11 Concrete with aggregates and surrounding ITZ.

The thickness of the ITZ zone is in the same range as the size of the cement grains, about 30  $\mu\text{m}$ , measured by SEM (scanning electron microscope) according to Caré and Hervé (2002) and depends on the type of cement and not on the aggregate size distribution. In the report by Jin-yang et al. (2012) a thickness of 20  $\mu\text{m}$  is stated. Sun et al. (2012) present the ITZ thickness as 30-50  $\mu\text{m}$ . All these recommendations assume a constant thickness. According to Scrivener et al. (2004) the effect of the ITZ is most significant in the first 15-20 micrometer closest to the aggregate and has an effect on the first approximate 50 micrometers. As for the rest of the concrete the diffusion coefficient of the ITZ changes with time, due to the hydration process.

For smaller aggregate particles, the ITZ area relative to the aggregate volume, is larger compared to the same relation for larger aggregates. This means that small aggregate particles will increase the effective diffusion coefficient of the concrete, while large aggregates will decrease the effective diffusion coefficient because of the blocking (impermeable) volume. The aggregates need to be much larger than the cement particles in order to form an ITZ layer. To get a hint of the proportions and sizes that are involved, calculations were made and presented in Figure 2.12. It can be seen that if the ITZ zone has the thickness 0.045 mm then the volume of ITZ and

aggregates is the same at an aggregate radius of about 0.017 mm, but if the ITZ zone instead has the thickness 0.025 mm the volumes will be the same at an aggregate radius of about 0.1 mm. Figure 2.12 also shows how the volume of the aggregates becomes much larger than the volume of the ITZ as the radius grows larger and the other way around when the radius decreases. This is only a geometrical analysis, for complete comparison the diffusion coefficient of the ITZ must be known.

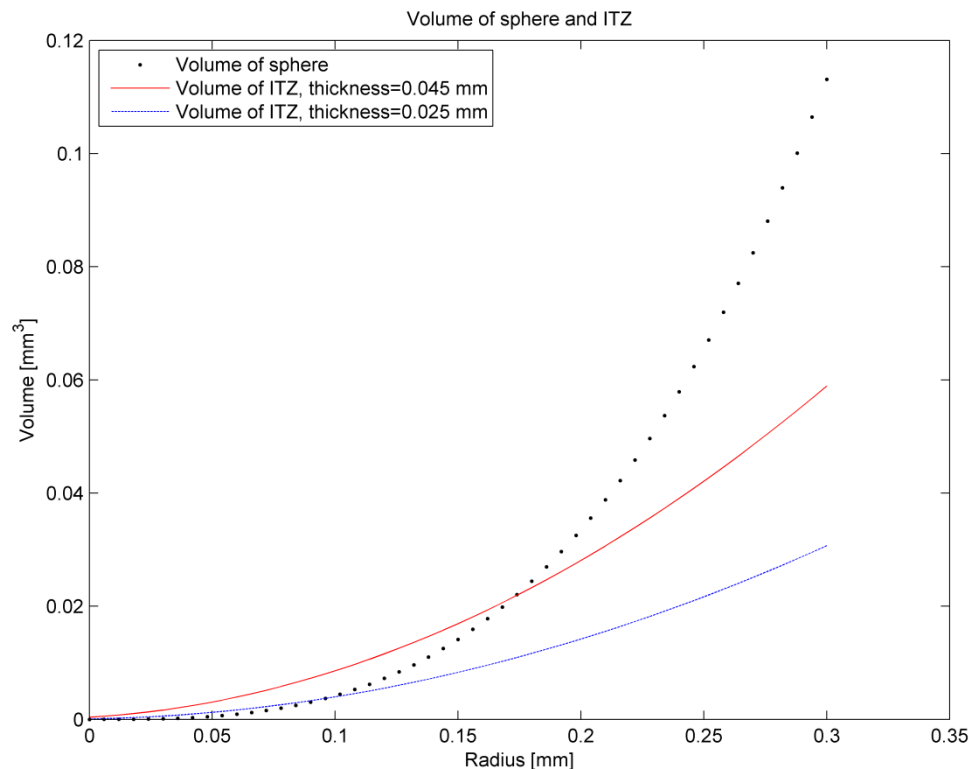


Figure 2.12 Comparison between volume of ITZ and volume of a sphere for different radius.

Zheng et al. (2009) studied the influence of the ITZ on steady-state chloride diffusivity of concrete and mortars, by use of a three phase composite sphere model. This three phase model consisted of aggregates, bulk cement paste and the ITZ, which is similar to the FE model in this study. They found from their model that the effective chloride diffusivity for the concrete decreased by increase of aggregate volume fraction, curing time and size of the maximum aggregate diameter. It was also found that the diffusivity increased with increase of ITZ thickness and w/c ratio. The most influencing factors found were those that controlled the porosity of the concrete, i.e. the w/c ratio, curing age and aggregate content. The effect of the ITZ on the effective chloride diffusivity was rather small and they meant that the diffusivity mainly depends on the volume fraction of the aggregates and the micro geometry of the pore structure in the cement paste.

Jin-yang et al. (2012) specified an expression for the diffusion coefficient of the ITZ, equal to equation ( 2-9 ) except that it is the porosity of the ITZ instead of the cement paste.

$$D_{ITZ} = D_{ow}(0.001 + 0.07\varphi_{ITZ}^2 + 1.8 \cdot H(\varphi_{ITZ} - \varphi_{cri}) \cdot (\varphi_{ITZ} - \varphi_{cri})^2) \quad (2-13)$$

From this model, relations for the porosity and the diffusion coefficient between the ITZ and the bulk cement paste were calculated for pastes with different water cement ratios. It was found that highest difference in porosity between the ITZ and the cement paste was for the paste with lowest water cement ratio ( $w/c = 0.20$ ), about 6 times higher. For the diffusion coefficient, the largest difference was found for the paste with  $w/c$  ratio equal to 0.45 around 12 times higher for the ITZ. The relation for  $D_{ITZ}/D_{cp}$  was reaching from about 2 to 12, for  $w/c$  ratios from 0.2 to 0.7. The highest values were found for the pastes with the intermediate  $w/c$  ratios.

Guowen et al. (2011) found in their study that the diffusion coefficient of ITZ is 12 times that of the cement paste for mortars and 17 times larger than the value of the cement paste for concrete. The reason of the difference was explained as the dependence of particle size distribution and volume fraction of aggregates.

If the aggregate fraction increases it means that the distance between aggregate particles and consequently the distance between ITZ zones decreases. Eventually the ITZ zones will connect to each other and create a system of continuous ITZ zones with higher diffusivity than the cement paste that covers a substantial part of the concrete. Winslow, et al. (1994), found that at an aggregate fraction of around 50 %, this behavior appears.

## 2.7 Chloride threshold value

The chloride threshold value has been investigated by numerous researches over the years. Varying techniques for measurements are available to determine chloride threshold values, but there are a lot of uncertainties which make it difficult to rely on the results totally and a wide range of threshold values has been the consequence, Ann and Song (2007).

It was suggested in early works that only free chlorides affect the corrosion, but it is most common to express the threshold value in total chlorides, (free + bound). This has the advantages that it is easier to measure the total chloride content and also the fact that when corrosion is initiated, if the pH value drops, a great part of the surrounding bound chlorides will be released and contribute to the corrosion, Ann and Song (2007).

In Bertolini et al. (2004), an important factor described is the electrochemical potential of steel, which highly depends on the availability of oxygen at the steel surface. Therefore the state of moisture essentially influences the threshold value. For submerged condition the threshold value is higher than for conditions above sea level and it can be more than one order of magnitude larger. Also the voids close to surface of the reinforcement bar is a factor to account for. When the volume of air voids was decreased from 1.5 % to 0.2 %, the threshold value, which was defined as the chloride content when corrosion initiated, was increased by a factor of 10 from 0.2 % to 2 % of cement weight, Bertolini et al. (2004).

The chloride binding capacity influences the threshold value as well, where especially the amount of  $C_3A$ , (related to the AFm phase), in the cement paste affects the binding capacity. It has been shown that the threshold level increased when the  $C_3A$  content for plain cement increased, Ann and Song (2007). If only the free chlorides contribute to the corrosion it is reasonable to assume that for increased binding capacity, the corrosion risk will be lower and the threshold value higher. Although this positive effect of binding, the bounded chlorides, as mentioned, may be released when the pH drops and contribute to the corrosion.

A wide range of different threshold values that have been suggested in literature is stated in a table by Ann and Song (2007). The range reaches from 0.079 up to maximum 2.9 (total chloride % by cement weight) or 0.014 % to 0.5 % of concrete weight for the Bakkasund Bridge, depending on varying detection methods, specimens and conditions.

In the report by Sandberg (1998) experiments on concrete specimens from the Swedish west coast, Träslövsläge, were analysed. For concrete with w/c ratio of 0.4 and 5 % silica fume, similar to the Bakkasund Bridge, threshold values from 0.8 % to 1.4 % by cement weight were found, which represent 0.14 % to 0.24 % of concrete weight for the Bakkasund Bridge.

In Arya et al. (2014) the authors used a threshold value of 0.05 % of concrete weight when studying chloride profiles of concrete exposed to cyclic wetting and drying.

Fluge (2003) suggests a threshold value of 0.72 % chlorides of cement weight, which represents 0.12 % by concrete weight for the Bakkasund Bridge, based on measurement in 110 locations of the Gimsøystraumen Bridge in Norway. From the measurements of corrosion the results are divided into five groups, no corrosion, start of depassivation, corrosion, heavy corrosion and heavy corrosion and pitting. The threshold value was defined as when corrosion has occurred. The level for start of depassivation was found to be 0.44 % of cement weight or 0.08 % of concrete weight.

In Ann and Song (2007) a table is shown giving threshold values (% by cement weight) that are stated in different standards. The standards are BS 8110, ACI 201, ACI 357 and ACI 222 and values are given for prestressed concrete, reinforced concrete exposed to chlorides in service, reinforced concrete that will be dry or protected from moisture during service and for other reinforced concrete. The threshold value is lowest for prestressed concrete, 0.06-0.10 % by cement weight or 0.01-0.02 % by concrete weight, and for reinforced concrete exposed to chlorides the value is 0.10-0.20 % by cement weight or 0.02-0.04 % by concrete weight and this is the category for which the Bakkasund Bridge will be placed in. The highest value given is 0.40 % by cement weight or 0.07 % by concrete weight and it is for dry, reinforced concrete.

In the report which describes the DuraCrete model, The European Union – Brite EuRam III (2000), critical chloride threshold values are specified for different concrete types and environments. For submerged conditions, these threshold values are very high, 1.6 % to 2.3 % relative to binder. For the tidal and splash environment and for a concrete type with water binder ratio equal to 0.4, the threshold value is stated to 0.8 % relative to binder, which represents 0.145 % by concrete weight for the Bakkasund Bridge. These values are characteristic values and have to be divided by partial factors.

### 2.7.1 Summary

Various suggestions of the threshold value were found and one factor is the spread in measurement techniques. Also, the difference between design and characteristic values is not always easy to determine.

Because of the wide variation of suggested threshold values in the literature it seems reasonable to define a span with a minimum limit below which there is no significant risk of corrosion and a maximum limit where values above relate to high risk of corrosion. A conservative maximum value would be 0.12 % chlorides of concrete weight due to the results from Fluge (2003) and the results from Sandberg (1998) at Träslövsläge. A minimum of 0.04 % might be reasonable by reason of the stated values in the codes and the result from Fluge (2003) where the depassivation starts at 0.08 % by concrete weight.

### 3 The Bakkasund Bridge

The Bakkasund Bridge, see Figure 3.1, is a concrete bridge built in 1999 located close to Bergen at the west coast of Norway, see Figure 3.2. It has a length of 342.5 meters with totally 4 spans and with a largest span of 173 m. The bridge is located in a marine environment exposed to chlorides, mainly coming from the seawater. De-icing salts from vehicles during winter time may, even if the influence is very small, also be a source to account for and is included in the measurements. Different parts of the bridge were cast during different weather conditions because the construction period was over the whole year. The columns were cured one day and the box girders three days before the formwork was removed, Larsen<sup>2</sup>, (2014).



Figure 3.1 Picture of the Bakkasund Bridge. (Photo: Claus K Larsen<sup>2</sup>, 2013)



Figure 3.2 Map of the south of Norway with the Bakkasund Bridge and Oslo inside the red lined squares, (google.se/maps, 2014).

<sup>2</sup> Claus K Larsen, Chief Engineer at Statens Vegvesen, Oslo.

Many bridges built before 1989 in Norway are suffering from chloride ingress and corrosion of the reinforcement, mainly due to the use of concrete with too high diffusion coefficients, Larsen<sup>3</sup> (2014). For example, the reinforcement in the Gimsoystraumen Bridge in Norway, built in 1981, suffered from corrosion due to chloride ingress already after 10 years. In 1989 changes in concrete specifications were made, introducing concrete with lower diffusion coefficients. For example concrete like the one used in the Bakkasund Bridge with a water-binder ratio lower than 0.4 and with about 5% silica fume. In 1995 the design guidelines were changed increasing the cover depth from 30 mm to 60 mm +15 mm tolerance which was used for the Bakkasund Bridge. This means that the minimum concrete cover for the Bakkasund Bridge is 60 mm. Common practice is to perform inspections of bridges such as the Bakkasund Bridge every 5th year. In this bridge only smaller cracks have been found. In the columns investigated in this thesis, one crack was detected, located at the bottom of one of the columns. It was approximate 0.10 mm wide at the surface and went into the depth of the reinforcement. The crack was investigated further and no chloride ingress in the crack could be measured, Larsen<sup>3</sup>, (2014).

### 3.1 The concrete composition

The concrete has a binder consisting of 95% OPC (Ordinary Portland Cement), 5% silica fume and a water binder ratio of less than 0.4. The dry weight of different components in the concrete is shown in Table 3-1.

Table 3-1 Dry weights and densities for the components in the binder.

Material	Weight, m [kg/m <sup>3</sup> ]	Particle density, ρ [kg/m <sup>3</sup> ]
Cement <sup>4</sup>	408	3140
Silica fume <sup>5</sup>	20	2200
Sand, 0-8 mm	820	2600
Gravel, 8-16 mm	930	2600
Rescon P	1.7	
Rescon HP-SF	4.3	

Rescon P is a plasticizer and Rescon HP-SF is a super-plasticizer. Sieve curves for the aggregate in the concrete have been produced by NCC and were received from Larsen<sup>3</sup>, (2014). One of the sieve curves was for the sand with the dimension of 0 mm to 8 mm and one was for the gravel with the dimension of 8 mm to 16 mm. The two sieve curves are shown in Figure 3.3 and Figure 3.4.

<sup>3</sup> Claus K Larsen, Chief Engineer at Statens Vegvesen, Oslo, mail correspondence in May 2014.

<sup>4</sup> Domone and Illston, (2010)

<sup>5</sup> SFA, (2005)

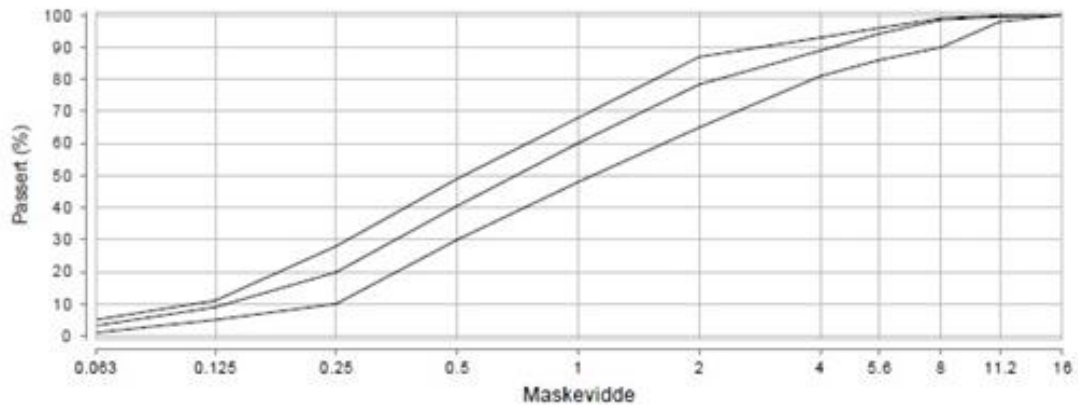


Figure 3.3 Sieve curve for the sand, 0-8 mm.

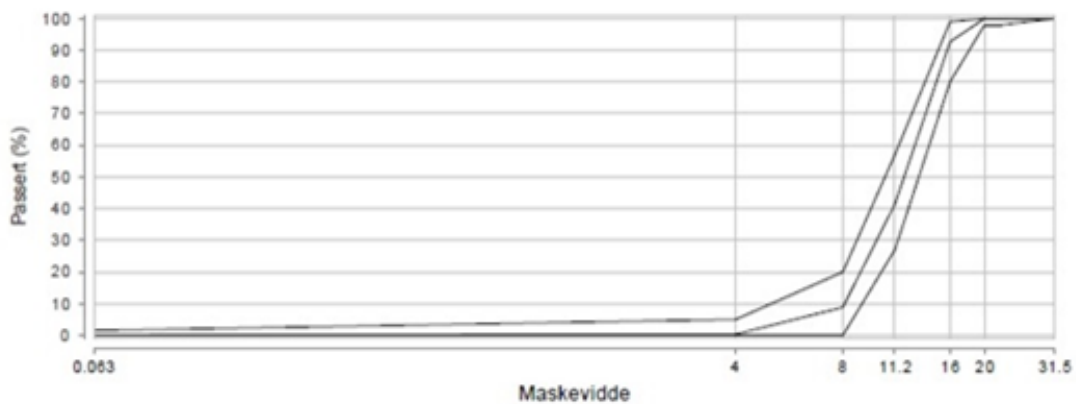


Figure 3.4 Sieve curve for the gravel, 8-16 mm.

Larger figures of the sieve curves can be seen in Appendix E. The aggregates were occupying 67 % of the volume.

## 3.2 Data from measurements at the Bakkasund Bridge

Measurements have been made at the Bakkasund Bridge during 2013, where drilled cores were taken at various locations of the bridge. The locations are named with letters A to L and a figure with their positions can be seen in Appendix C. All samples have been taken from one of the two columns that stand in the water but at different heights and sides. Dust samples were obtained by profile grinding the drilled cores in laboratory.

### 3.2.1 Chloride content

The dust samples were analyzed in laboratory; dissolved in acid and tested for chloride content. The results from the dust samples can be seen in Table 3-2 where the chloride concentration is shown at different depths.



Table 3-2 Measurements from the Bakkasund bridge in 2013 in chloride weight- % of concrete.

Location	Depth [mm]	Cl % of concrete by weight								
		A	B	C	E	F	G	H	I	L
	1	0,15	0,25	0,06	0,06	0,115	0,1	0,075	0,085	0,085
	3	0,25	0,24	0,08	0,065	0,1	0,08	0,055	0,06	0,06
	5	0,24	0,17	0,15	0,045	0,085	0,04	0,03	0,02	0,025
	7	0,29	0,12	0,13	0,03	0,06	0,03	0,015	0,005	0,015
	9	0,18	0,11	0,11	0,02	0,035	0,01	0,01	0,005	0,005
	12,5	0,14	0,07	0,08	0,015	0,015	0,01	0,005	0	0,005
	17,5	0,08	0,03	0,01	0,01	0,005	0,005	0	0	0
	22,5	0,01	0,01	0	0,005	0	0	0	0	0
	27,5	0,01	0,01	0	0,005	0	0	0	0	0
	32,5	0,01	0,01	0	0	0	0	0	0	0
	37,5	0,01	0,01	0	0,01	0,005	0	0	0	0
	42,5	0,01	0,01	0,03	0	0	0	0	0	0
	47,5	0	0,01	0	-	-	0,005	0	0	0

The drilled cores at the locations E, F, G, I and L were used to calculate the diffusion coefficient of the concrete. An accelerated chloride diffusion test according to NT Build 443 was made on the inner part of the concrete cores, i.e. concrete free from chlorides. NT Build 443 is a method for measuring of the diffusion coefficient cf. Jensen (2013). A value for the diffusion coefficient for each location is showed in Table 3-3.

Table 3-3 Measured diffusion coefficients.

	E	F	G	I	L	Average total
Average [x10 <sup>-12</sup> m <sup>2</sup> /s]	3,39	2,15	2,08	2,43	4,25	2,86

When diffusion coefficient analyses are made, waiting until steady state conditions would be preferable, but since it takes very long time to reach steady state it is not practical. Instead methods as the rapid chloride migration test and the method according to NT Build 443 have been developed. For input in the analytical models values from the rapid chloride migration test are supposed to be used. For concrete with CEM I and with 5 % silica fume the ratio  $D_{RCM}/D_{433}$  is 0.7 at an age of 97 days according to Larsen<sup>6</sup>. Therefore the measured diffusion coefficient by NT Build 443 was transferred to  $D_{RCM}$  with help of the factor 0.7.

Some of the measurements (A, B, E and F) were taken 2-3 meters from the water level on one of the columns while the rest (C, D, G and H) were taken at the upper part of the column and from the wall of the bridge's box girder at 12-13 m over water

<sup>6</sup> Claus K Larsen, Chief Engineer at Statens Vegvesen, Oslo, mail correspondence in May 2014.

level. The major difference between the results on the different locations is that the chloride content at A, B and C is higher than at the other locations, see Appendix C.

### 3.2.2 Cement content from calciumoxide

The content by weight of calciumoxide, CaO was also measured and the results can be seen in Table 3-4. The content of calciumoxide in the aggregates was assumed to be zero which means that all the calciumoxide should come from the cement. The cement used for the Bakkasund Bridge was "Norcem. Anl. cement" and the average calcium oxide content of this cement is 64%. The cement content is proportional to the calciumoxide content and the cement by volume percentage can be seen in Table 3-4.

Table 3-4 Measurements of the calciumoxide content in the concrete in the Bakkasund bridge.

Depth [mm]	CaO by weight [%]	Cement by weight [%]	Cement by volume [%]
0-2	16,7	26,1	21,5
2-4	12,6	19,6	16,1
4-20	10,9	17,0	13,9

The cement content used when calculating the aggregate content is about 14%. That seems to correspond well with the results from Table 3-4 since the cement percentage per volume is about 14 % in the third column, in depths larger than 4 mm. There is a difference in the first few millimeters in the real concrete that depends on the boundary effect, less aggregates gives more cement. However this effect could be considered as small compared with a depth of 60 mm where the minimum locations of the reinforcements are.

## 4 Analytical Models

Prediction of chloride ingress in concrete is possible to do by different analytical models. There exist both empirical and physical models. Below three models are described; empirical models, as the Simple error function model and the DuraCrete model, and physical, as the ClinConc model.

All the three analytical models are based on the error function, which is the solution of Fick's second law of diffusion. In this solution the diffusion coefficient needs to be specified. It is common to use the diffusion coefficient as a general term, but there exist different types of diffusion coefficients. In the report by Tang and Gulikers (2007) the authors try to explain the difference between different diffusion coefficients. The diffusion coefficient is time dependent and the integral of varying diffusion coefficients from time equal to zero to the actual time is called the apparent diffusion coefficient, which more simplified can be understood as the average diffusion coefficient over time. When  $D_0$  is stated in this report it refers to a measured diffusion coefficient by the rapid chloride migration test at the time  $t_0$ . When only diffusion coefficient is used as in Section 2.5 and 2.6, it refers to the diffusion coefficient more generally speaking.

### 4.1 The Simple error function model

A model based on the error function can be derived from a Fick's second law solution; the model is in this report called the Simple error function model. This model is the base for the other analytical models presented in this report. Assuming constant chloride surface concentration and constant diffusion coefficient, the result according to Bertolini et al. (2004) is showed in equation ( 4-1 ).

$$c(x, t) = c_s \left[ 1 - \operatorname{erf} \left( \frac{x}{2\sqrt{D_{App} \cdot t}} \right) \right] \quad (4-1)$$

where

$c$	Chloride concentration, [ $kg/m^3$ ]
$c_s$	Chloride surface concentration, [ $kg/m^3$ ]
$x$	Distance, [ $cm$ ]
$D_{App}$	Constant apparent diffusion coefficient, [ $cm^2/s$ ]
$t$	Time [ $s$ ]

A weakness is that all transport mechanisms that occur in the concrete are represented by the diffusion coefficient. However, experience show that the diffusion coefficient

in a good way represents the other transport mechanisms. Also, this model does not separate free chlorides from bound chlorides hence all chlorides contribute to the driving potential.

The model can be used by curve fitting with measured values to estimate the apparent diffusion coefficient of a concrete sample and also to estimate the chloride ingress at any time,  $t$ . But since the apparent diffusion coefficient changes over time a constant diffusion coefficient will be too much on the conservative side as the time increases.

## 4.2 The DuraCrete model

The DuraCrete model is based on the Simple error function model. The model introduces a time dependent apparent diffusion coefficient and constants validated for different exposure conditions. According to The European Union – Brite EuRam III (2000) the equation, can be expressed as

$$c(x, t) = c_s \left[ 1 - \operatorname{erf} \left( \frac{x}{2\sqrt{D_{App} \cdot t}} \right) \right] \quad (4-2)$$

$$c_s = A_{c,s,cl} \cdot \left( \frac{w}{b} \right) \quad (4-3)$$

$$D_{App} = k_{e,cl}^c \cdot k_{c,cl}^c \cdot \left( \frac{t_0}{t} \right)^{n_{cl}^c} \cdot D_0 \quad (4-4)$$

where

$c$	Chloride concentration, [ $kg/m^3$ ]
$c_s$	Chloride surface concentration, [ $kg/m^3$ ]
$A_{c,s,cl}$	Constant given in DuraCrete model, (Regression factor)
$\left( \frac{w}{b} \right)$	Water binder ratio, [-]
$x$	Distance, [ $cm$ ]
$D_0$	Diffusion coefficient measured in diffusion coefficient test, [ $cm^2/s$ ]
$D_{App}$	Apparent diffusion coefficient, [ $cm^2/s$ ]
$t$	Time, [ $s$ ]
$k_{c,cl}^c$	Curing factor, [-]

$k_{e,cl}^c$	Environmental factor, [-]
$t_0$	The age of the concrete when the compliance is performed, [s]
$n_{cl}^c$	Age factor [-]

The strengths of this model are that it is easy to use and covers different environmental conditions and concrete compositions.

It is also rather general in the way that a whole environmental condition is treated in the same way which means it is a very sharp distinction between the different conditions. In reality the differences between environmental zones appear gradually. Also for this model, it does not distinguish between free and bound chlorides but considers all chlorides to influence the driving potential.

The diffusion coefficient test made for the measurement at the Bakkasund Bridge was the NT Build 443 and not the rapid chloride migration test, which should be used. As was mentioned in Chapter 3, after the concrete age of 97 days the ratio  $D_{RCM}/D_{433}$  was measured to 0.7.

### 4.3 The ClinConc model

The ClinConc model uses free chlorides instead of total chloride content as driving potential, which corresponds to reality in a more correct way. The ClinConc model by Tang (2008) is performed in two main steps. First it simulates the free chloride penetration through the pore system by use of Fick's second law, with free chlorides as the driving potential, see equation ( 4-5 ). Then by use of the mass balance equation combined with non-linear chloride binding, the total chloride concentration is calculated, see equation ( 4-6 ).

$$c = c_s \left( 1 - \operatorname{erf} \left( \frac{x}{2 \cdot \sqrt{\frac{k_D \cdot D_0}{1-n} \cdot \left[ \left( 1 + \frac{t_{ex}'}{t} \right)^{1-n} - \left( \frac{t_{ex}'}{t} \right)^{1-n} \right] \cdot \left( \frac{t_{6m}'}{t} \right)^n \cdot t}} \right)} \right) \right) \quad (4-5)$$

where

$c, c_s$	Free chloride concentration in pore system and at the surface, [ $kg/m^3$ ]
$t$	Duration of exposure, [s]
$t_{ex}'$	Age of concrete at the start of exposure, [s]

$t_{6m}$	Age of concrete 6 months of exposure, [s]
$x$	Distance, [cm]
$n = -0.45a_t^2 + 0.66a_t + 0.02$	Age factor, [-]
$D_0 = \frac{(0.8a_t^2 - 2a_t + 2.5) \cdot (1 + 0.59K_{b6m}) \cdot k_{TD}}{1 + k_{OH6m} \cdot K_{b6m} \cdot k_{Tb} \cdot f_b \cdot \beta_b \cdot \left(\frac{c_s}{35.45}\right)^{\beta_b - 1}} \cdot D_{6m}$	Initial apparent diffusion coefficient, [cm <sup>2</sup> /s]
$K_{b6m} = \frac{W_{gel6m}}{1000 \cdot \varepsilon_{6m}}$	Constant depending on gel content and water accessible porosity, [kg/m <sup>3</sup> ]
$k_{TD} = e^{\frac{E_D}{R} \left(\frac{1}{T_0} - \frac{1}{T}\right)}$	Temperature factor for diffusion coefficient, [-]
$k_{Tb} = e^{\frac{E_b}{R} \left(\frac{1}{T} - \frac{1}{T_0}\right)}$	Temperature factor for chloride binding, [-]
$k_{OH6m} = e^{0.59 \cdot \left(1 - \frac{0.043}{OH_{6m}}\right)}$	Factor describing the effect of alkalinity, [-]
$\beta_b$	Chloride binding exponent, [-]
$f_b$	Chloride binding coefficient, [-]

When the free chloride concentration in the pore system is determined, the total chloride concentration can be calculated as

$$C = \frac{\varepsilon \cdot (c_b + c_f)}{B_c} \cdot 100 \text{ mass \% of binder} \quad (4-6)$$

where

$c_b = f_t \cdot k_{OH6m} \cdot K_{b6m} \cdot k_{Tb} \cdot f_b \cdot c^{\beta_b}$	Bound chloride concentration, [g/l]
$f_t = a_t \cdot \ln\left(\frac{c}{c_s} \cdot t + 0.5\right) + 1$	Time dependent factor for chloride binding, [-]
$\varepsilon$	Water accessible porosity, [-]
$B_c$	Cementitious binder content, [kg/m <sup>3</sup> ]

It should be noted that the equations above are based on the assumption of submerged conditions where the chloride solution is in constantly contact with the concrete surface, which is not true for the measured locations in the Bakkasund Bridge. For input values see Appendix G.

## 4.4 Results from analytical models

The results from the analytical models were compared to the measurements from the bridge. The measurements were divided into two groups, splash zone and atmospheric zone, where the measurements from the splash zone showed considerable higher values than the ones from the atmospheric zone. Only the measurements, see Chapter 3, that were considered to be in the splash zone were compared with the analytical models.

Graphs of the results from the analytical models are shown together with the chloride profiles from the measurements in Figure 4.1 to Figure 4.3. The input data used for the three models are shown in Appendix G.

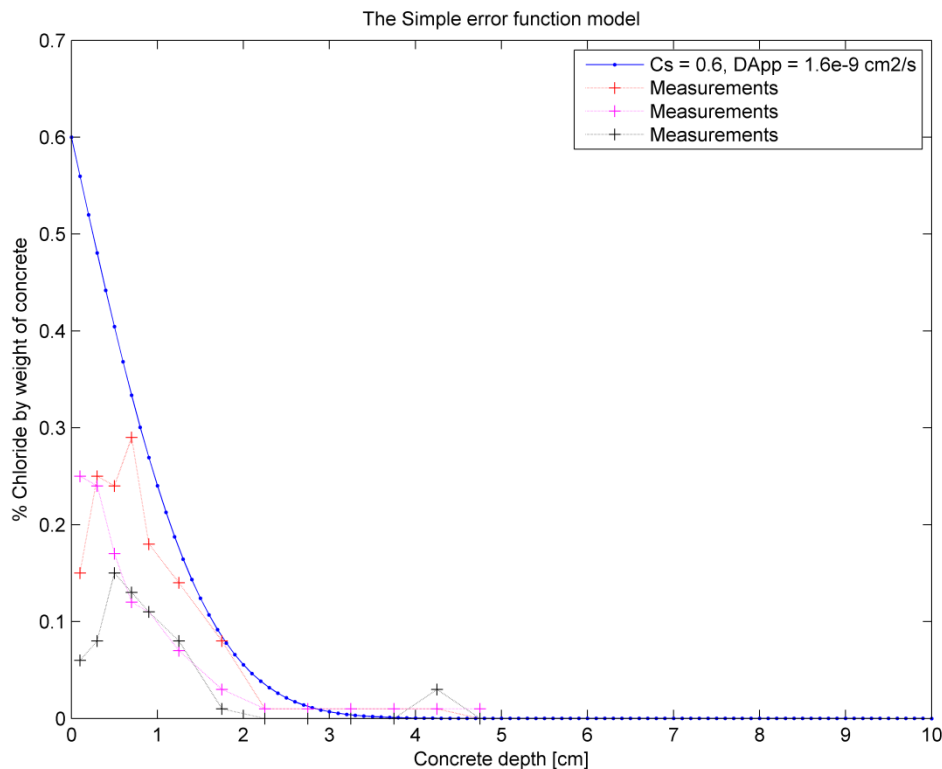


Figure 4.1 The Simple Error Function compared with measurements at 14 years.

In the Simple error function model, there is only the chloride surface concentration and the diffusion coefficient that the user should vary. These variables were varied in such way it fitted the measurements, but it should be noticed that the profile in Figure 4.1 only is one of many possible ways of fitting the measurements by varying the inputs.

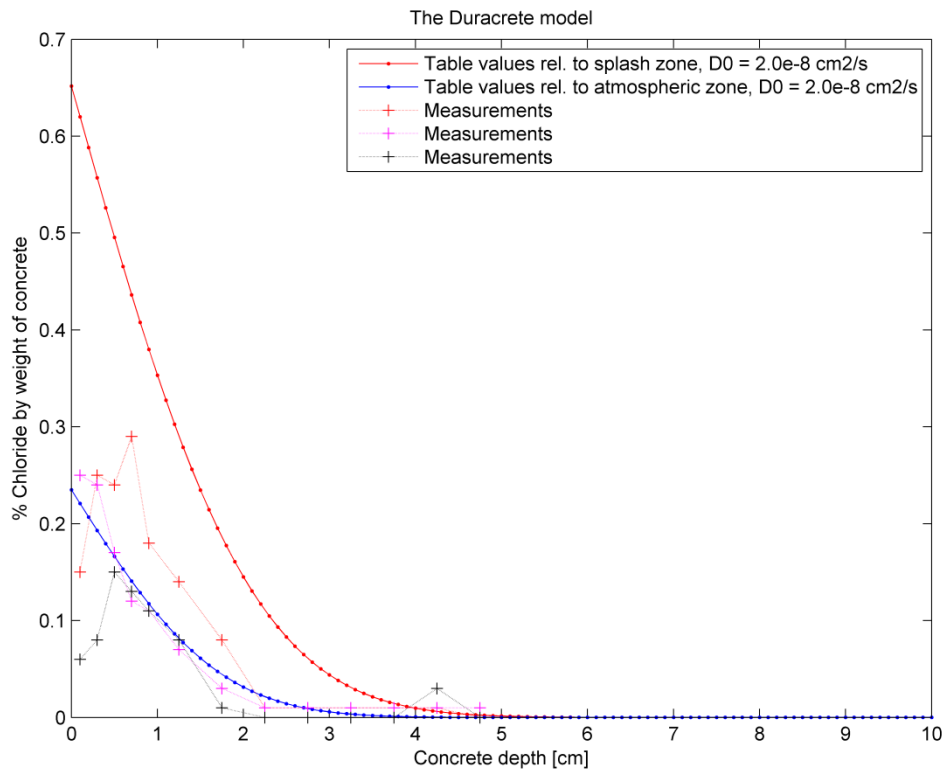


Figure 4.2 The DuraCrete model compared with measurements at 14 years.

The input values for the DuraCrete model were taken from the guide, The European Union – Brite EuRam III (2000), for splash and atmospheric zone. The diffusion coefficient was taken as the value measured in the diffusion coefficient tests, by Jensen, (2013).



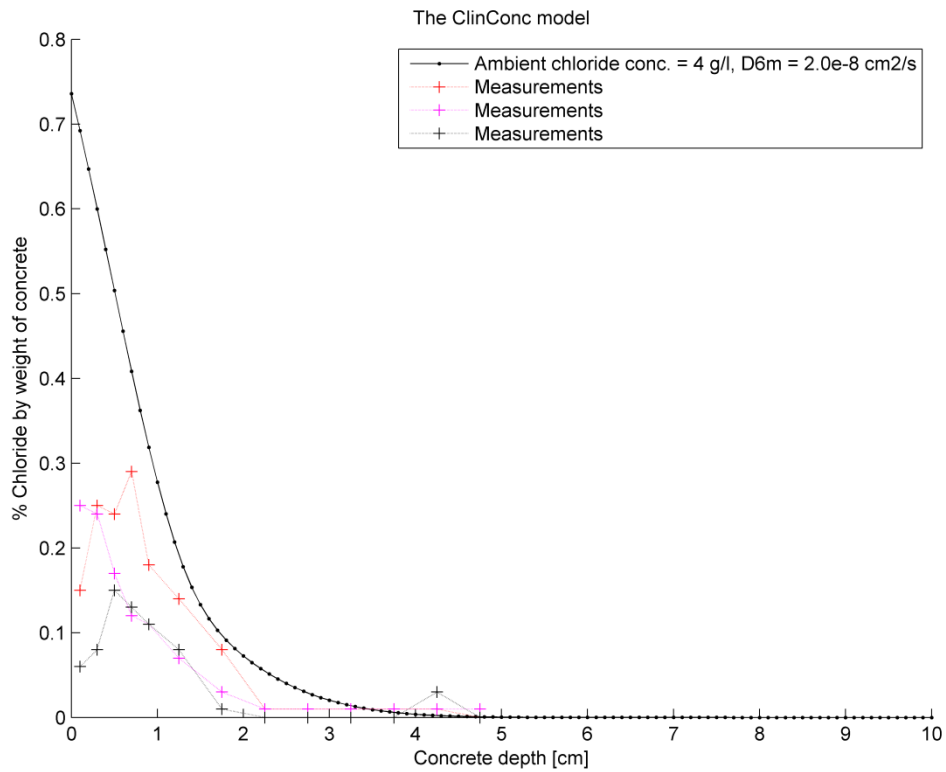


Figure 4.3 The ClinConc model compared with measurements at 14 years.

The input values for the ClinConc model were taken from the report by Tang, (2008), except diffusion coefficient which was the same as for the DuraCrete model.

In Figure 4.4 the profiles from the analytical models that fit the measurements at 14 years are shown, but for the service life of 100 years. The profiles are shown together with the location of the reinforcement and the maximum and minimum threshold limits taken from Section 2.5.

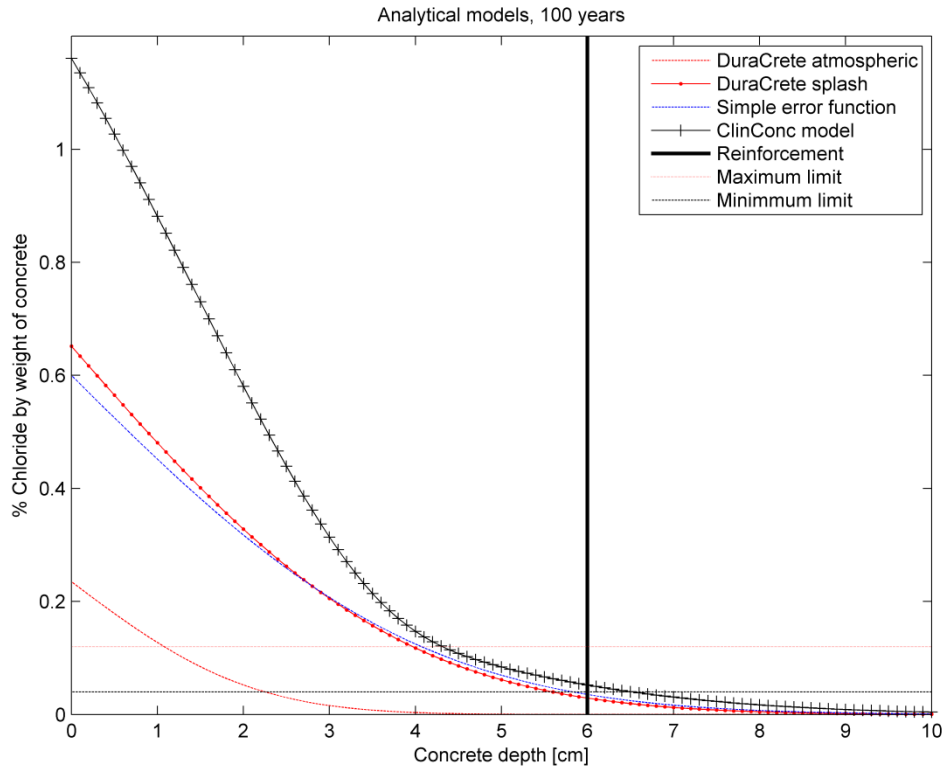


Figure 4.4 The profiles that fits measurements at 14 years, for the time 100 years.

## 4.5 Comments on the analytical models

The input values for the models are challenging to get accurate so that the models reflect the certain situation in a reliable way. The DuraCrete model has few inputs and is rather easy, while it describes different factors depending on different environment zones, empirically though. This in comparison to the ClinConc model which has more input values, but it should describe the behaviour of the chloride ingress in a more realistic way. For usage of the Simple error function, only the chloride surface concentration and the diffusion coefficient need to be specified, which makes it simple to use.

The time  $t_0$  in the DuraCrete model, which is the age of concrete when the compliance test was performed, should according to the model be taken as 14 years, because this is the time when the diffusion coefficient test was performed. This factor influences the change of the apparent diffusion coefficient in time, see equation ( 4-4 ), and because of the hydration process both the measured diffusion coefficient and the apparent diffusion coefficient will decrease with time. According to Tang (1996) the measured diffusion coefficient does not change much after 6 months and can be considered as constant after this time. After recommendation from Tang Luping at Chalmers University of Technology, a reasonable value of the time  $t_0$  was chosen to 6 months instead of 14 years in the DuraCrete model. It can be seen in Figure 4.2 that the profile according to splash zone overestimates the measurements, while the profile for the atmospheric zone fits rather well.

For the ClinConc model, there is no regression parameter specified for calculation of the chloride surface concentration. The chloride surface concentration is as described

a parameter that varies a lot depending on many factors. Due to this uncertainty and for simplicity, an average value for these 14 years is chosen in such way that the chloride profiles fit the measurements. A constant chloride surface concentration was chosen to 4 g/l, and then the diffusion coefficient was adjusted to fit the measurement. The ClinConc model is only verified for submerged conditions which is important to keep in mind, and the chloride surface concentration is changed to fit the measurements without considering other effect that might give.

The input parameters for the Simple error function model, the apparent diffusion coefficient and chloride surface concentration, was adjusted in such way it fitted the measurements.

The purpose with the use of the analytical models in this work was to compare the results with the 3D FE model after time exceeding the measurement time of 14 years. In Figure 4.4 the profiles that fitted the measurements at 14 years are shown for 100 years. It can be seen that the curves are rather close to each other except for the DuraCrete in atmospheric zone. The ClinConc model is a little bit higher but cannot be relied on completely, when it is modelled in splash zone.

## 5 3D Mesoscale FE Model

Concrete is a well known heterogeneous material which simplified can be divided into cement paste and aggregates. If the size of the aggregates is well distributed they fill most of the space and the cement paste will due to the hydration process glue everything together. The permeability of the cement paste is much larger than the permeability of the aggregates and therefore the permeability of the aggregates can be considered to be zero. The difference in permeability of cement paste and aggregates makes the heterogeneity of concrete important when analyzing the flux of water and chloride ions in concrete. The highly porous contact area between the cement paste and the aggregates, the ITZ, influences the flux and the diffusivity increases gradually closer to the aggregates due to the higher porosity and presence of voids, Wriggers and Moftah (2005). This ITZ zone has a thickness of 15-50 micrometer, Caré and Hervé (2002), Jin-yang et al. (2012) and Sun et al. (2012). The ITZ is the red-colored area in Figure 5.1.

A 3D mesoscale FE model for moisture and chloride transport in concrete has been developed by Nilenius (2014) at Chalmers University of Technology. Mesoscale is in this project the level of scale where concrete can be considered as a three phase material consisting of cement paste, aggregates and ITZ in comparison to macroscale where it is only concrete. The aim with this model is to make it possible to consider the heterogeneity of concrete in a realistic and accurate way. This by modelling the heterogeneity of the concrete and then by numerical computational homogenization transfer the heterogeneities in the mesoscale to the macroscale. In Figure 5.1, a statistical volume element is shown, which will be further described in next subsection.

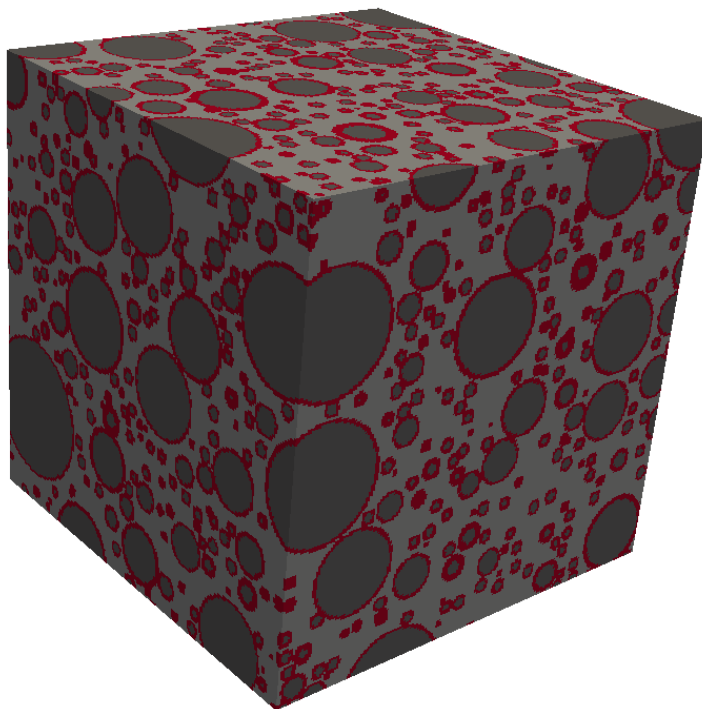


Figure 5.1 Statistical volume element, SVE.

## 5.1 Generation of statistical volume elements, SVEs

In order to run analyses in the FE-model, so called statistical volume elements, SVEs, have to be generated. The SVEs are cubes which consist of three phases, cement paste, aggregates and ITZ, and should in this project represent the concrete from the Bakkasund Bridge. The SVEs are filled with aggregates which are placed randomly. The sizes of the aggregates come from the sieve curves from the concrete in the Bakkasund Bridge. The placing of aggregates in the SVEs starts with the largest aggregate and ends with the smallest aggregate. If a position is already taken when an aggregate is placed a new position is instead randomly selected. The center of the aggregate is placed on a specific coordinate in the SVE and to allow for pieces of aggregates to be included in the SVE and not only whole particles, the placing occurs in a larger box than the specified SVE, see Figure 5.2. Although aggregates in reality have all kinds of shapes, they are for simplicity in this model assumed to be spherical. The algorithm that places the aggregates continues until the aggregate fraction is sufficiently close to the input value. It checks the aggregate fraction in the large box, why the resulting aggregate fraction in the SVEs always gets smaller than the input value. Even if the same input values are used, different SVEs will be obtained due to the randomness when the generations are performed. These different SVEs are called realizations.

In the beginning of the project the generation was done as shown in Figure 5.2, with the possibility of having cut aggregates on all boundaries. Later small changes in the code was made in such way that there was no longer possible for aggregates to be cut at one boundary, which resembles the reality in a more correct way, see Figure 5.3. When concrete is cast no aggregates are able to cross the mould, why this way to model is more correct from this projects view. If the purpose is to model a piece of concrete a distance in from the surface, then the way shown in Figure 5.2 is more correct. A space of 2 mm between the aggregates and that specific boundary was also created, because it corresponds to reality better. The number of 2 mm was an assumption from the authors. Due to this change the resulting aggregate fraction in the SVE becomes higher than the input value. This is because no aggregates can be placed outside one boundary, see the marked area in Figure 5.3, but the algorithm will still account for this area when it checks the aggregate fraction. This area will be empty, why the other part will be denser with aggregates.

With the aggregates in place the SVE can be meshed with an arbitrary mesh size where the aggregates will be more spherical for smaller element sizes. All the different input-parameters: aggregate content, aggregate size, size of SVE and mesh density affects how well the SVE represent the real concrete.

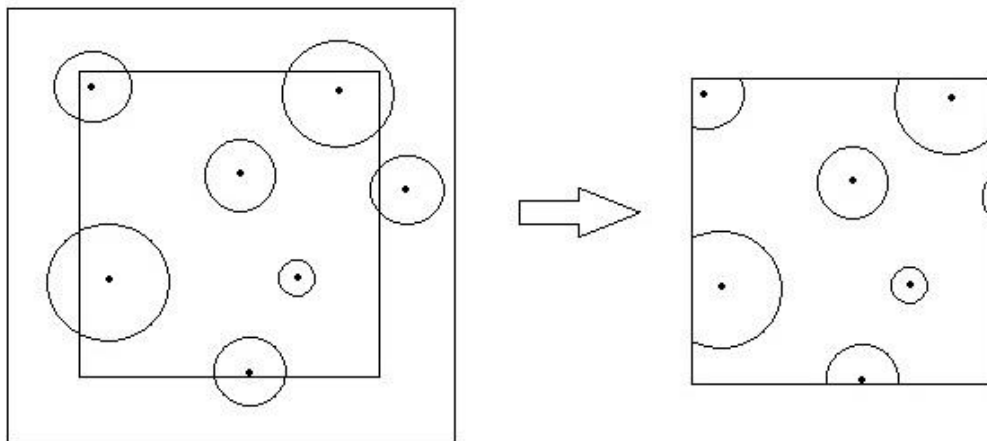


Figure 5.2 How SVEs were created when aggregates did cut the surface boundary.

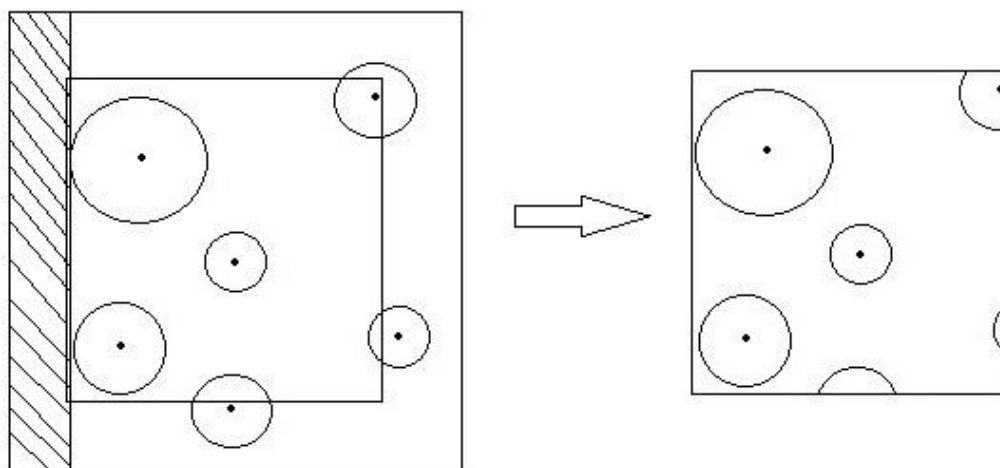


Figure 5.3 How SVEs were created when aggregates did not cut the surface boundary.

## 5.2 Transient analysis in the FE model

A general description of how the transient analysis is performed in the model is shown in this section, from the balance equation of mass transport to FE-formulation.

The flux of chloride ions is described by equation ( 5-1 )

$$\frac{\partial C_{tot}}{\partial t} = -div(J_{cl}) \quad (5-1)$$

Where  $C_{tot}$  is the total amount of chlorides and  $J_{cl}$  is the flux. The time derivative can be rewritten as

$$\frac{\partial C_{tot}(C_f)}{\partial t} = \frac{\partial C_{tot}}{\partial C_f} \cdot \frac{\partial C_f}{\partial t} \quad (5-2)$$

Where  $C_f$  is the amount of free chlorides. By doing this equation ( 5-1 ) is written as

$$\frac{\partial C_{tot}}{\partial C_f} \cdot \frac{\partial C_f}{\partial t} = -div(J_{cl}) \quad (5-3)$$

$$\frac{\partial C_{tot}}{\partial C_f} \cdot \frac{\partial C_f}{\partial t} + div(J_{cl}) = 0 \quad (5-4)$$

Equation ( 5-4 ) can be written on FE-form

$$\mathbf{C}\dot{\mathbf{a}} + \mathbf{K}\mathbf{a} = \mathbf{f} \quad (5-5)$$

where

$$\mathbf{C} = \int_{\Omega} \mathbb{N}^T \frac{\partial C_{tot}}{\partial C_f} \mathbb{N} dV \quad (5-6)$$

$$\dot{\mathbf{a}} = \frac{\partial C_f}{\partial t} \quad (5-7)$$

$$\mathbf{K} = div(D) = \nabla \cdot D \quad (5-8)$$

$$\mathbf{a} = C_f \quad (5-9)$$

The flux  $div(J_{cl})$  is equal to  $\nabla \cdot D \cdot C_f$ , where  $D$  is the diffusion coefficient. Contributions are later added to the stiffness matrix  $\mathbf{K}$  and the force vector  $\mathbf{f}$  from Newton's convection boundary conditions, described in Section 6.4. More extensive information is described in Nilenius, (2014).

## 6 Calibration of the Model

For calibration of the 3D mesoscale FE model with the measurements from the Bakkasund Bridge, efforts were made to create SVEs that resemble the concrete.

The input parameters that are needed to create an SVE are

- $L_{\text{box}}$ , which is the length of a side of the cubical SVE.
- Aggregate fraction, which is the volume percentage of the aggregates that are included in the SVE
- The radius of the aggregates which are included in the SVE and their percentage of all the included aggregates.
- The number of finite elements that the SVE should be divided into.

The aggregate fraction and aggregate sizes are taken from the sieve curves, see Chapter 2. The value of  $L_{\text{box}}$  depends on boundary effects which are described in Section 6.3 and the number of finite elements was determined by mesh size studies in Section 6.2.

In the beginning of the project, the ambition was to model the concrete down to as small scale as possible. In order to model small aggregates the SVE needs to be divided into small finite elements in order to get reasonable shapes of the smallest aggregates and to get accurate results. Later in the project new discoveries were done and SVEs were created with a different aim. Model it down to as small aggregates as possible was no longer the goal, but instead the SVE increased in size, due to boundary effects described in Section 6.3. Due to this, the mesh size had to be increased because of the increase of computational time. Then the smallest aggregate size also had to be increased.

When SVEs are created, analyses of the chloride ingress can be made and in order to perform a transient analysis in the model, the following main input parameters are required.

- The convective coefficient.
- The ambient chloride concentration.
- The chloride binding capacity.
- The time (steps and step size).
- The diffusion coefficients of cement paste/mortar and ITZ.

Each of these input parameters was investigated regarding their effect on the chloride ingress profiles.

### 6.1 Aggregates, size and amount

The amount of aggregates used in the 3D model was determined by the smallest size of aggregates that were modelled in the SVEs. Smaller aggregates than a specific value was simply neglected and assumed as a part of the homogenous cement paste. To model the concrete as good as possible could mean trying to model as small particles as possible. The size of the smallest aggregate that was considered in the 3D model depended on computational time and the size of the elements. As each aggregate is placed individually, a smaller size requires a larger amount to reach the



same volume hence it takes longer total time to place. A larger total amount of aggregates also makes it harder to find empty spots where new aggregates can be placed without having to randomly find a new spot because it was already occupied. The sieve curves given for the Bakkasund Bridge ranged down to 63  $\mu\text{m}$  and also specified the quantities for aggregates below 63  $\mu\text{m}$ . Modelling the aggregates down to 63  $\mu\text{m}$  or even below would need enormous computational power or take extremely long time. For the mesh size studies the smallest aggregates were first chosen to 1.5 mm (the mean value between 2 mm and 1 mm in the sieve curve). This gave the aggregate fraction of 48 %. The aggregates smaller than 1 mm was assumed to be a part of the mortar and these aggregates represent almost 20 % of the aggregate volume fraction. The effect from the aggregates that were parts of the mortar, both the effect from the non-permeable aggregate and the effect from the highly permeable ITZ zone was assumed to be taken care of through the diffusion coefficient of the mortar. Later the size of  $L_{\text{box}}$  was increased to 10 cm and the smallest aggregate size was increased to 4.8 mm.

## 6.2 Influence of the mesh size

The size of the mesh determines how small the smallest aggregate can be and how spherical the aggregates will be. As the mesh gets finer the aggregates will go from cubes to more spherical shapes, see Figure 6.1.

Mesh size analyses were done for different amount of elements, where the input variable  $n_x$  was equal to 50, 100, 150 and 200 nodes. Figure 6.2 shows the definition of  $n_x$ ,  $n_y$  and  $n_z$ , which in this case are equal. This means that  $(n_x - 1)$  to the power of three gives the total amount of elements for an SVE.



Figure 6.1 Same SVE, but with different mesh size,  $n_x$  equal to 50, 100, 150 and 200 nodes.

In the upper left figure, with  $n_x$  equal to 50, it seems like there is extremely much ITZ. However, this is misleading because, simplified described, if an element contains a boundary element of an aggregate (ITZ) it will be visualized like the whole element is ITZ. But the effect of the ITZ on that element comes from its property, which is the diffusivity times the thickness. This means that the rougher meshed SVE does not have more ITZ than the finer meshed SVE, even if it looks like that in the figures.

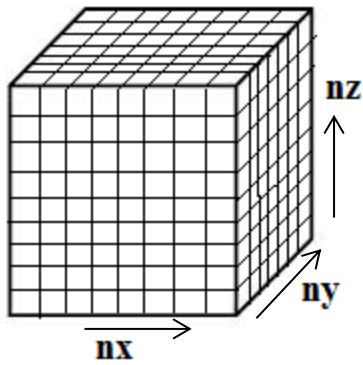


Figure 6.2 Definition of the number of nodes in each direction.

Analyses were made for  $n_x$  equal to 300 but due to long computational time this was not made for all analyses. In the beginning of the mesh size studies, the size of the SVEs were 50 mm (or  $50^3 \text{ mm}^3$ ), which gave the element size of 1 mm, 0.5 mm, 0.33 mm and 0.25 mm. The limit for the smallest aggregate size from the sieve curves was chosen to 1.5 mm and from the different mesh sizes, this smallest aggregate was divided in 1.5, 3, 4.5 and 6 elements.

Four different checks were made for different mesh sizes:

- The change of aggregate fraction
- The change of aggregate surface area
- The change of flux for stationary analysis
- The change of flux for transient analysis

In Figure 6.3 and Figure 6.4, the change of aggregate fraction and the change of aggregate surface area with changing mesh size are shown. The aggregate fraction was from the sieve curves specified to 48 %. Because of the randomness when generating the SVEs, 10 realizations were made for each mesh size and the mean values were plotted in Figure 6.3 and Figure 6.4. The input for aggregate fraction were chosen to 54 % and 56 % to get as close to 48 % as possible, this because the model gives lower aggregate fraction than specified, when placing is allowed at all boundaries, i.e. before the code was changed as explained in Section 5.1.

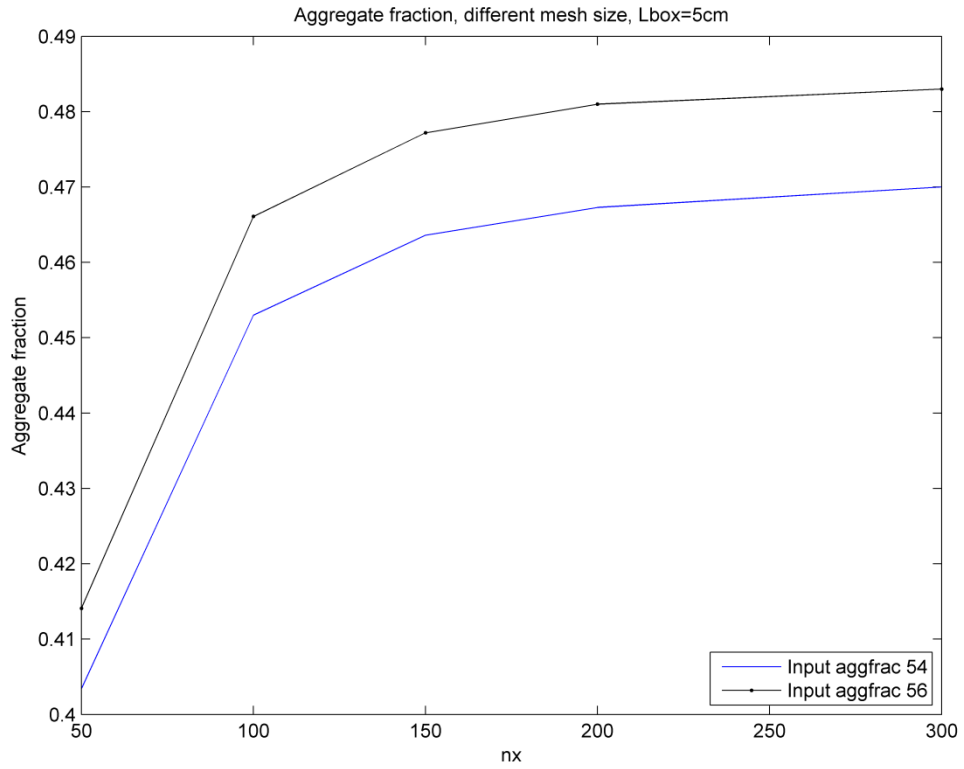


Figure 6.3 The aggregate fraction with varying mesh size.

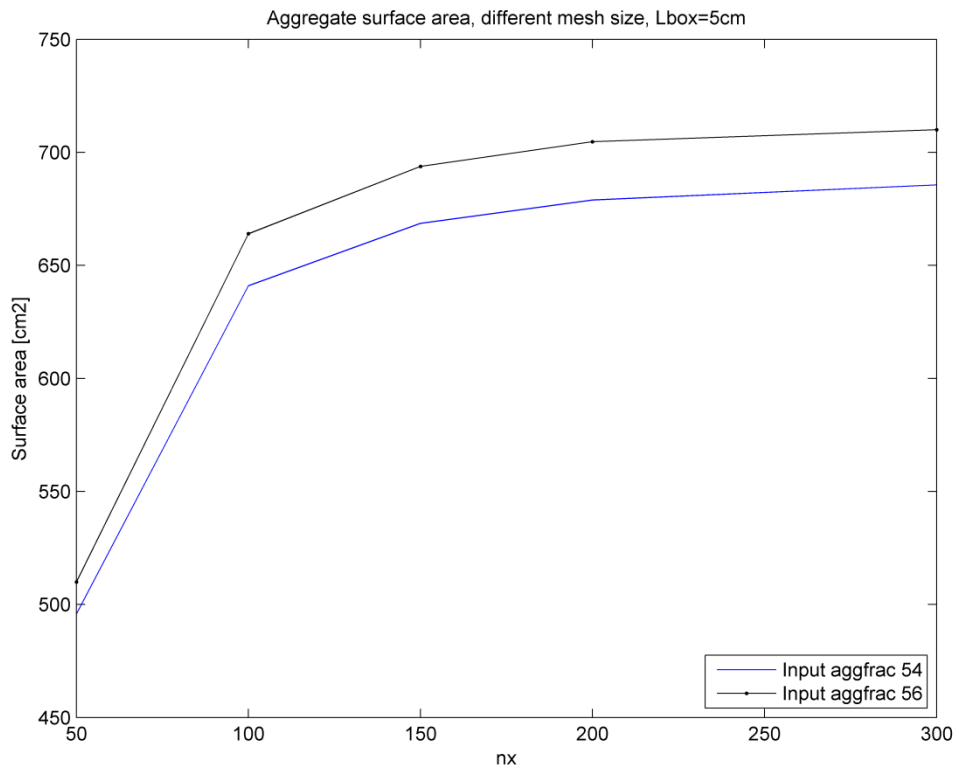


Figure 6.4 The aggregate surface area with varying mesh size.

The largest difference in aggregate fraction and aggregate surface area was between  $n_x$  equal to 50 and 100, 12 % higher respective 29 % higher for 100. Between  $n_x$  equal to 100 and 150 the difference was lowered to 2 % respective 4 %. The average stationary flux for different mesh sizes was calculated and is shown in Figure 6.5.

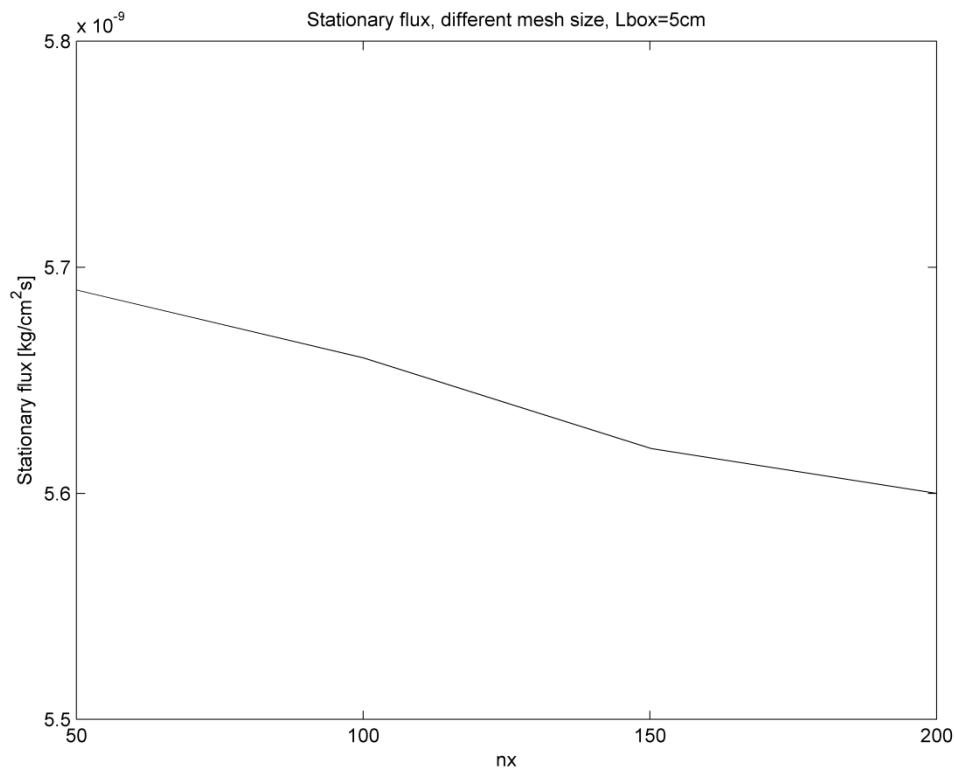


Figure 6.5 Stationary flux with varying mesh size.

The average stationary flux through the SVEs shows no big difference with different mesh sizes according to Figure 6.5. The difference between 50 and 200 is 1.5 %. This is due to the increase in blocking volume and ITZ equalize each other. Another analysis was made for the stationary flux on an SVE with  $L_{\text{box}}$  equal to 10 cm. More mesh sizes were included and in Figure 6.6 the result is shown. It can be seen that the largest change of flux is for rough mesh sizes and the profile seems to converge at  $n_x$  equal to about 100, which means mesh size of 0.1 mm.

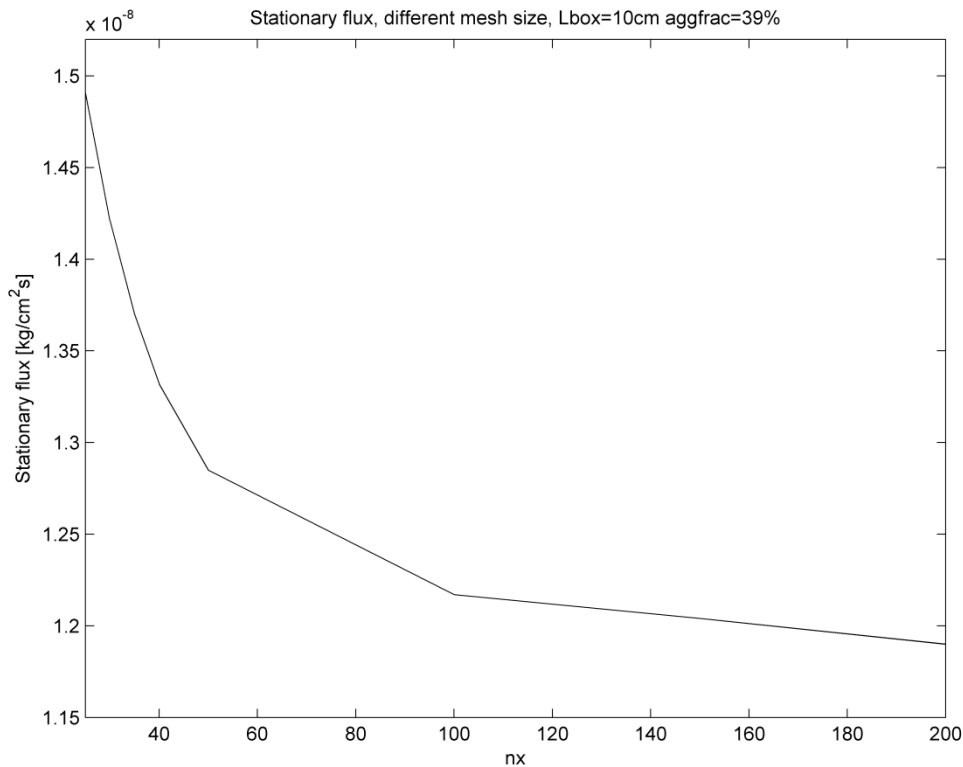


Figure 6.6 Stationary flux with varying mesh size.

The difference in profile shape between Figure 6.5 and Figure 6.6 is because the profile in Figure 6.6 is calculated from SVEs with larger span of mesh sizes. The profile in Figure 6.5 starts at  $n_x$  equal to 50 and  $L_{\text{box}}$  for that case were 5 cm. This gives the mesh size of 0.1 mm for the roughest mesh, which was the mesh size where the profile in Figure 6.6 seemed to converge.

For the transient analysis chloride profiles were compared. The same properties were used for each curve, but with different mesh size, and were made for three different times, 1 year, 14 years and 50 years. Note that the input value for  $C_s$  and the diffusion coefficient is just arbitrary values. As can be seen in Figure 6.7 and Figure 6.8 the start value for the curves is not the same for the different mesh sizes. This is because the profiles are plotted as average chloride concentration in the Y-Z plane for the specific X-value and the curves were made by SVEs created as in Figure 5.2, with cut aggregates at the boundary. This means that the chloride concentrations are mean values of 2D slices of the SVEs. When the mesh gets finer the aggregate volume increases and there will be more nodes with in-flux equal to zero, which will decrease the average chloride content in that Y-Z plane. Neglecting these boundary points the profiles for 50 years follow each other rather well.

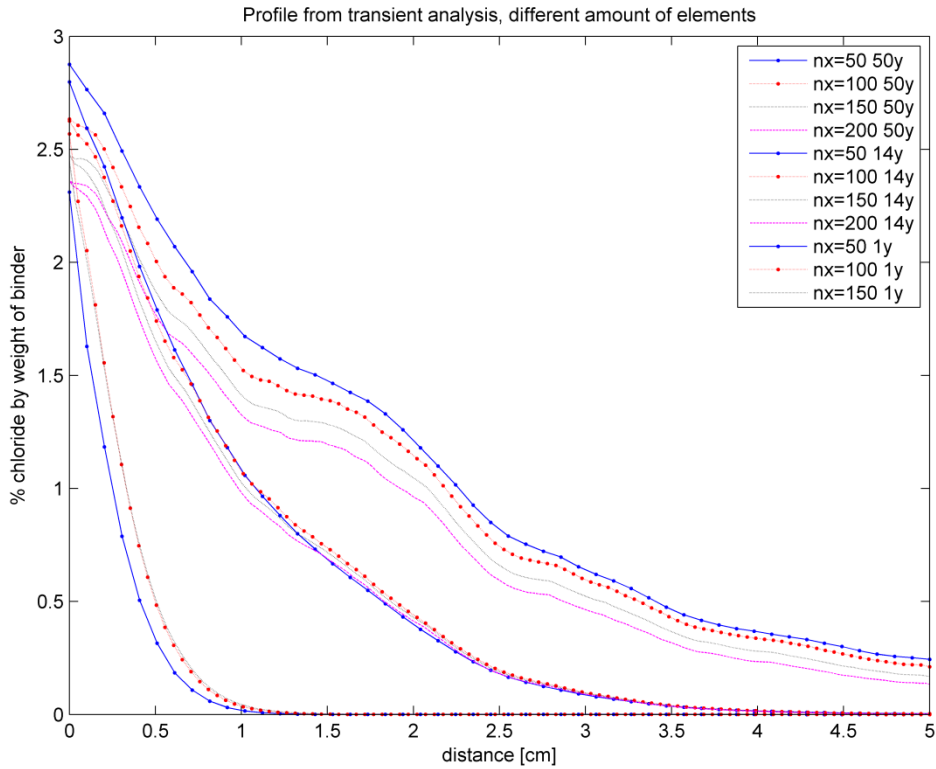


Figure 6.7 Chloride profiles with different number of elements for different years.

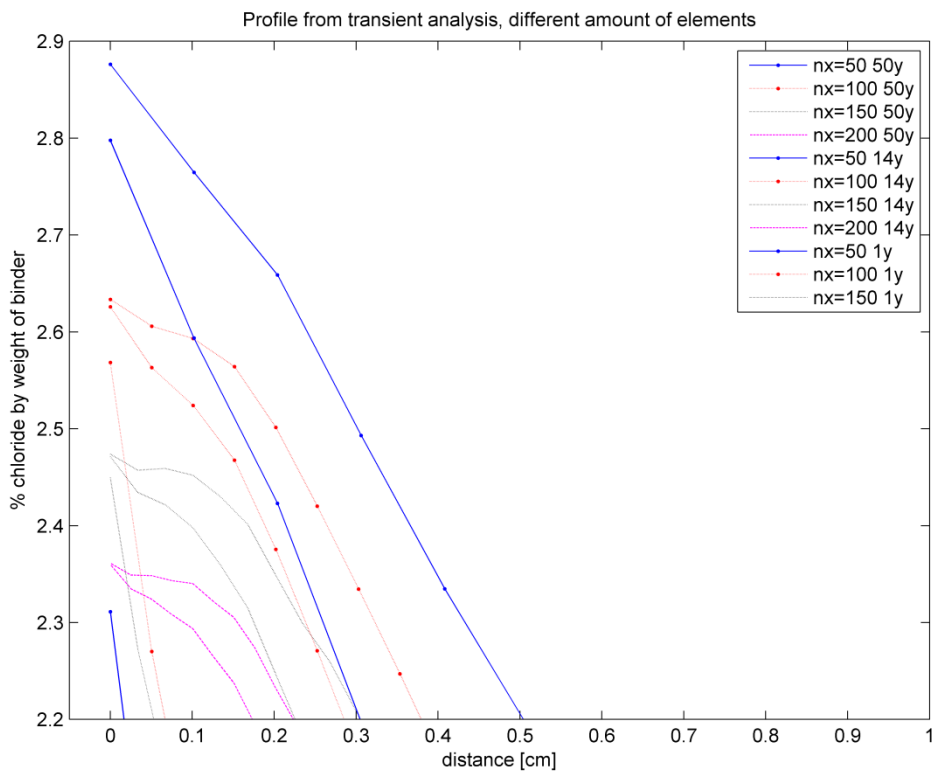


Figure 6.8 Zoomed in on the previous Figure 6.7 to show how the profiles differ close to the surface.

The code was changed and there was no longer cut aggregates at the outer surface, which resulted in that all curves had the same value in nodes in the outer surface, see Figure 6.9. It is displayed in Figure 6.10 that the flux in the transient analysis decreased when the mesh size was decreased. The difference also increased with a longer time even though the start value was the same. A reason for this could be due to the increase in volume of the aggregates for a smaller mesh size results in larger obstacles and a longer transport path for the flux. The increasing surface area, which corresponds to the ITZ, does not have the same impact on the flux as the increasing path distance. Note that the curves in Figure 6.10 is made on an SVE with size 10 cm and smallest aggregate size 4.8 mm, instead of size 5 cm and smallest aggregate 1.5 mm as in Figure 6.7. It is the same principle though.

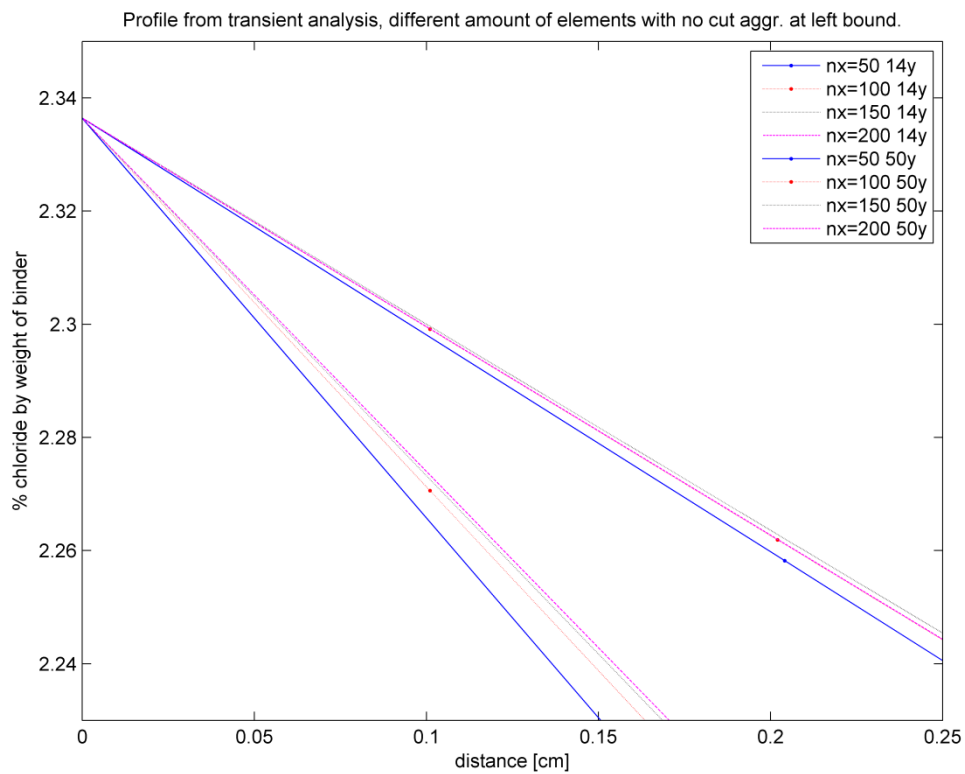


Figure 6.9 Zoomed in on Figure 6.10, profiles with no cut aggregates at the outer surface.



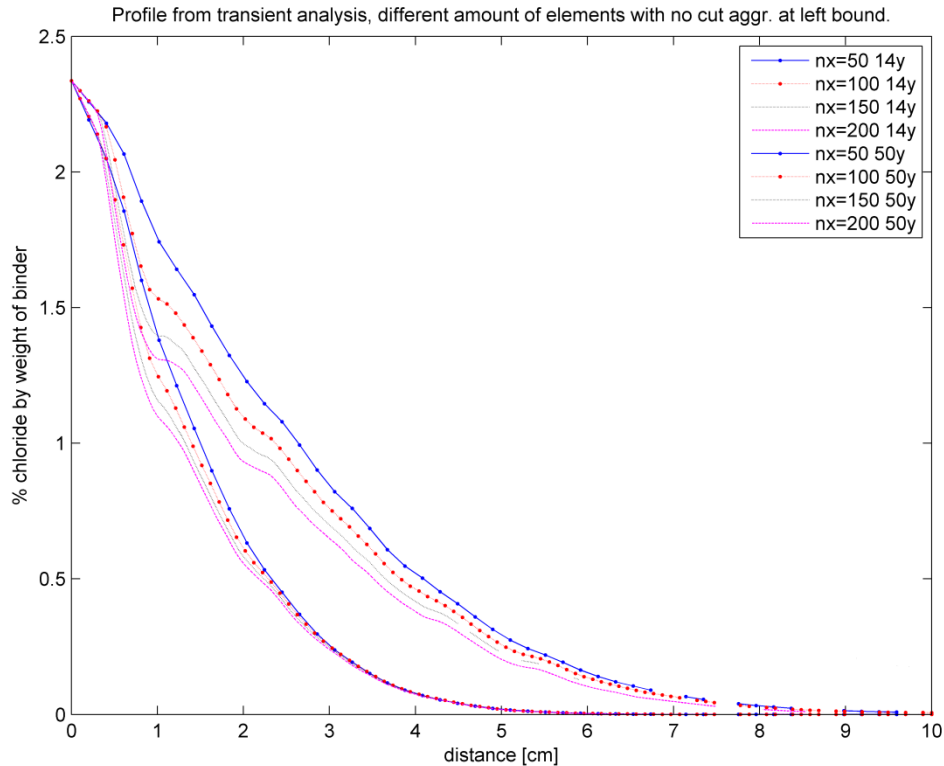


Figure 6.10 Shows chloride profiles with different number of elements for different number of years with no cut aggregates at the outer surface.

Another sound explanation why the profile decreases for a decreased mesh size would be that these chloride profiles cannot directly be translated to the flux through the SVE. It is actually the mean chloride concentration in each X-Y-plane that is plotted and for an increased aggregate volume the mean value in each plane will therefore be lower, due to that there is only chlorides in the cement paste/mortar. One could think of that the chloride concentration in the nodes that does not consists of aggregates would increase in such case, but it seems that this is not the situation or anyway the impact from this is not as large as the impact from the increasing volume. If this explanation would have been completely correct, the difference between the profiles would have been the same through the whole depth. This is not the case, the percentage difference decreases with depth. It should be noticed that the missing points in the profiles in Figure 6.10 was due to a small mathematical error in the code and this was changed later in the project.

In Figure 6.11 below, analyses with different amount of elements for the time 50 years, where made on 4 different realizations to check the variance in between different realizations. Small differences can be seen, but the profiles are similar.

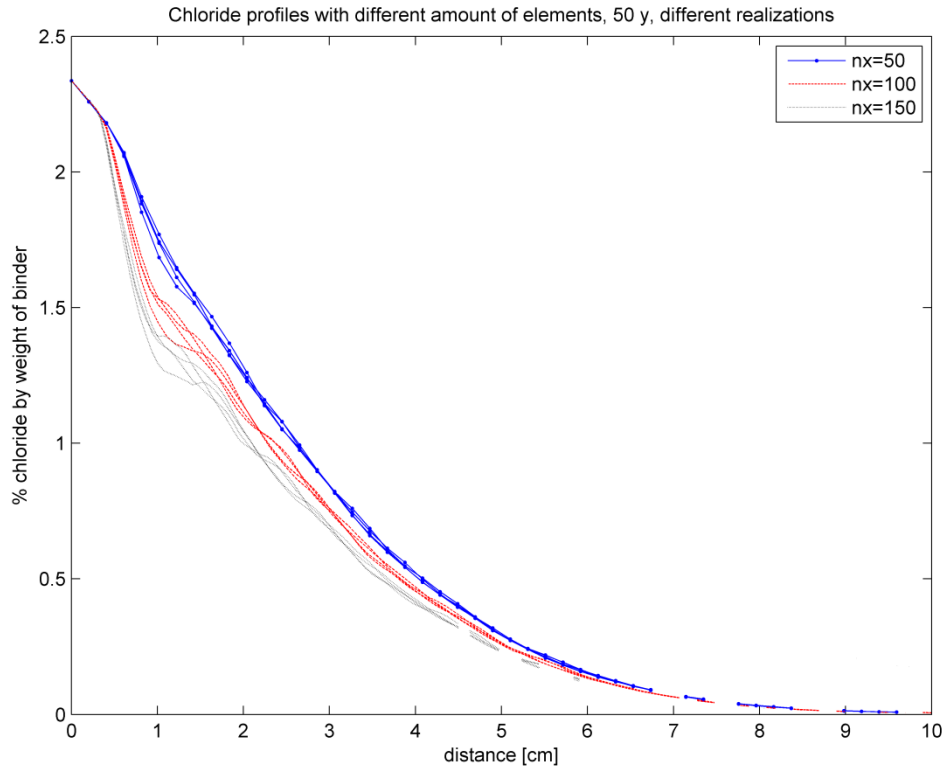


Figure 6.11 Chloride profiles for different realizations and different number of elements.

From these studies, no straight forward conclusions can be drawn about what mesh size that is correct to use. Although it is found that, a sufficiently small mesh is needed to get spherical shapes of the smallest aggregates included. The stationary flux analyses showed that for a mesh size of 0.1 mm and smaller the flux seemed to converge. The differences between various realizations with approximate the same aggregate fraction is not that big, which means it does not have large impact.

### 6.3 Influence of the size of the SVE

The size of the SVE created depends on the input parameter  $L_{\text{box}}$ , which determines the side length of the cube. This means that  $L_{\text{box}}$  also determines how deep the chloride profile predictions will be. The measurements were done on a depth up to 50 mm, but the reinforcement is located at a depth of minimum 60 mm, therefore  $L_{\text{box}}$  needs to be at least 60 mm.

Since the only surface where boundary conditions were prescribed was the outer surface, i.e. x-coordinate equal to zero, there was no flux through any other surface. One can imagine an SVE as a closed box with only one of the six surfaces open. It is possible in the model to define boundary conditions on other surfaces as well but due to the difficulties in defining the ambient concentration outside these surfaces this was not made. The surfaces perpendicular to the outer surface will have some, but not very large impact on the resulting profile, but the inner surface parallel to the outer surface will act as a wall and keep all chlorides from leaving of the box. This does not correspond to reality as the concrete structure is much larger than the concrete cover of 60 mm and the chlorides should have the possibility to move further. A solution for this is to make an  $L_{\text{box}}$  large enough to give a value of the chloride concentration close

to zero at the inner surface. A chloride concentration close to zero means that basically no flux would appear further than that slice anyhow.

To get an estimation of how large the SVEs need to be, transient analysis were done on an SVE containing no aggregates see Figure 6.12. A curve was first fitted to the measurements from the Bakkasund Bridge at 14 years. Then SVEs of different sizes were created and the time was increased to 100 years. Curves of the transient analysis for 100 years with different values of  $L_{\text{box}}$  are shown in Figure 6.12 together with the measurements and the fitted curve after 14 years. From Figure 6.12 it can be seen that the fitted curve is on the safe side. Overestimations for the profiles with the time 100 years in  $L_{\text{box}} = 5 \text{ cm}$  and  $L_{\text{box}} = 7.5 \text{ cm}$  can be seen. There is also a small deviation between the profile with  $L_{\text{box}} = 10 \text{ cm}$  and  $L_{\text{box}} = 15 \text{ cm}$ . The chloride concentration from the estimation at 100 years at 10 cm is 0.0062, thus the amount of chlorides that are hindered at the border at 10 cm is small and would not affect the results very much. From these analyses the size of the SVEs were chosen to 10 cm for further studies. An SVE of 10 cm also covers both the depth of the measurements, 5 cm, and the depth of the reinforcement, 6 cm. The depth of the reinforcement would have been the deciding part if the profile would not have been overestimated.

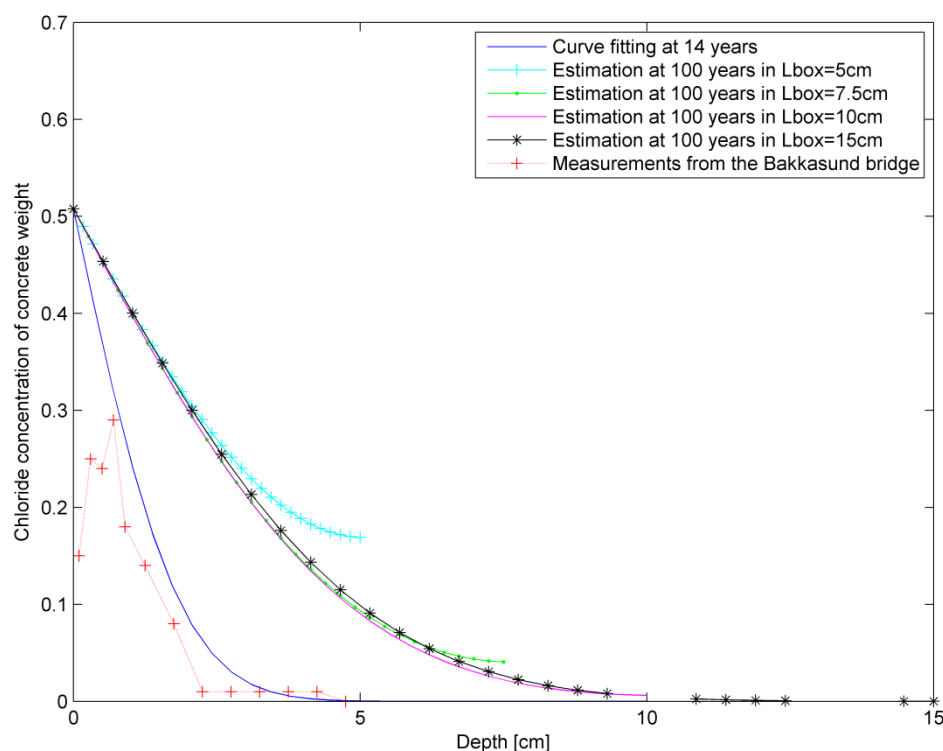


Figure 6.12 Chloride profiles for different sizes of  $L_{\text{box}}$  after 100 years together with measurements and curve fitting at 14 years.

## 6.4 Boundary conditions

The boundary condition in the FE-model is applied as Newton's convection boundary condition, equation ( 6-1 )

$$q_n = \alpha(c_s - c_\infty) \quad (6-1)$$

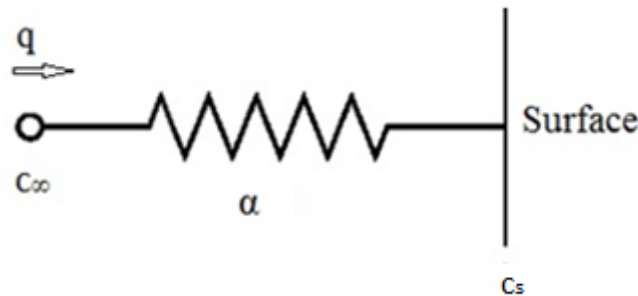


Figure 6.13 Describing how the boundary conditions are implemented in the model.

In Ottosen and Petersson (1992), the potential difference in equation ( 6-1 ) is specified as temperature difference, but it is analogical for chloride concentration. This convective boundary condition contributes both to the stiffness matrix and the boundary force vector in the FE-model. In this FE-model input values for both the convective coefficient and the ambient chloride concentration should be specified and are evaluated further in Section 6.4.1 and Section 6.4.2.

Variables in equation ( 6-1 ):

$q_n$	Flux through the boundary with the unit normal vector, $n$ , $\left[ \frac{kg}{m^2s} \right]$
$\alpha$	Convective coefficient, $\left[ \frac{m}{s} \right]$
$c_s$	Chloride concentration at the surface, $\left[ \frac{kg}{m^3} \right]$
$c_\infty$	Ambient chloride concentration, $\left[ \frac{kg}{m^3} \right]$

In Section 2.4 the chloride surface concentration,  $C_s$ , was evaluated and it was concluded that this value varies depending on many factors. In the FE-model the chloride surface concentration is defined as the value in the first node, i.e. the value exactly at the surface, see variable  $c_s$  in Figure 6.13. In Appendix B hand calculations are shown how the ambient chloride concentration was implemented in the FE model.

### 6.4.1 Influence of the ambient chloride concentration

The ambient chloride concentration depends on environmental conditions. In marine environment this condition varies depending on the location of the surface. If it is submerged the ambient value is close to constant, i.e. the chloride concentration in the sea water. For splash zone and atmospheric zone, this value is more complicated to specify. It varies according to weather condition and season.

It might be reasonable to assume a constant average ambient chloride concentration for a specific location. In Burn (2002) there were intentions on how to model the ambient chloride concentration in other environments than submerged. Proposals were made according to a statistic normal distribution function, for description of the annual chloride concentration. There are still difficulties to rely on these models though, why it might be most practical and due to simplicity, to use a constant average value, which is curve fitted to the measurements.

#### **6.4.2 Influence of the convective coefficient and tolerance in calculations**

The convective coefficient describes the resistance for the chloride ions to move from the ambient environment to the surface. No confident measurements or experiments were found where the convective coefficient has been studied for chloride movement.

Analyses were made on how varying convective coefficient affect the chloride ingress profile at a certain diffusion coefficient. In Appendix D figures are shown with different diffusion coefficients but with same relations to the convective coefficient. From these figures it can be concluded that the magnitude of the diffusion coefficient does not have any impact as long as the relation between the diffusion coefficient and the convective coefficient and time is the same. In the beginning of the analyses, the influence of the tolerance in the calculations was not found yet and therefore profiles which stopped in early iterations were obtained. The figures in Appendix D still holds for their purpose; to show that it is the relation between the diffusion coefficient and the convective coefficient that is important and not the magnitude.

The most realistic behaviour for chloride transportation through the surface boundary is that for a low resistance a large amount of chlorides should be transported from the ambient to the surface and the opposite for a high resistance. It is also most reasonable to obtain the profile with highest chloride concentration from the highest convective coefficient. In each time step the model iterates until the results are within a certain given tolerance. If the given tolerance is too large the model will stop the iterations further away from the result where it is completely in equilibrium. If the given tolerance instead is very small it will find a result very close to the equilibrium but with a large number of iterations and high cost of computational power.

In order to evaluate how the tolerance influences the results, analyses were made with a diffusion coefficient of  $1 \cdot 10^{-8}$  [ $cm^2/s$ ] and with a convective coefficient of  $1 \cdot 10^{-2}$  [ $cm/s$ ] and varying tolerance. The default tolerance of  $1 \cdot 10^{-6}$  was used in the first analyses, which resulted in that the iterations stopped. In Figure 6.14 it can be seen that a decrease in the tolerance gives room for more iterations and clearly affects the chloride profile. For a decreasing tolerance the results will eventually converge.

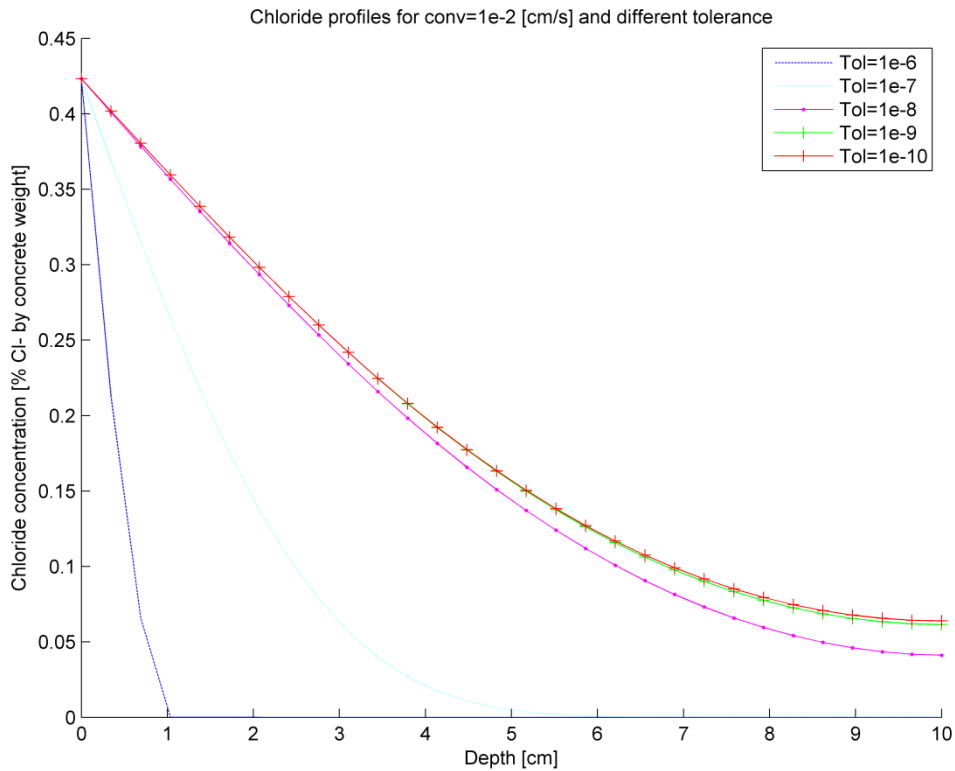


Figure 6.14 Chloride profiles with a constant convective coefficient and diffusion coefficient and varying tolerance.

The same calculations were done for another value of the convective coefficient, the results can be seen in Figure 6.15. The results are very similar to those in the previous figure, but for another range of tolerance.

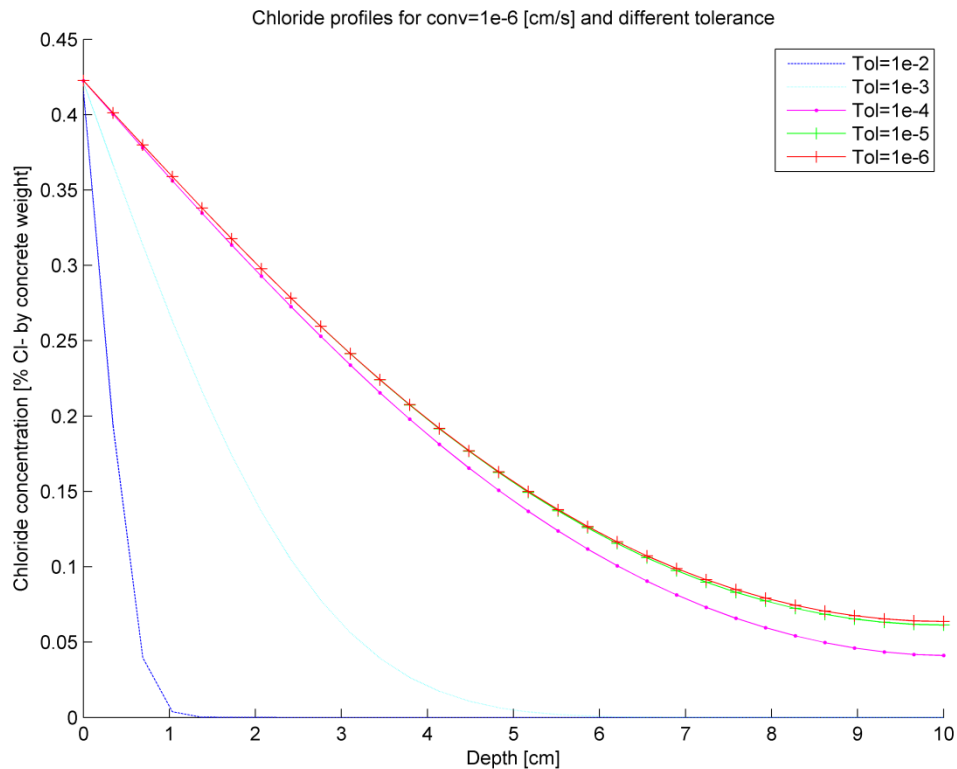


Figure 6.15 Chloride profiles with a constant convective coefficient and diffusion coefficient and varying tolerance.

From these figures it can be seen that the tolerance is very important to account for to get correct results. In Figure 6.16 the convective coefficient was varied with a tolerance of  $1 \cdot 10^{-10}$ . It was previously checked that a tolerance of  $1 \cdot 10^{-10}$  was enough for a convective coefficient of  $1 \cdot 10^{-2}$  and then also enough for lower convective coefficients. From Figure 6.16 it can be seen that a low convective coefficient gives a high resistance and a lower curve. As the convective coefficient increases the resistance will be so small that it will eventually almost not make any difference ( $1 \cdot 10^{-2}$  to  $1 \cdot 10^{-7}$  are on top of each other), and that feels reasonable. The point when the convective coefficient stops to influence the results seems to be when it grows a lot larger than the resistance on the other side of the node, i.e. the nodes for the elements in the concrete, in this case is the diffusion coefficient equal to  $1 \cdot 10^{-8} \text{ cm}^2/\text{s}$ .

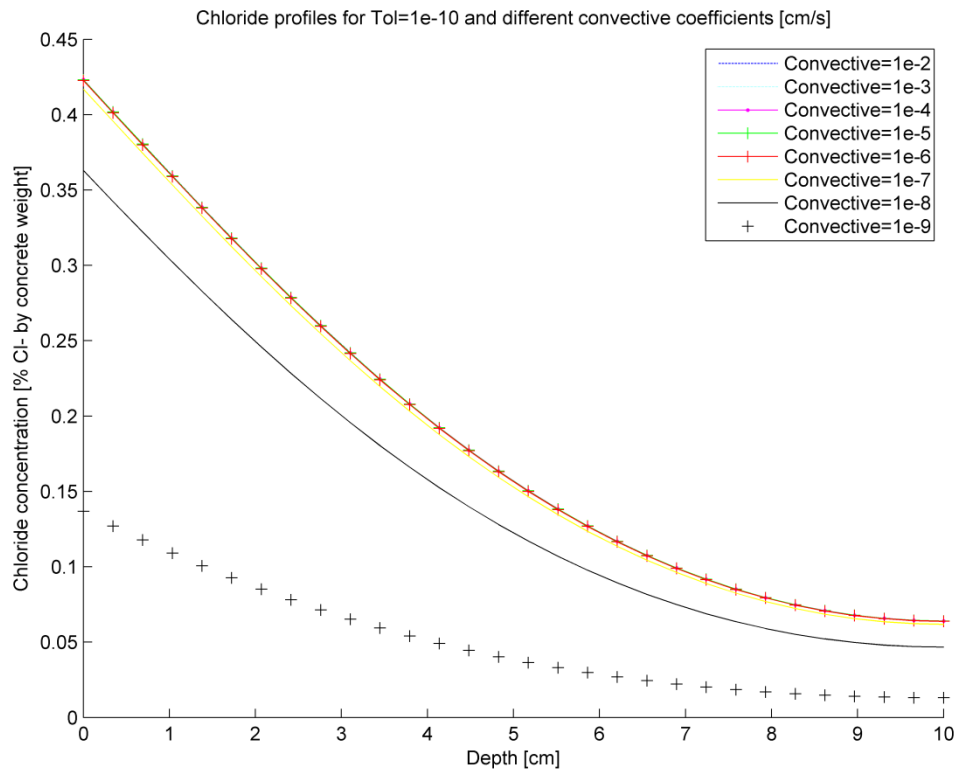


Figure 6.16 Chloride profiles with a constant tolerance and diffusion coefficient with varying convective coefficient.

Some concluding remarks could be drawn from this. Right now it is hard to calibrate the value of the convective coefficient with data that is available from the Bakkasund bridge. Instead the aim could be to use a convective coefficient that gives a stable value almost as the prescribed ambient one. In order to do that, the convective coefficient should be high enough, to not significantly influence the profile. Figure 6.14 and Figure 6.15 show that the choice of tolerance is important for different relations between convective coefficients and diffusion coefficients and Figure 6.16 at what magnitude the convective coefficient stops to influence the result. The relation between the diffusion coefficient and the convective coefficient where the influence is insignificant is around 10 times the diffusion coefficient (the diffusion coefficient for the profiles in Figure 6.16 is  $1 \cdot 10^{-8} \text{ cm}^2/\text{s}$ ).

Swatekititham (2001) describes a model which simulates the chloride ion movement in the surface layer of concrete. The concept is that the chloride ions move by adsorption and diffusion. The movement by adsorption is always going inwards while the movement by diffusion is controlled by the concentrations at the different layers. This could be a part of the physical behavior that the convective coefficient should try to capture.

### 6.4.3 Influence of the chloride binding capacity

In Section 2.3 the chloride binding capacity was introduced and the physical and chemical reactions which take place were described. Further the importance of the chloride binding capacity was explained and in the end a relationship between free chloride concentration and chloride binding capacity was proposed. This chapter



describes how the chloride binding capacity was used in the 3D model and some effects that were needed to be considered.

In the 3D FE model the chloride profile is calculated by

$$C \cdot \dot{a} + K \cdot a = f \quad (6-2)$$

where

<b><i>C</i></b>	Storage matrix depending on chloride binding capacity
<b><i>K</i></b>	Resistance matrix
<b><i>f</i></b>	Force vector
<b><i>a</i></b>	Solution vector, free chloride concentration in each node.

Equation ( 6-2 ) is calculated for each time step and it is also iterated several times to get a solution vector within a certain tolerance. Efforts were made trying to include a varying binding capacity according to the relation in Figure 2.5. A new binding capacity was calculated according to Equation ( 2-5 ) for each element for each new time step by use of the previous time step's solution vector. The chlorides that were not bound, the solution vector ***a***, were at each time step multiplied with the binding capacity to get the total amount of chlorides. Problems occurred though when this method was tried to be implemented. If the solution from the previous time step should be used as initial values for the present time step, the step size needed to be small for accuracy. This results in heavier and more time consuming computations. Convergence problems also occurred when the step size was decreased too much.

Figure 6.17 shows the problem with varying binding capacity, when a too large step size is used. For the same actual time, the profiles are different depending on the step size.

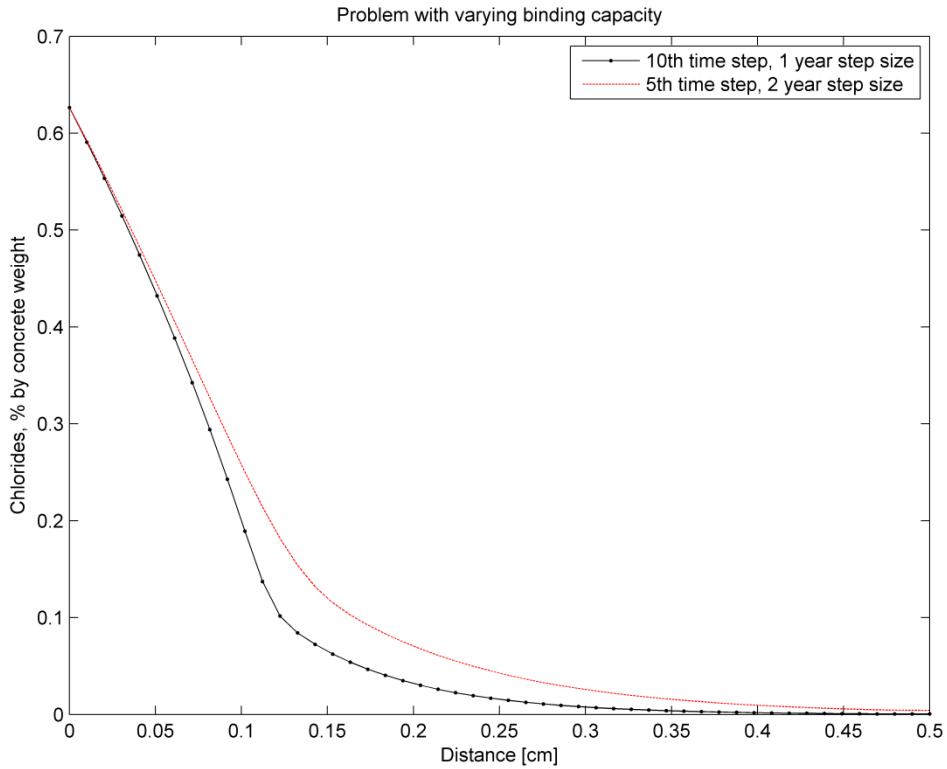


Figure 6.17 Problem with too large step size, when varying binding capacity is used.

Due to the problems by introducing the varying chloride binding capacity, a constant value was decided to be used instead. This was made for the estimation of the chloride ingress at the Bakkasund Bridge at the service life of 100 years, see Chapter 7.

Figure 6.18 below shows the effect of different constant binding capacities on the chloride profiles. The other properties are the same for the different curves and arbitrary. Both free and total amount of chlorides are shown, where the low curves represent the free chlorides and the higher represent the total amount of chlorides. It can be seen that for a low binding capacity there will be rather low total chloride concentration at the surface, but the curve will be flat in comparison to a higher binding capacity, where there will be a high concentration at the surface but the curve will be steeper.

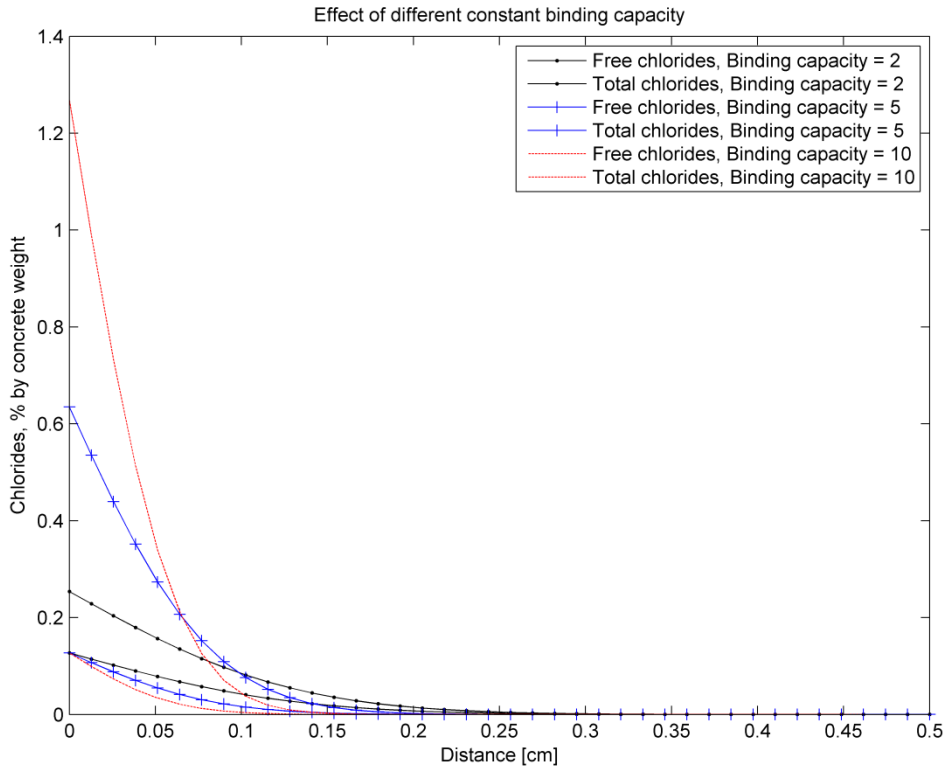


Figure 6.18 Profiles with different constant binding capacity

#### 6.4.4 Comments on the chloride binding capacity

An assumption of a constant binding capacity has been done by Liang et al. (2010) and the proposal is that the bound chlorides should be twice as many as the free chlorides, but since the binding capacity varies both with time and with the free chloride concentration, this is a rough approximation. One question is how large error the approximation of a constant chloride binding would give. Also, if implementing a varying chloride binding capacity, the question is how well known the varying binding capacity for the concrete in the Bakkasund Bridge actually is.

If varying chloride binding capacity should be used and it uses the solution vector of the free chloride concentration from the last time step to calculate the present binding capacity, it gives a too high binding capacity. This is because of the “lagging” effect when the previous solution is used. One solution to this is to decrease the step size which gives higher accuracy, but as mentioned, convergence problems occurred when trials of this was made. Another solution is to make iterative calculations for the binding capacity within each time step, but this would make the program heavier. Also, if one binding capacity is calculated for each time step and for each element, from the previous step’s free concentration, the program becomes much heavier than if a constant binding capacity was used.

Another thing to consider, when including varying binding capacity, is the maximum binding capacity. In elements where the free chloride concentration is close to zero the chloride binding capacity goes to infinity which causes troubles in the calculations. If the binding capacity is too high the model needs more iterations to solve the equations. The maximum number of iterations that the model does can be

chosen but if the iterations needed are a high number, it will result in long computational time.

Also, if varying chloride binding capacity is implemented in such way it uses the previous time step's solution, the first time step needs to be specified in the model because no solution vector exists for the first time step. It is difficult to know what the binding capacity is for the first time step, but most reasonable would be to specify a large value due to the fact that the binding capacity is high for low free concentrations, see Figure 2.5, but is dependent on the step size. As it was done in the trials in this project, all elements were given the same binding capacity for the first time step which is an approximation. Instead, estimations of the chloride profile after the first time step could be done and further calculate different binding capacities for each element for the first time step.

For further work recommendations would be to use a numerical iterative method within each time step to obtain the present binding capacity for each element. It gives a heavier model than if just the previous step's solution vector is used, but a more accurate result. But still, the relation between free and total chlorides in this thesis has only been verified in submerged conditions, by Tang (2008). In other conditions such as "splash" and "atmospheric" the relation might differ.

#### **6.4.5 Influence of the time**

One of the input parameters that there was good information about was the time. The bridge was constructed in 1999 and the measurements of the chloride ingress were taken in 2013, 14 years later and the lifetime should be at least 100 years. In all calculations where the time was of importance it was set to either 14 or 100 years. But one could argue that it is not really correct. The time could be interpreted as for how long time diffusion is taking place in the concrete, and that is not the same as the total time. Especially not on the surface which is sometimes dry and sometimes wet. A shorter time could be used for the analysis, but further in the concrete, diffusion probably occurs constantly, because it does not have time to dry out. Instead, it is assumed that the diffusion coefficients take care of the dry periods through curve fitting with the measurements which are created with the natural variation of wet and dry cycles.

The time step size has to be specified in the transient analyses. On one hand greater step sizes are preferred to give shorter calculation time. On the other hand shorter step sizes give more accurate results. An analysis was made to check the influence of the step size, see Figure 6.19. Transient analyses on an SVE with only cement paste for the total time 100 years were made with four different step sizes. Step size equal to 1 year, 10 years, 25 years and 100 years, which gave the number of steps equal to 100, 10, 4 and 1. It can be seen that only the profile with one time step deviates a lot. A constant binding capacity was used.

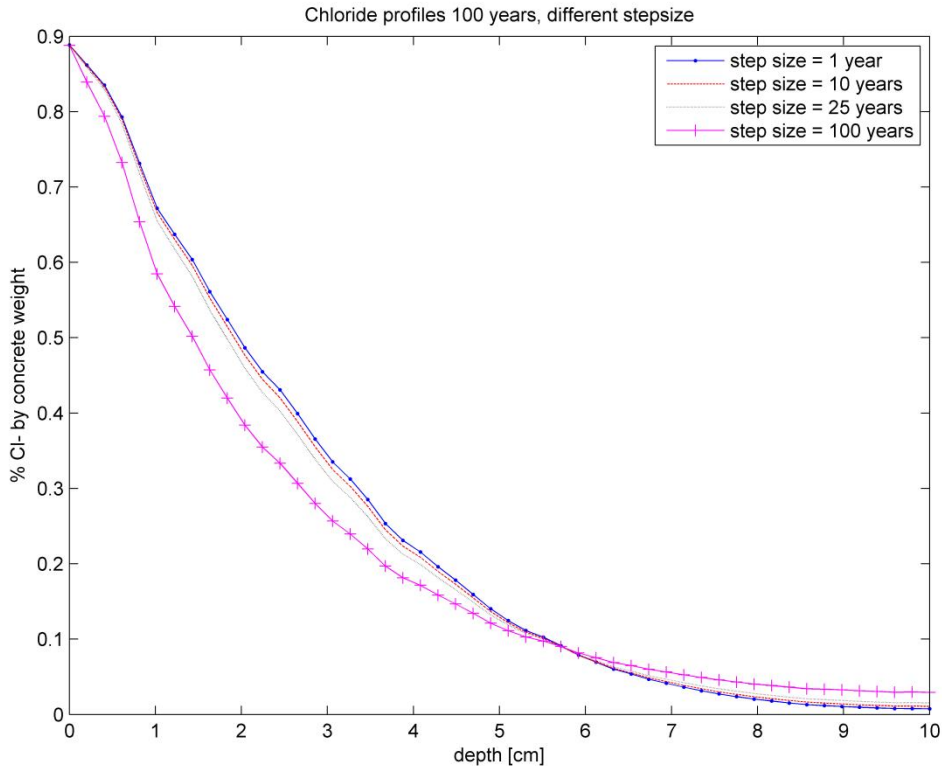


Figure 6.19 Influence of step size

## 6.5 Diffusion coefficients

In the model the diffusion coefficients should be specified for the three different phases, cement paste, aggregates and the ITZ. The diffusion coefficients for the aggregates are assumed to be zero due to its extremely low permeability in comparison to the mortar. For the cement paste/mortar and the ITZ the values may vary in different concrete types with different properties.

The diffusion coefficient of the cement paste/mortar was discussed in Section 2.5, where analytical formulas were found in the literature. However, for the 3D FE model, the diffusion coefficient was calibrated in such way it fitted the measurements, which could be done in various ways, see Chapter 7.

It is not the diffusion coefficient of “pure” cement paste that should be used as input in the model; it should instead represent the mortar with cement paste and the small aggregates that are too small to be included in the model as aggregates. The aggregates below the specified size limit were assumed to be included in the cement paste/mortar and therefore these aggregates contribute to the effective diffusion coefficient of the paste. The ratio between the blocking volumes of the aggregates in comparison to the aggregate surface area which corresponds to the permeable ITZ is of interest for the aggregates not included. For small aggregates the surface area will be high in comparison to the blocking (impermeable) volume relative larger aggregates.

The diffusion coefficient of the ITZ was discussed in Section 2.6, where the thickness of the zone was found to approximate 15-50  $\mu\text{m}$  and the diffusivity to about 10-15

times the diffusion coefficient of cement paste. The varying thickness and diffusivity of the ITZ is commonly modeled by a constant thickness and diffusion coefficient  $c_f$ . Garboczi and Bentz (1996), which was also done for the 3D FE model in this project. The influence of the ITZ is set as the product of the diffusion coefficient times the thickness of the ITZ. In the FE model the SVE is divided in equally sized finite elements (cubes) and for the elements located at the surface of the aggregates, the ITZ layer is applied as a “plate” with an area which is the element size in square and with the specified thickness. This “plate” is rotated in the element according to the normal of the plate related to its location on the analytical spherical aggregate, Nilenius (2014). This means that for smaller mesh sizes, the shape of the ITZ (or the surface of the aggregate) will approach the analytical spherical shape.

An analysis was made on an SVE with all properties constant except the ITZ properties. Five different profiles were obtained were the thickness and the diffusivity of the ITZ were varied, see Figure 6.20. It is displayed how the profile with the highest effective diffusion coefficient of the ITZ (diffusivity times the thickness) is highest and the opposite way around. However, on this SVE (which resembles the concrete from the Bakkasund Bridge) with aggregate fraction of about 39 %, the difference between the profiles is not very large, with this span of property variation. The variation was chosen to the span found in the literature as was described in Section 2.6.

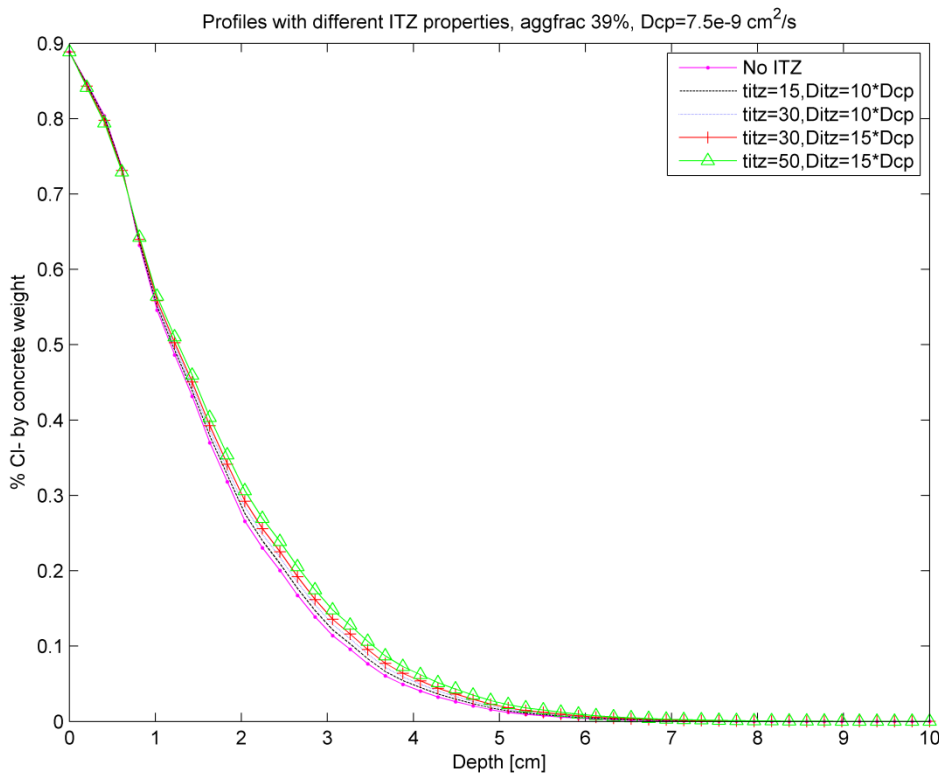


Figure 6.20 Test of ITZ properties, same SVE and cement paste properties as Figure 7.2.

## 6.6 Comparison between homogeneous and heterogeneous modelled concrete

Transient analyses were made on an SVE with 37 % aggregate fraction with different amount of elements and the profiles are shown in Figure 6.21. Then, stationary analyses were made to obtain the effective diffusion coefficient,  $D_e$ . The different  $D_e$  was then used on SVEs with homogeneous concrete as can be seen in Figure 6.21.

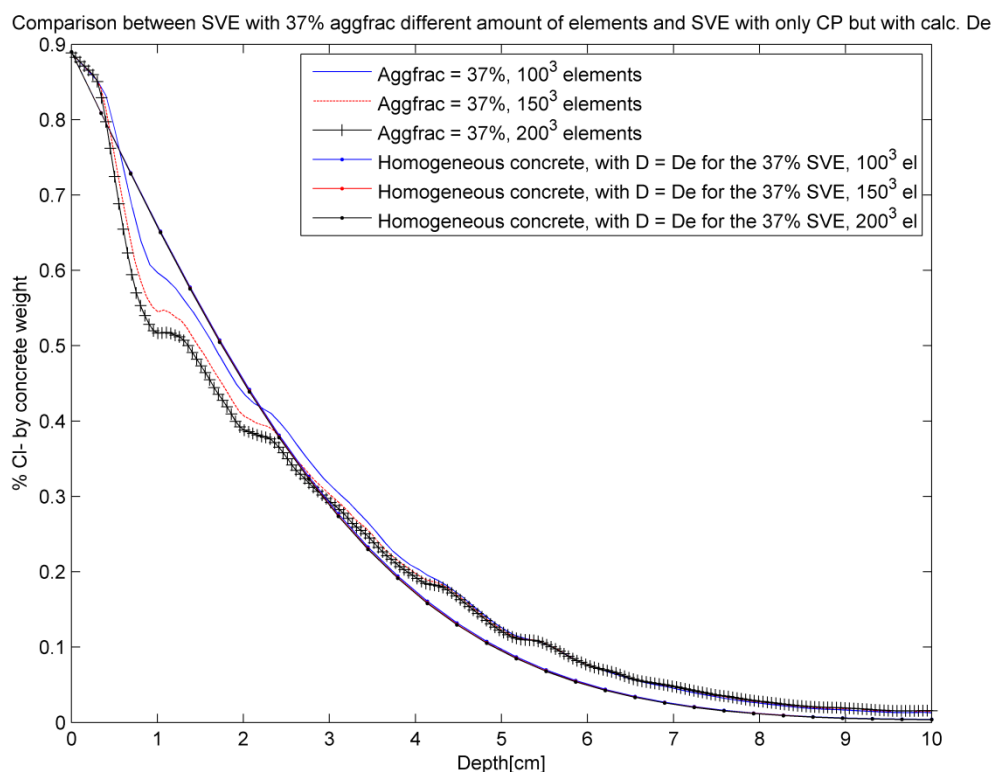


Figure 6.21 Comparison between homogeneous and heterogeneous modelled concrete

The values of  $D_e$  was smaller for denser mesh, but was very close to each other, why it seems like there is only one curve for the homogeneous concrete. What was interesting was that by modelling the heterogeneity of the concrete, the chloride profile gets slightly higher than if only a homogeneous concrete would have been modelled with the calculated  $D_e$ .

The same constant chloride binding capacity was used in all the analysis but a reason for the difference between the homogeneous and heterogeneous concrete might still be due to the chloride binding. Since aggregates do not bind any chlorides the chloride binding capacity per volume will be lower including aggregates and a lower binding capacity gives higher flux. This can be important when modelling chloride ingress with heterogeneous concrete. The difference at the depth of the reinforcement, 6 cm, with a binding capacity of 7.78 is about 50 %, see Figure 6.21, which is a significant difference. The difference should increase with increasing chloride binding capacity and decrease with decreasing chloride binding capacity. This because with a lower binding capacity, the binding capacity per volume does not change as much when aggregates are included as if the binding capacity is higher.

## 6.7 Constants in the FE model

The chloride binding capacity influences the apparent diffusion coefficient over time and it also influences the total amount of chlorides at the surface. This means that it should exist some relationship between these three parameters.

When performing various analyses a relationship between the parameters was noticed and that is mathematically shown in this chapter.

Starting from the FE- formulation:

$$\Phi \int \mathbb{N}^T \mathbb{N} dV * \dot{\mathbf{C}}_f + D \int \mathbb{B}^T \mathbb{I} \mathbb{B} dV * \mathbf{C}_f + \alpha \int \mathbb{N}^T ds * \mathbf{C}_f = \alpha \mathbf{C}_\infty \int \mathbb{N}^T ds \quad (6-3)$$

where

$\Phi$	Chloride binding capacity
$\dot{\mathbf{C}}_f$	Free chloride concentration
$\alpha$	Convective coefficient
$\mathbf{C}_\infty$	Ambient chloride concentration

$$\mathbf{C}_{tot} = \Phi * \mathbf{C}_f \Rightarrow \mathbf{C}_f = \frac{\mathbf{C}_{tot}}{\Phi} \quad (6-4)$$

Replace  $\mathbf{C}_f$  in equation ( 6-3 ) with equation ( 6-4 ) and if  $\Phi$  is not time dependent, it can be put outside of the integral.

$$\frac{\Phi}{\Phi} \int \mathbb{N}^T \mathbb{N} dV \dot{\mathbf{C}}_{tot} + \frac{D}{\Phi} \int \mathbb{B}^T \mathbb{I} \mathbb{B} dV \mathbf{C}_{tot} + \frac{\alpha}{\Phi} \int \mathbb{N}^T ds \mathbf{C}_{tot} = \alpha \mathbf{C}_\infty \int \mathbb{N}^T ds \quad (6-5)$$

Which means that for the equation to always give the same answer, the following conditions needs to be fulfilled.

$$\frac{D}{\Phi} = constant_1 \quad (6-6)$$

$$\frac{\alpha}{\Phi} = constant_2 \quad (6-7)$$



$$\alpha C_{\infty} = constant_3 \quad (6-8)$$

If  $\alpha$  is constant the three conditions can be cut down to two as follows.

$$\frac{D}{\Phi} = constant_1 \quad (6-9)$$

$$\Phi C_{\infty} = constant_4 \quad (6-10)$$

The conclusion is that no matter which values that are set for the three parameters above to get a certain curve, the results will be the same for any time, provided that the convective coefficient is so large that the resistance at the surface is negligible. This means that if the results are fitted to the measurements, it is then of no importance which values are set for the three variables above. And since the error function model solves the same equation it is also valid for the error function model. Notice that these expressions only hold for linear FE-analyses.

## 6.8 Comparison between FE model and analytical models

In this chapter comparisons are done between the analytical models and the mesoscale model. A first comparison is between the Simple error function model and the mesoscale model. The analysis was done with the same diffusion coefficient, time and chloride surface concentration. The chloride binding capacity was set to one in the mesoscale model and the aggregate fraction was set to zero, which means a homogeneous material. Figure 6.22 shows that the results are almost the same, as could be expected. Even if the mesoscale model solves the problem in a different way it still gives the same result. These results also confirm that a chloride binding capacity of 1 is built into the error function, meaning that no chlorides are bound.

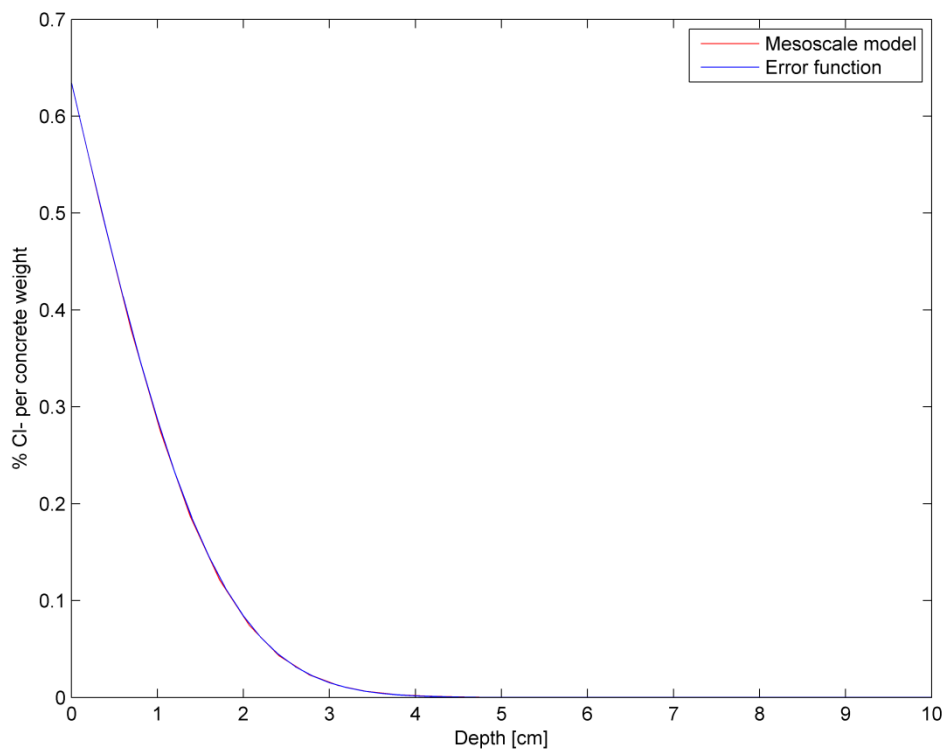


Figure 6.22 Chloride ingress with the mesoscale model and the error function.

Next comparison was made between the DuraCrete model and the mesoscale model. In Figure 6.23 the DuraCrete model was used to estimate the chloride ingress after 14 years and 100 years. Then the same apparent diffusion coefficient was used for the mesoscale model for analysis after 14 years and 100 years and did in the same way as the previous Figure 6.22 give very similar results. Also analyses were made with the same apparent diffusion coefficient as for 14 years but for 100 years with the mesoscale model. Figure 6.23 shows that a constant diffusion coefficient gives much higher concentrations than a varying one and even if that assumption is very wrong the results are still on the safe side.

$$D_0 k \left( \frac{t_0}{t} \right)^n \rightarrow D_{App} \quad (6-11)$$

where

$D_0$	Diffusion coefficient at $t_0$
$t_0$	Time when $D_0$ is measured
$t$	Actual time
$D_{App}$	Apparent diffusion coefficient
$k$	Coefficients from equation ( 4-4 )

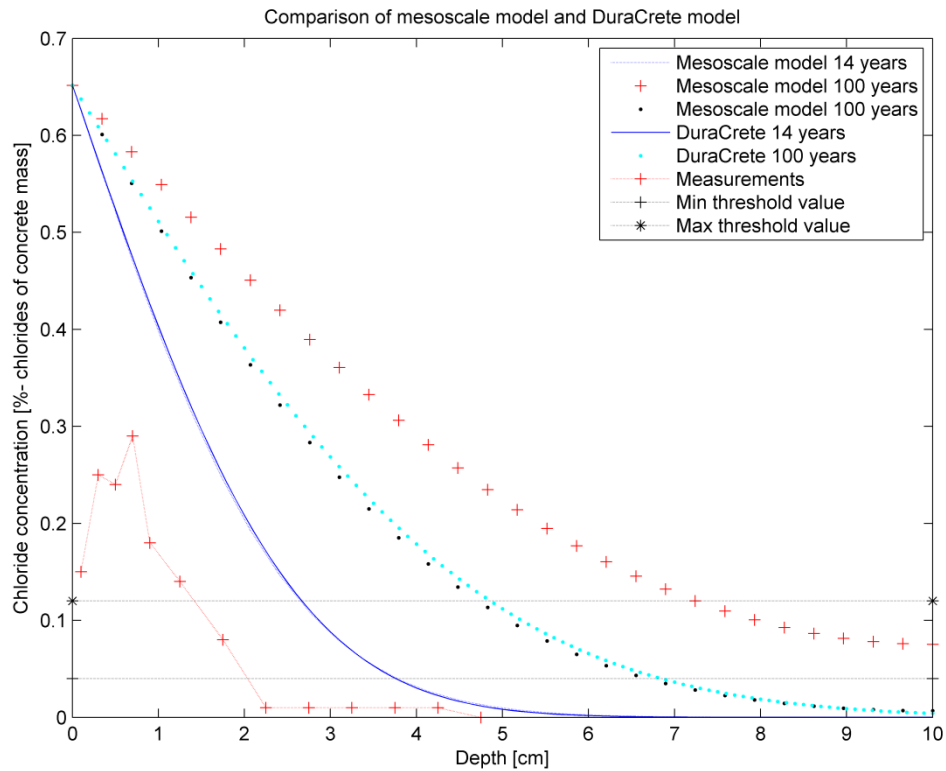


Figure 6.23 Chloride ingress from analysis with the mesoscale model and the DuraCrete model after 14 and 100 years.

The ClinConc model differs between free and bound chlorides and includes a varying chloride binding capacity. Comparing those models under submerged conditions and for concrete with 5 % silica fume the ClinConc model gives slightly higher results for times over about 5 years, Tang, et al. (2012).

## 7 Estimation of the corrosion risk

The Norwegian Public Roads Administration wanted information about the risk of corrosion for the reinforcement at the Bakkasund Bridge at the service life of 100 years. Input values were chosen such that the chloride profile fitted to the measurements in splash zone at 14 years and then analysis with same properties were made, but for the time 100 years. As described in Section 2.3 the chloride binding capacity has a non-linear behaviour and trials were made for application of this in the model. Due to uncertainties in the results with the non-linearity implemented, it was decided to use a constant binding capacity instead when estimating the chloride ingress. This constant was chosen to be the secant of the binding capacity curve, see Figure 7.1. The slope of the secant, i.e. the constant binding capacity, depends on the assumed maximum free chlorides that are in the pore-system. To display the influence of the difference, a rather large span was chosen for the maximum free chlorides; 18 g/l, 6 g/l, 2 g/l to 0.5 g/l.

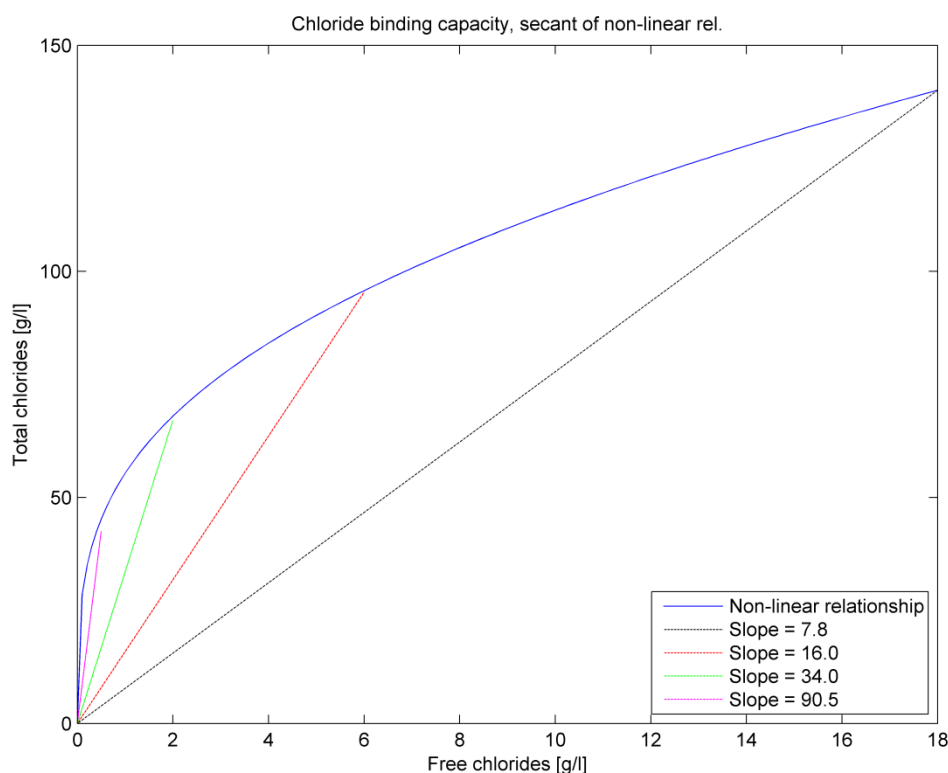


Figure 7.1 Chloride binding capacity as secant of the non-linear relationship between free and total chlorides.

These maximum free chlorides in the pore-system were taken as the ambient chloride concentration. Estimations were made with the ambient chloride concentration equal to 18 g/l, 6 g/l, 2 g/l and 0.5 g/l and with corresponding binding capacity equal to 7.8, 16.0, 34.0 and 90.5 shown in Figure 7.2 to Figure 7.5. In Figure 7.6 are the total chloride concentrations at 100 years compared with the location of the reinforcement and the maximum and minimum concentration limits. In the Bakkasund Bridge the reinforcement was placed with a concrete cover of 60 mm + 15 mm tolerance and the maximum and minimum limits are taken from Section 2.5.

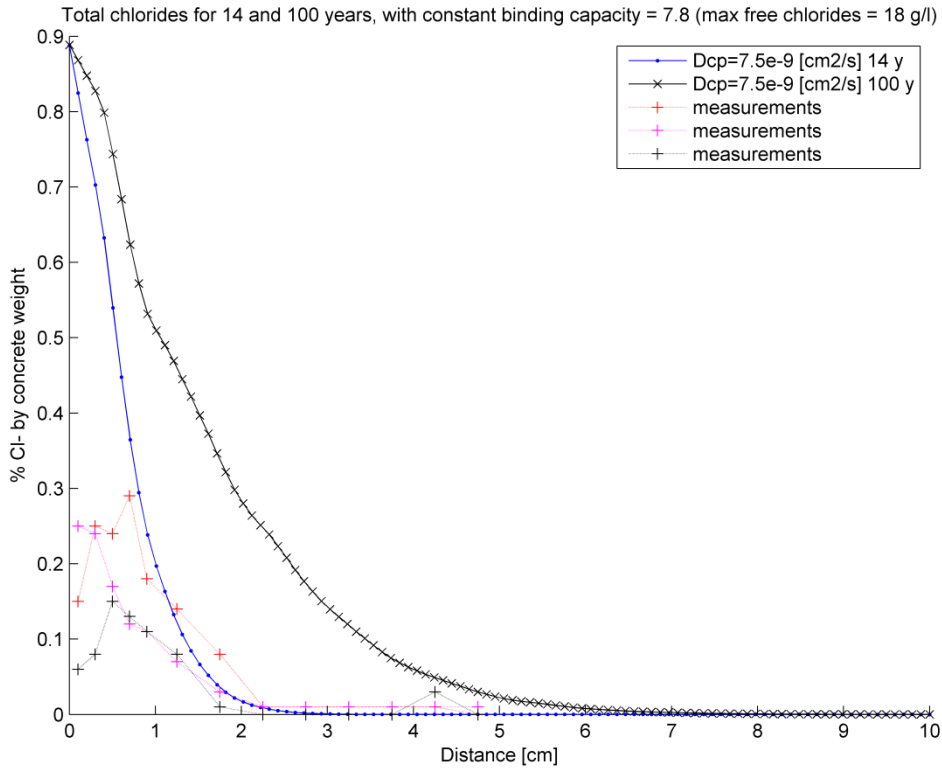


Figure 7.2 Total chloride concentration at 14 and 100 years, max free chlorides 18 g/l.

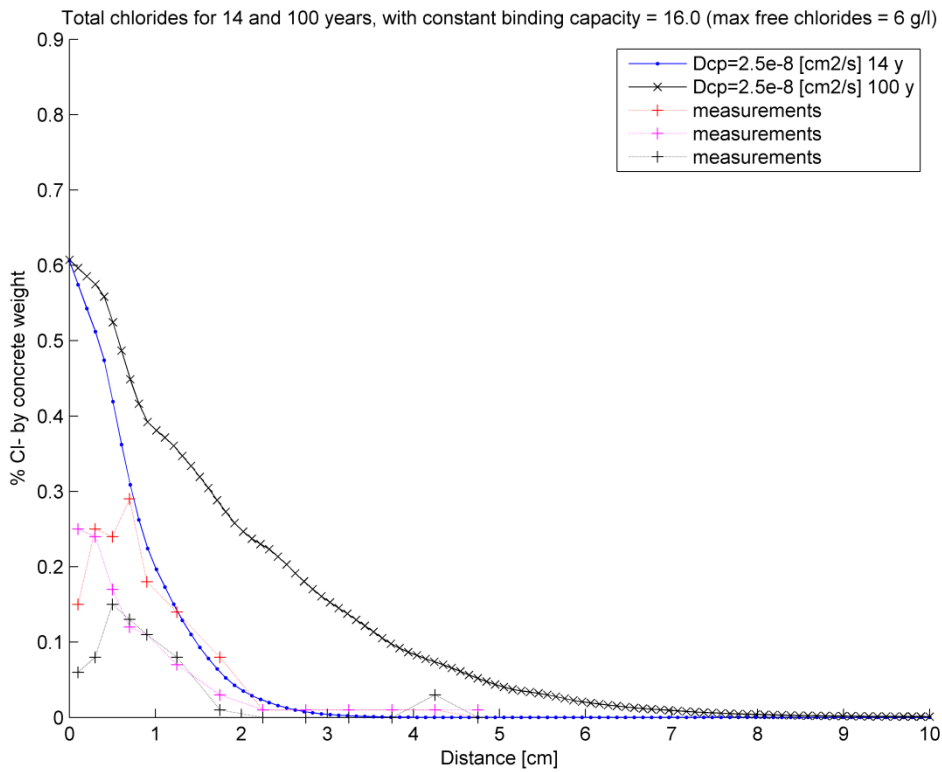


Figure 7.3 Total chloride concentration at 14 and 100 years, max free chlorides 6 g/l.

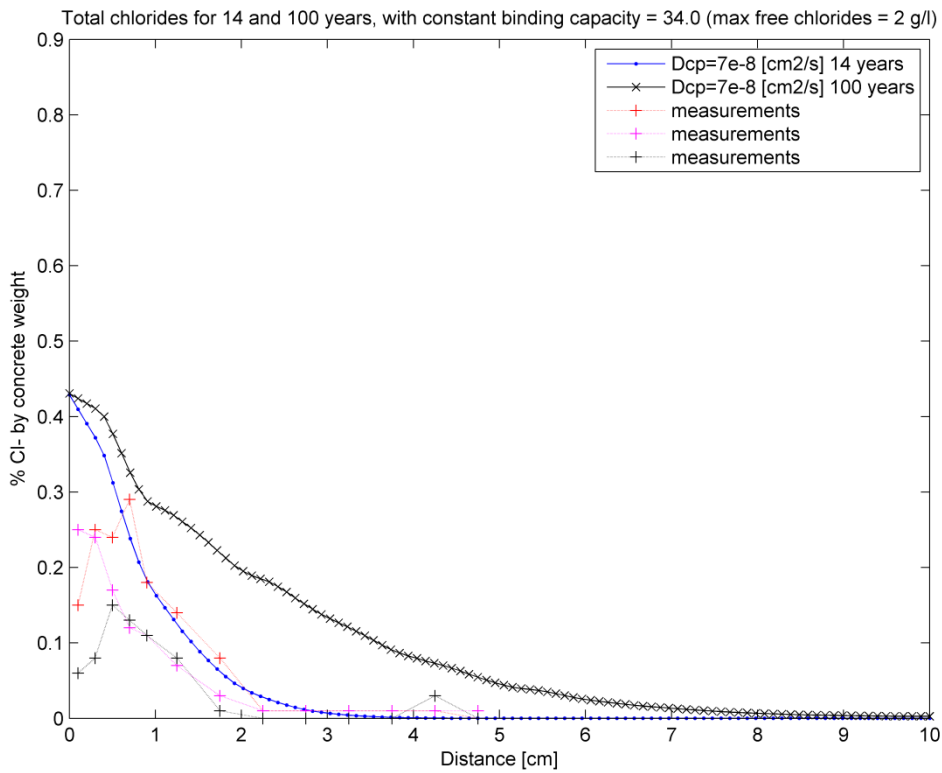


Figure 7.4 Total chloride concentration at 14 and 100 years, max free chlorides 2 g/l.

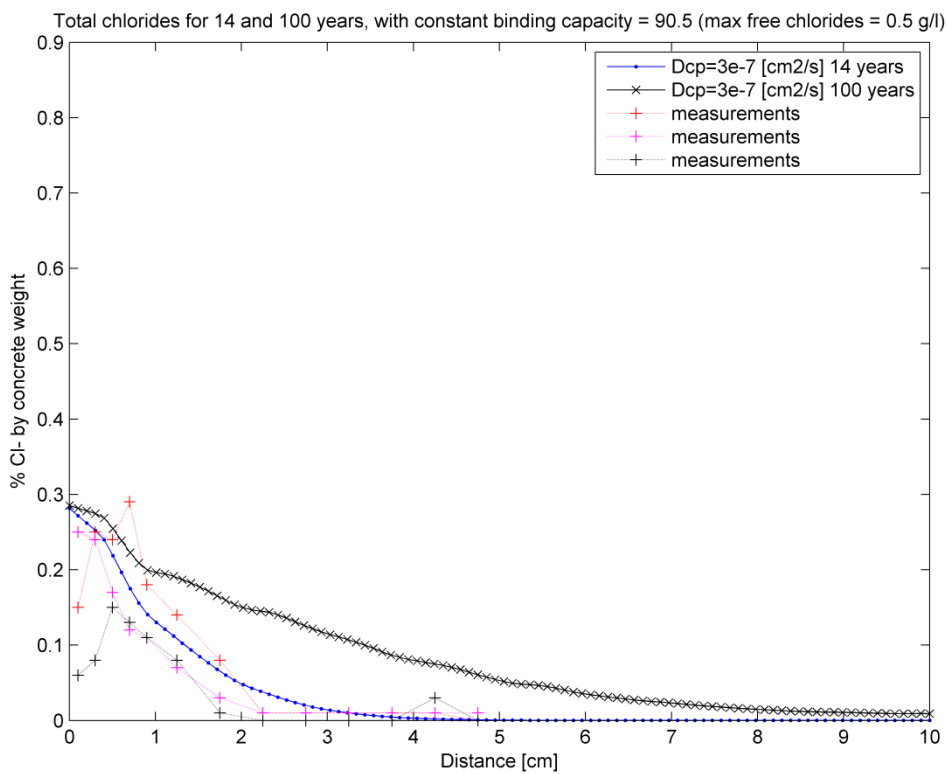


Figure 7.5 Total chloride concentration at 14 and 100 years, max free chlorides 0.5 g/l.

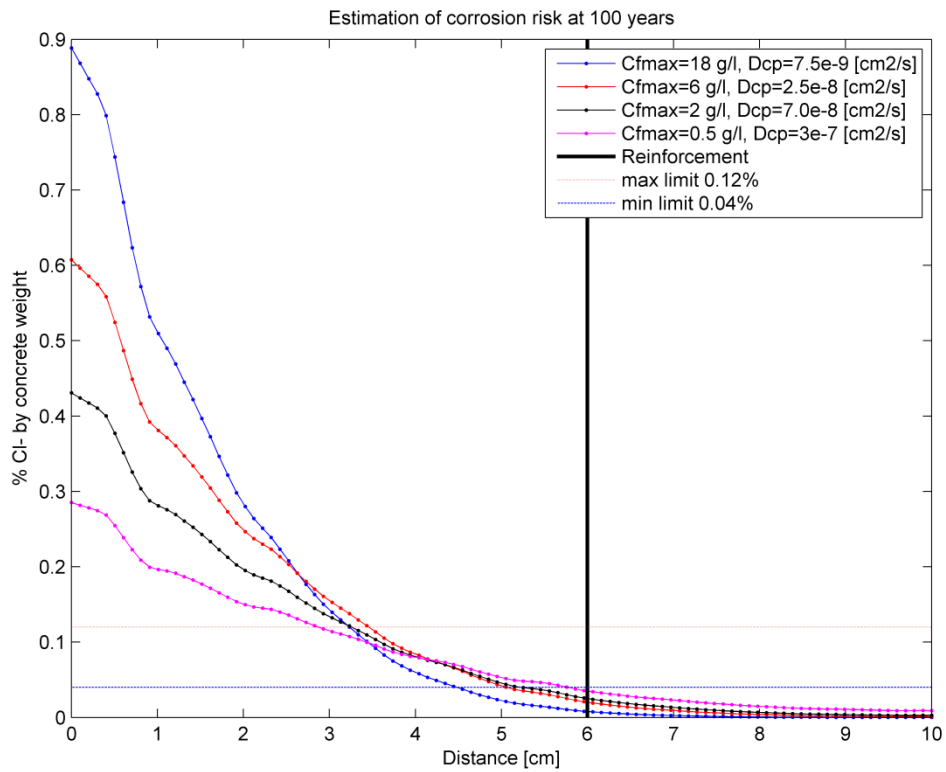


Figure 7.6 Estimation of the corrosion risk at 100 years, for the four different profiles.

The diffusivity of the ITZ was in all four analyses chosen to, 30  $\mu\text{m}$  thickness and diffusion coefficient equal to 15 times the diffusion coefficient of cement paste.

In Figure 7.7 are the results from the analytical models from Chapter 4 shown.

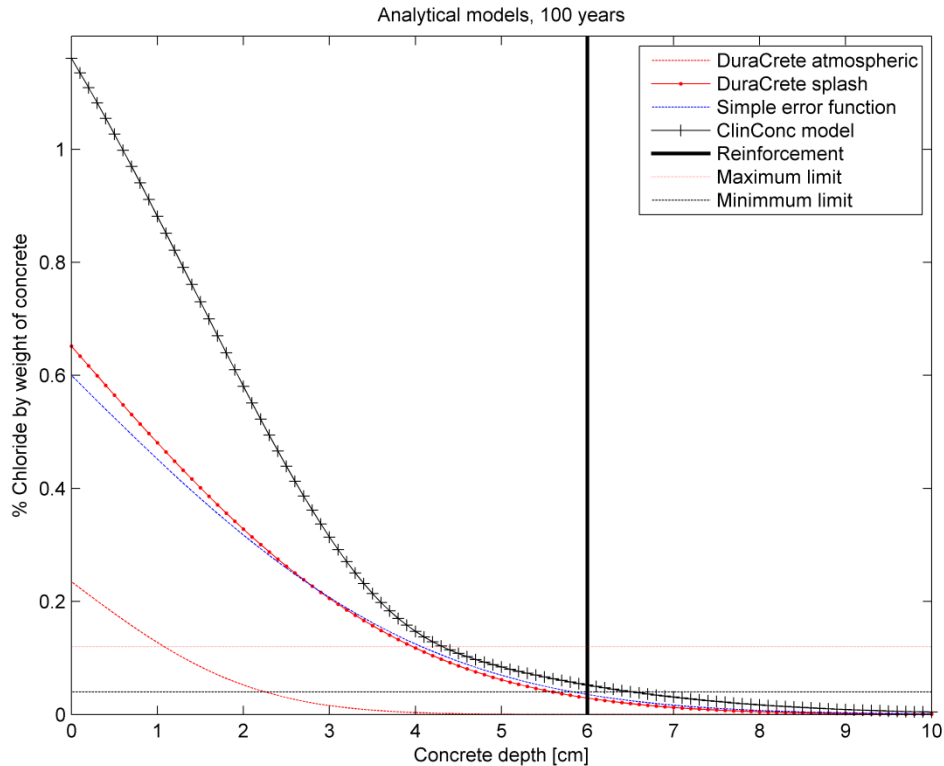


Figure 7.7 Profiles from analytical models that fits measurements at 14 years, for the time 100 years

In Section 2.5 values of the diffusion coefficient for the cement paste/mortar was calculated from analytical formulas. Formula ( 2-8 ) gave  $1.6 \cdot 10^{-8} \text{ cm}^2/\text{s}$  and formula ( 2-9 ) gave  $4.7 \cdot 10^{-8} \text{ cm}^2/\text{s}$ . These values correspond in best way with the profile representing ambient chloride concentration equal to 6 g/l in Figure 7.6. This means that these analytical formulas can be used for estimation of the diffusion coefficient of the cement paste/mortar if the other constants are defined as previously. Many uncertainties still exist though, but this is one attempt to be able to make estimations of the chloride ingress without measurements.

According to these results the cover thickness for the Bakkasund Bridge seems sufficient for the service life of 100 years, due to the fact that none of the curves have passed the minimum limit of 0.04 % chloride concentration by concrete weight. It has to be mentioned though that this formula does not take the possibility of cracks into account, which might increase the profile essentially.



## 8 Discussion

In this thesis, the use of a 3D mesoscale FE model, which has been developed at Chalmers University of Technology, was investigated. The purpose was to calibrate the model with measurements from the Bakkasund Bridge at the Norwegian West coast and thereafter study the chloride ingress at the service life of 100 years.

Mesoscale is the scale where the concrete can be considered as a three phase material. By dividing the concrete in aggregates, cement paste and the ITZ, the properties of each separate phase can be investigated and the aim is to get an accurate effective concrete property. The FE- model gives the possibility to study concrete with different amount of aggregate fraction, due to the creation of statistical volume elements, derived from sieve curves. The sieve curves usually have a large span between the smallest aggregate size and the largest aggregate size, where it for the Bakkasund Bridge reached from 63  $\mu\text{m}$  up to 20 mm.

At the generation of SVEs, the aggregates will approach analytical spherical shapes, as the mesh becomes finer, which is a simplification. Instead the fact that the model creates the randomness of the size and location of the aggregates are of most importance. In the beginning of this project the aggregates were cut on all the boundaries, but in reality this should not be done on one of the boundaries due to the presence of moulds. The code was changed to include this effect.

The size of the SVE is important to account for since all the boundary effects at the surface parallel to the influx surface should be avoided. Due to the difficulties of specifying boundary conditions on that surface, the size of the SVE should be large enough, so that the profile is close to zero at that inner surface. To represent the concrete in the most reasonable way it would have been beneficial to model all aggregate sizes with their respective fraction. This is difficult, because the smaller size of the aggregates that should be modelled, the smaller mesh sizes are needed to get sufficient element division of the aggregates. A smaller element size means more elements and more time-consuming computations. Therefore in this project the minimum size of the aggregates modelled was eventually chosen to 4.8 mm. The aggregate fraction for all aggregates in the concrete was about 67 %, but when the limit was drawn to 4.8 mm, the aggregate fraction left was approximate 40 %, which was used as the input when generating the SVEs. This percentage of excluded aggregates has of course influence on the resulting properties, but the intention was to take care of this by adjusting the diffusion coefficient of the cement paste/mortar.

The generated SVEs did resemble the concrete from the Bakkasund Bridge sufficiently. In the end the results from the mesoscale model were compared with the measurements and the diffusion coefficient given in the mesoscale model was adapted accordingly. This means that how the SVEs were generated was of less importance since the effective diffusion coefficient would have been almost the same anyway. But if the diffusion coefficients are connected to the composition of the SVE through an equation the generation of SVEs would be of great importance. Since the SVEs in this project did resemble the concrete from the bridge, when reasonable input parameters for diffusion and size of ITZ are put, the results match the measurements in a good way. An even more accurate generation of SVEs should together with calibrated expressions for the diffusion coefficients give a good estimation for the chloride ingress without comparing with measurements.

When an SVE is created transport analysis can be made. Different input parameters had to be specified - the ambient chloride concentration, the convective coefficient of chloride ions at the boundary, the diffusion coefficients of the cement paste/mortar and the ITZ, the chloride binding capacity and the time (step size and number of steps). The ambient chloride concentration varies a lot in zones other than submerged and is hard to define. The variable is included in Newton's convection boundary condition and affects, together with the convective coefficient, the chloride surface concentration. In the literature, this chloride surface concentration is usually taken as a curve fitted value according to Fick's second law and measurements. It is commonly a "drop effect" the first approximate 10 mm due to various effects, but this is difficult to include in the model, why it was assumed sufficient to use the curve fitting approach. The convective coefficient of chloride ions could not be found in the literature, but its effect on the chloride ingress was studied. A higher convective coefficient means a lower resistance and the opposite way around. Due to the fact that no confident value of this variable could be found it felt most reasonable to use a high value, low resistance, in such way that the chloride surface concentration took the value of the ambient concentration immediately after one time step. The diffusion coefficient of the cement paste/mortar should be specified and in the literature some suggestions on how to model it was found. Equation ( 2-8 ) and ( 2-9 ) gave the most trustworthy and similar value to the curve fitted. The properties and influence of the ITZ have been analysed by a lot of researches and described in the literature. The suggestions varies, but seems to be somewhere between 15-50  $\mu\text{m}$  in thickness and 10 to 15 times the diffusion coefficient of the cement paste/mortar.

The binding capacity should in the model be specified as a constant value, because linear finite element analyses are used. However, when studying the literature a non-linear relationship was found between free and bound chlorides. Isotherms that describe the relationship between free and bound chlorides in the equilibrium state were found, the Freundlich isotherm and a modification by Tang Luping at Chalmers Univerist of Technology. Efforts were made trying to implement the modified isotherm in the model, but only by using the previous time steps result of the free chloride concentration as values for determination of the chloride binding capacity in the present time step. This makes the analysis very step size dependent, which means the size of the steps should be really small for accuracy. This makes the calculations heavy and time consuming and there were also convergence problems when the step size was decreased. For implementation of this relationship in the model, non-linear finite element analyses is needed, with iterations over each time step to determine the chloride binding capacity. It should be noticed that this modified relationship is made for submerged conditions, why it in other conditions such as splash and atmospheric conditions may deviate. The reason for the choice of the modified relationship was to get some reliable values of the needed constants, which has been calibrated to measurements.

Due to the problems described, a constant binding capacity was chosen as the secant of the non-linear relationship, which should represent the average chloride binding capacity for the varying depths. This is a simplification, but as long as there exist uncertainties about the non-linear relationship in the splash zone, this assumption seems sufficiently accurate. The slope of the secant depended on the assumed maximum free chloride concentration in the pore system, which means that the chloride biding capacity was higher for a lower free chloride concentration and the opposite way around. Four different analyses were made with different assumptions

of the maximum free chloride concentration, which was equal to the ambient chloride concentration. A low free chloride concentration gives a high binding capacity, which means that the diffusion process of free chlorides will be slower than for a high free chloride concentration where the binding capacity is lower.

The surface concentration varies as well when the free chloride concentration, equal to the ambient chloride concentration, varies. These four analyses were made by first calibrate the total amount of chlorides with the measurements at 14 years and then the time was increased for estimation of the chloride ingress at 100 years. All these analyses fitted the measurements at 14 years, but with different assumptions of the ambient and the maximum free chloride concentration in the pore system. For the assumption of the free chloride concentration equal to 18 g/l, which was the highest assumption, the chloride surface concentration was highest, which generated the lowest diffusion coefficient to fit the measurements. The lowest assumption of the free chloride concentration was 0.5 g/l, which due to the reason above gave the highest diffusion coefficient. This resulted in that the highest profile at 100 years was given for a low free chloride concentration but with a high diffusion coefficient, the “flattest” profile.

Comparisons were also done between the mesoscale model and the analytical models. A constant diffusion coefficient and constant chloride binding capacity should give higher chloride ingress and due to this, these factors gives results on the safe side. Since Tang (2008) found a relationship between the age factor,  $n$ , and the time dependent factor for chloride binding capacity there are reasons to believe that the time factor,  $n$ , in the DuraCrete model expresses the same physical behaviour. This means that neglecting the varying chloride binding capacity results in a constant diffusion coefficient and calculations on the safe side.

However the fact that the chloride surface concentration is constant may be on the unsafe side, since in the literature some proposals were that the surface concentration should increase with time and results in more chloride ingress. In the concrete recipe, the water-binder ratio was specified to be below 0.4. This was although assumed to be 0.4 which is on the safe side.

The relationship between the ambient chloride concentration, the diffusion coefficient and the chloride binding capacity, which showed that the same profile will appear no matter how the variables are changed in between, holds as long as the quotients for the two relations, ( 6-9 ) and ( 6-10 ) do not change and the convective coefficient is constant. For time or concentration dependent variables there seems to be a more complicated relationship.

It is the highest concentration close to the reinforcement that will eventually cause corrosion and there might be variations in the diffusion at different locations for example due to cracks, which means that high local concentrations can occur. This pitting corrosion is not accounted for in the model, but it is instead the mean chloride concentration in each element slice. This is on the unsafe side. There is also a question on how reliable certain measurement values are. In the analysis when curves are fitted, a lot of trust is put on about three values that in the end should represent the whole concrete. Even if these values are the highest measured it is hard to know how much they vary in different locations and with time.

The diffusion coefficient of concrete barely changes after 6 months. But the apparent diffusion coefficient does and that is also considered in the analytical models. The

difference between these diffusion coefficients is according to Tang (2008) to a great extent attributed to a time dependent chloride binding capacity.

According to the analytical models, even if the diffusion coefficient and chloride binding capacity indirectly varies with time in the DuraCrete model it is still a mean value over depth and time. The ClinConc model further divides the chlorides into free and bound and includes a with free chloride concentration varying chloride binding capacity. What is possible in the mesoscale model is to include a within each element and each time step varying chloride binding capacity. The consideration of the concrete as a three phase material in the mesoscale model is not done in the analytical models. If properties of these three phases are known then an effective diffusion coefficient can be calculated and the influence from each parameter can be examined. But if none of these parameters are time dependent the diffusion coefficient of the concrete could as well be known.

## 9 Conclusions and Outlook

- The possibility of resembling the concrete of interest more accurately is beneficial with the mesoscale model in comparison to conventional models. This gives the opportunity to include the different properties for the different phases.
- From the calibration it was found that:
  - It is hard to specify a “correct” mesh size to use. If a too rough mesh size is used, the smallest aggregates will not be sufficiently divided to approach a spherical shape and the smallest aggregate might be larger than wanted. However, this must not mean that the concrete is much worse resembled, because in reality the aggregates are not spherical. A smaller mesh gives with more calculation nodes, more accurate results though. A smaller mesh gives larger aggregate volumes, but at the same time larger surface area. Analysis of the stationary flux were made, which displayed that the flux eventually converged, when the mesh becomes smaller.
  - The SVEs must be large enough to exclude any boundary effect at the inner surface.
  - Different realizations are due to randomness possible to create. When analyses were made for different realizations with similar aggregate fraction, size and input parameters, some deviations between the realizations were shown. But the deviations were close to insignificant when estimations of chloride ingress were made.
  - The ambient chloride concentration shows a large variation within a cycle of one year in other zones than submerged. An assumed variation by time can be included in the model, but for simplicity and due to the fact that the time variation is not known, a constant ambient concentration is to prefer.
  - The convective coefficient for chloride ions could not be found in the literature, hence it is difficult to specify a value for the resistance. Therefore it felt most reasonable to use a very high value, which means a very low resistance, which in turn means that the free chloride surface concentration will almost take the value of the ambient chloride concentration. The influence of the tolerance in the calculations is important to account for to get correct results.
  - Suggestions of analytical formulas were found in the literature on how to calculate the diffusion coefficient of the cement paste. Two of the three models, gave reasonable diffusion coefficients when compared with the measured ones. In the future, when measurements might not have been made, i.e. curve fitting cannot be made, it would be beneficial to be able to assume a diffusion coefficient from an analytical formula for estimations of the chloride ingress.
  - The ITZ was found to have a thickness of approximate 15-50  $\mu\text{m}$  and a diffusivity of 10 to 15 times larger than the cement paste/mortar. This is rather uncertain, since the properties of the cement paste/mortar varies depending on input parameters in the mesoscale model.

- It was found that the chloride binding capacity has a non-linear relationship. However, a constant binding capacity was used, due to difficulties to include this in the model.
  - Using the mesoscale model without including varying chloride binding capacity is equivalent to using the error function model. The mesoscale model gives basically the same result as the error function, given that the input values are the same. The DuraCrete model is a development of the Simple error function model, where empirical input constants have been the result from tests. If the varying chloride binding capacity is included in the model, it should then be similar to the ClinConc model, dividing the chlorides into bound and free. But in that case also including different chloride binding capacities in time. The ClinConc model is only verified for submerged conditions, but can with a questionable reliability be curve fitted to the measurements and used for estimation of the chloride ingress at 100 years.
  - The possibility to vary geometry and diffusion coefficients of aggregates and ITZ gives the possibility to examine the effect from each of them and also to calibrate a formula for calculation of diffusion coefficient depending on the aggregate fraction and concrete composition. The effect of varying ITZ was studied on an SVE that resembled the concrete from the Bakkasund Bridge. Differences were shown, but were not very large. The span of variation was taken from suggestions in the literature.
  - A relationship between the ambient chloride concentration, the diffusion coefficient and the chloride binding capacity has been found, which showed that no matter how the variables are changed in between, as long as the two relations, described in Section 6.7, are the same and the convective coefficient is constant, the same profile will appear. However, to have the variables constant does not reflect the reality completely.
  - At the moment the mesoscale model is not necessarily more accurate than the analytical models, because of the linear input parameters which can be transferred to an effective parameter for the concrete. As long as the models, both the mesoscale and the analytical, are calibrated to measurements in the same way, the results at 100 years are reasonable for all the different models. The true benefit with the 3D mesoscale FE model is that all the non-linearities and especially the binding capacity can be implemented. But as long as there still exist so many uncertainties about chloride ingress at the field of material science, the true potential of this accurate numerical model cannot be shown.
- The chloride ingress at the service life of 100 years was calculated with the limitations and simplifications explained in the report. At the minimum concrete cover of 60 mm, the chloride profiles from the mesoscale model are approximate at the lower limit of the chloride threshold values. This means that there is a small risk of corrosion. These thresholds limits are not a specific value, but it was instead specified as a ranged due to different proposals in the literature. The profiles from the analytical models are in the same range, although some deviation is shown.

There are several aspects that are interesting for further studies in this subject and these are summarized below.

- Studies on how chloride binding capacity behaves in splash zone conditions and inclusion of that relationship with help of non- linear FE analysis. In such case the chloride binding capacity should also be connected to the diffusion coefficient.
- Study threshold values closer and express it in free chloride concentration and include various effects close to the reinforcement.
- Study transport mechanisms and reactions close to the surface and include for example the effect of carbonation in the model.
- Study maximum chloride concentrations at the location of the reinforcement and compare it to threshold values representing the maximum chloride concentration.
- One could also go to a smaller scale and model the pores themselves but that feels more complicated.

## 10 References

- Ann, K.Y. et al. (2007): The importance of chloride content at the concrete surface in assessing the time to corrosion of steel in concrete structures. *Construction and Building Materials*, Vol. 23, No. 2009, December 2007, pp. 239-245.
- Ann, K.Y., Song, H-W. (2007): chloride threshold level for corrosion of steel in concrete. *Corrosion Science*, Vol. 49, No. 2007, June 2007, pp. 4113-4133.
- Arya, C. et al. (2014): Modelling chloride penetration in concrete subjected to cyclic wetting and drying. *Magazine of Concrete Research*, Vol. 66, No. 7, February 2014, pp. 364-376.
- Bertolini, L. et al. (2004): *Corrosion of Steel in Concrete*. WILEY-VCH Verlag GmbH & Co., Weinheim, Germany, 2004, 392 pp.
- Bioubakhsh, S. (2011): *The penetration of chloride in concrete subject to wetting and drying: measurement and modelling..* Civil, Environmental and Geomatic Engineering Department of University College London, London, United Kingdom, 2011, 355 pp.
- Burn, S. red. (2002) 9<sup>th</sup> International Conference on the Durability of Building Materials and Components - Prediction Of Chloride Penetration Into Concrete Exposed To Various Exposure Environments. 17<sup>th</sup> – 21<sup>st</sup> March, 2002, Brisbane.
- Burström, P.G. (2007): *Byggnadsmaterial – Uppbyggnad, tillverkning och egenskaper*. Studentlitteratur, Lund, p. 228.
- Caré, S., Hervé, E. (2002): Application of a n-Phase Model to the Diffusion Coefficient of Chloride in Mortar. *Transport in Porous Media*, Vol. 56, No. 1, July 2004, pp. 119-135.
- Domone, P., Illston, J. (2010): *Construction Materials – Their Nature and Behaviour*. Spon Press, New York, United States, 2010, 567 pp.
- Fagerlund, G. (2011): *The threshold level for initiation of reinforcement corrosion in concrete - Some theoretical considerations*. Division of building materials. Lund Institute of Technology, Report TVBM-3159, Lund, Sweden, 2011, 47 pp
- Fluge, F. (2003): *Marine chlorides – A probabilistic approach to derive durability related provisions for NS-EN 206-1*. The Norwegian Road Administration, Publication no. 19, Oslo, Norway, 2003, 22 pp.
- Garboczi, E.J., Bentz, D.P. (1996): The Effect of the Interfacial Transition Zone on Concrete Properties: The Dilute Limit. *An electronic monograph: Modeling and measuring the structure and properties of cement-based materials*. <http://ciks.cbt.nist.gov/garbocz/paper89/> (2014-03-02).
- Global Sea Temperature. (2014): <http://www.seatemperature.org/europe/norway/> (2014-04-22)
- Guowen, S. et al. (2011): Multi-scale Modeling of the Effective Chloride Ion Diffusion coefficient in Cement-based Composite Materials. *Journal of Wuhan University of Technology-Mater. Sci. Ed.*, Vol. 27, No. 2, April 2012, pp. 364-373.



- Halamickova, P. et al. (1995): Water permeability and chloride ion diffusion in portland cement mortars: Relationship to sand content and critical pore diameter. *Cement and Concrete Research*, Vol. 25, No. 4, January 1995, pp. 790-802.
- Jin-yang, J. et al. (2012): Numerical calculation on the porosity distribution and diffusion coefficient of interfacial transition zone in cement-based composite materials. *Construction and Building Materials*, Vol. 39, No. 1, June 2012, pp. 134-138.
- Jensen, V. (2013): *NBTL' Prøvingsrapport*. Report of tests. Norsk betong – og tilslagslaboratorium AS, Trondheim, Norway, 2013, 103 pp.
- Justnes, H. (1998): *A review of chloride binding in cementitious systems*. Nordic Concrete Research, Publication no. 21, Oslo, Norway, 1998, 16 pp.
- Liang, M-T. et al. (2010): Revisited to the relationship between the free total chloride diffusivity in concrete. *Journal of Marine Science and Technology*, Vol. 18, No. 3, 2010, pp 442-448
- Martys, N.S. et al. (1994): Universal scaling of fluid permeability for sphere packings. *The American Physical Society*, Vol. 50, No. 1, July 1994, pp. 403-408.
- Montemor, M.F. et al. (2003): Chloride-induced corrosion on reinforcing steel: from the fundamentals to the monitoring techniques. *Cement & Concrete Composites*, Vol. 25, No. 2003, Lisboa, Portugal, pp. 491-502
- Nilenius, F. (2014): *Moisture and Chloride Transport in Concrete – Mesoscale Modelling and Computational Homogenization*. Ph.D. Thesis. Department of Structural Engineering, Chalmers University of Technology, Publication no. 3658, Gothenburg, Sweden, 2014, 28 pp.
- Ottosen, N., Petersson, H. (1992): *Introduction to the FINITE ELEMENT METHOD*. Prentice Hall, London, United Kingdom, 1992, 410 pp.
- Sandberg, P. (1998): *Chloride initiated reinforcement corrosion in marine concrete*. Division of Building Materials, Lund Institute of Technology, Lund, Sweden, 1998, 115 pp.
- Scrivener, K.L. et al. (2004): The Interfacial Transition Zone (ITZ) Between Cement Paste and Aggregate in Concrete. *Interface Science*, Vol. 12, No. 1, 2004, pp. 411-421.
- seHavnivå. (2014): seHavnivå - Vannstand og tidevannsinformasjon. <http://www.sehavniva.no/sted/Hordaland/Austevoll/Bakkasundbrua~1052805/tidevann.html> (2014-05-09).
- SFA (2005): *Silica Fume Users's Manual*, SFA, Lovettsville, United States, 2005, 194 pp.
- Song, H-W. et al. (2007): Factors influencing chloride transport in concrete structures exposed to marine environments. *Cement & Concrete Composites*, Vol. 30, No. 2008, September 2007, pp. 113-121.
- Sun, G.W. et al. (2012): Prediction of the Effective Diffusion Coefficient of Chloride Ions in Cement-Based Composite Materials. *Journal of Materials in Civil Engineering*, Vol. 24, No. 9, September 2012, pp. 1245-1253.

- Swatekititham, S. (2001): *Chloride Diffusivity of Self-Compacting Concrete With Limestone Powder*. Master of Engineering Thesis, Department of Infrastructure System Engineering, Kochi University of Technology, Kochi, Japan, 2001, 53 pp.
- Tang, L. (1996): *Chloride transport in concrete – Measurements and Prediction*. Ph.D. Thesis. Department of Building Materials, Chalmers University of Technology, Publication P-96:6. Göteborg, Sweden, 1996, 461 pp.
- Tang, L. (2008): Engineering expression of the ClinConc model for prediction of free and total chloride ingress in submerged marine concrete. *Cement and Concrete Research*, Vol. 38, No. 1, March 2008, pp. 1092-1097.
- Tang, L. et al. (2012): Validation of models and test methods for assessment of durability of concrete structures in the road environment. *CBI Betonginstituetet*, Vol. 2, No. 2012, 2012, 75 pp.
- Tang, L., Gulikers, J. (2007): On the mathematics of time-dependent apparent chloride diffusion coefficient in concrete. *Cement and Concrete Research*, Vol. 37, No. 2007, January 2007, pp. 589-595.
- Tang, L., Nilsson, L.O. (1992): Chloride binding capacity and binding isotherms of OPC pastes and mortars. *Cement and Concrete Research*, Vol. 23, No. 1993, December 1992, pp. 247-253.
- The European Union – Brite EuRam III (2000): *DuraCrete – Final Technical Report – General Guidelines for Durability Design and Redesign*, The European Union – Brite EuRam III, Lyngby, Denmark, 2000, 144 pp.
- Thomas, J.J. et al. (1999): The Surface Area of Hardened Cement Paste as Measured by Various Techniques. *Concrete Science and Engineering*, Vol. 1, No. 1, March 1999, pp. 45-64.
- Winslow, D. et al. (1994): Percolation and pore structure in mortars and concrete. *Cement and Concrete Research*, Vol. 24, No. 1994, 1994, pp. 25-37.
- Wriggers, P., Moftah, S.O. (2005): Mesoscale models for concrete: Homogenization and damage behaviour. *Finite Elements in Analysis and Design*, Vol. 42, No. 2006, November 2005, pp. 623-636.
- Xi, B.Y., Bazant, Z.P. (1999): Modeling chloride penetration in saturated concrete. *Journal of Materials in Civil Engineering*, Vol. 11, No. 1, February 1999, pp. 58-65.
- YR.no. (2014): <http://www.yr.no/place/Norway/Hordaland/Austevoll/Bakkasund/statistics.html> (2014-04-16).
- Zheng, J. et al. (2009): Assessing the influence of ITZ on the steady-state chloride diffusivity of concrete using a numerical model. *Cement and Concrete Research*, Vol. 39, No. 1, June 2009, pp. 805-813.

# Appendices

## A. Changes in the MATLAB code

Changes that were made in the code are summarized below

- Avoid cut aggregates at the left boundary and add 2 mm space:  
SVEclass.m line 157  

```
elseif centroid(k,1)<ballastRadii(iballastRadii)+0.2
    centroid(k,:) = zeros(1,3);
    radius(k) = 0;
    k = k - 1;
```
- Avoid calculation error with high convective coefficient by increasing the tolerance:  
SVEclass.m line 644  

```
a_new = minres(C + time.stepsize*K,C*a_old +
time.stepsize*f,[],70000,[],[],a_old);
```
- Get smooth curves with no cuts when plotting the profiles by increasing the max condition:  
SVEclass line 734  

```
[nodeSlice foo] = find(abs(NodeCoords(:,2)-
i*meshProperties.dx)<10*eps);
```
- Transfer the solution vector of free chlorides to total amount of chlorides (SC is binding capacity):  
SVEclass line 647  

```
a_total(dofs.cement.all,i+1)=a_new.*SC;
```

## B. Hand calculations

### Chloride surface concentration

Ambient chloride concentration

$$Amb1 = x \text{ g/l}$$

Porosity of the concrete

$$Porosity = 15\%$$

Concrete weight

$$C_w = 2363 \frac{\text{kg}}{\text{m}^3} = 2363 \frac{\text{g}}{\text{dm}^3}$$

Ambient chloride concentration when the porosity is considered and divided by concrete weight to obtain right unit

$$Amb2 = \frac{Amb1 * Porosity}{C_w} = x \% \text{ chlorides by } C_w$$

### For calculation of the binding capacity,

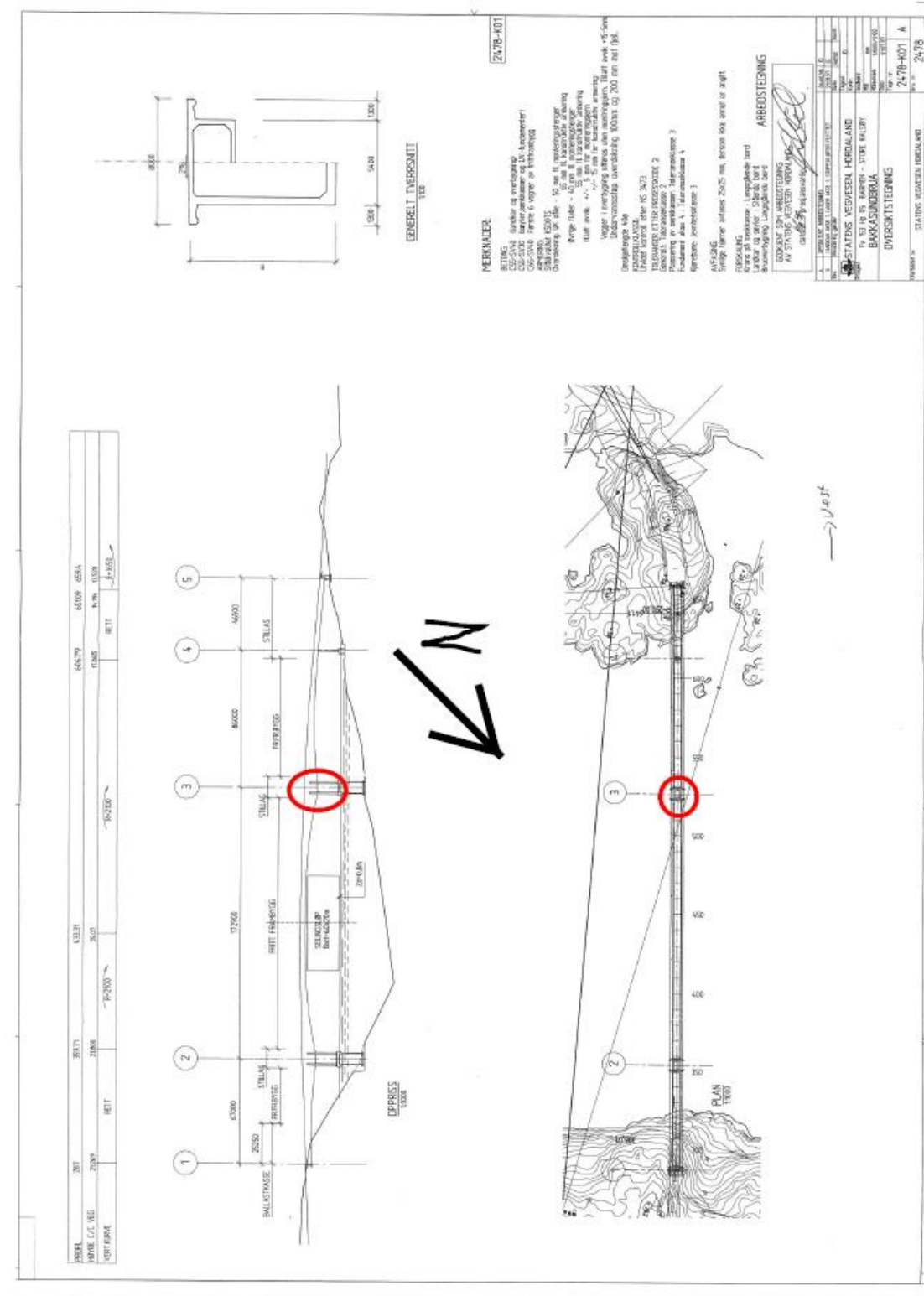
1 % chlorides by concrete weight, for 100 % porosity

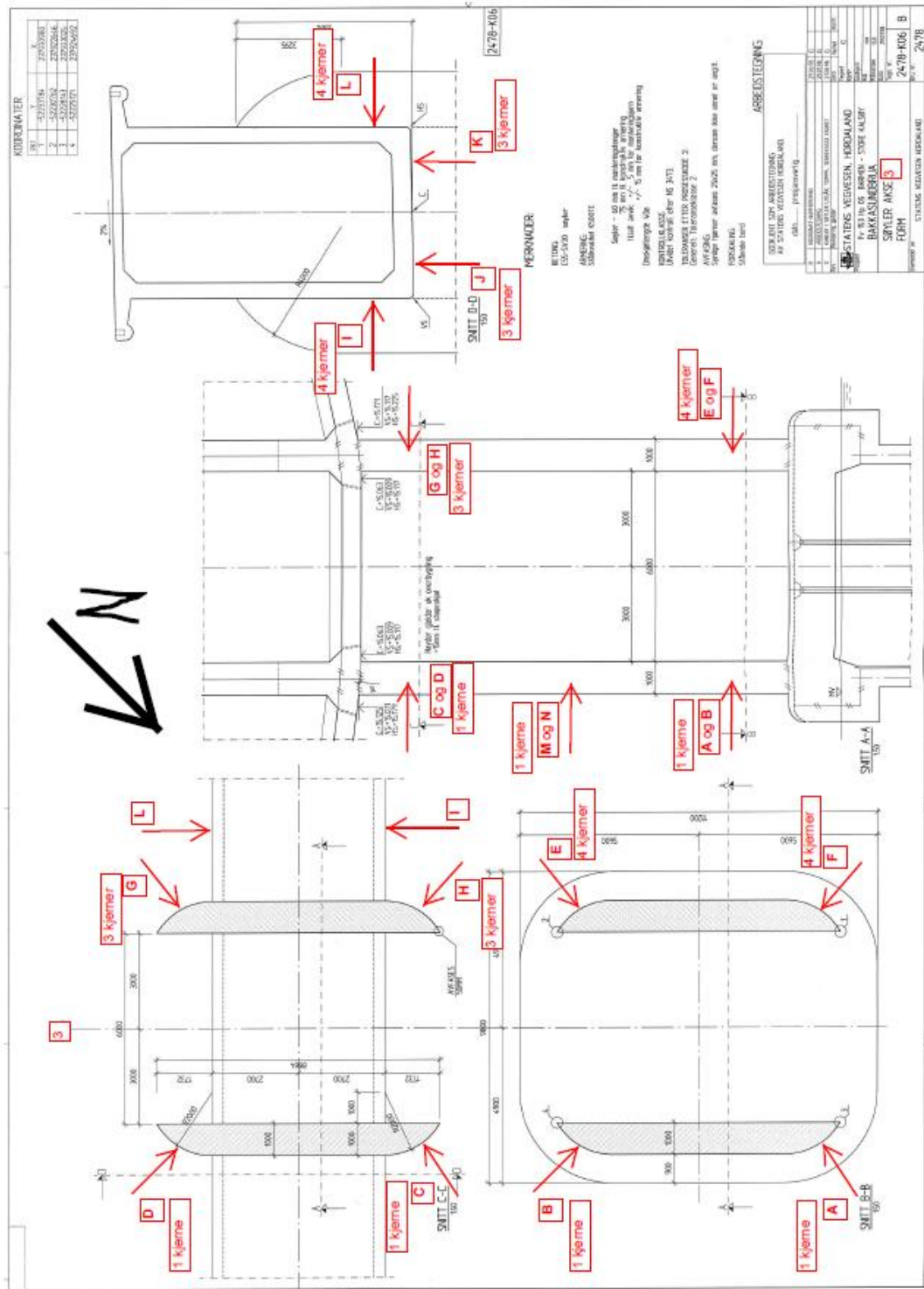
$$Cl(1\%) = 0.01 * C_w = 23.63 \frac{\text{g}}{\text{dm}^3}$$

1 % chlorides by concrete weight, for 15 % porosity

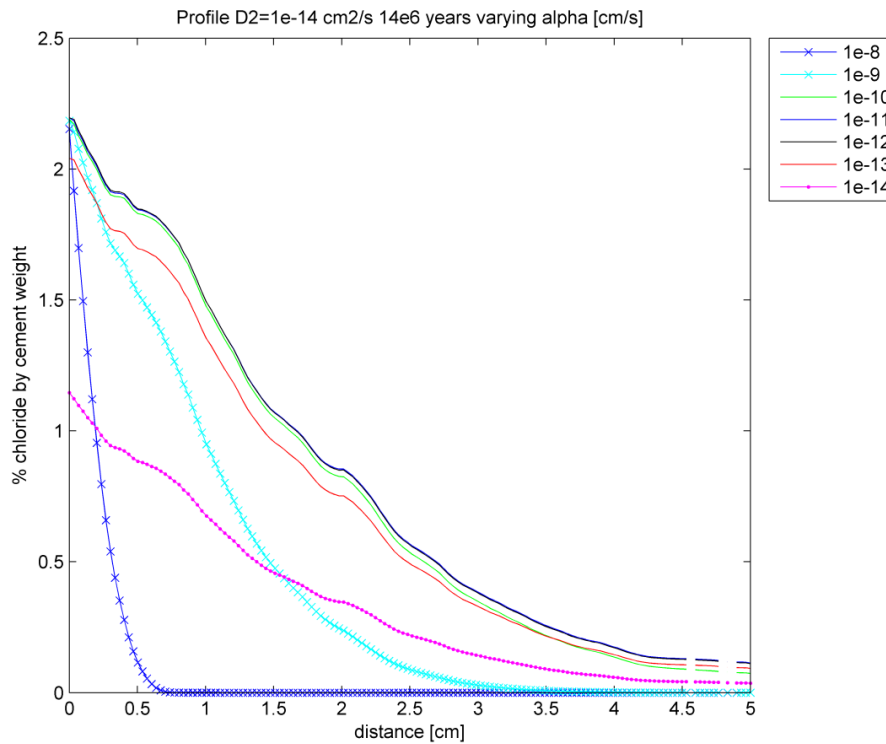
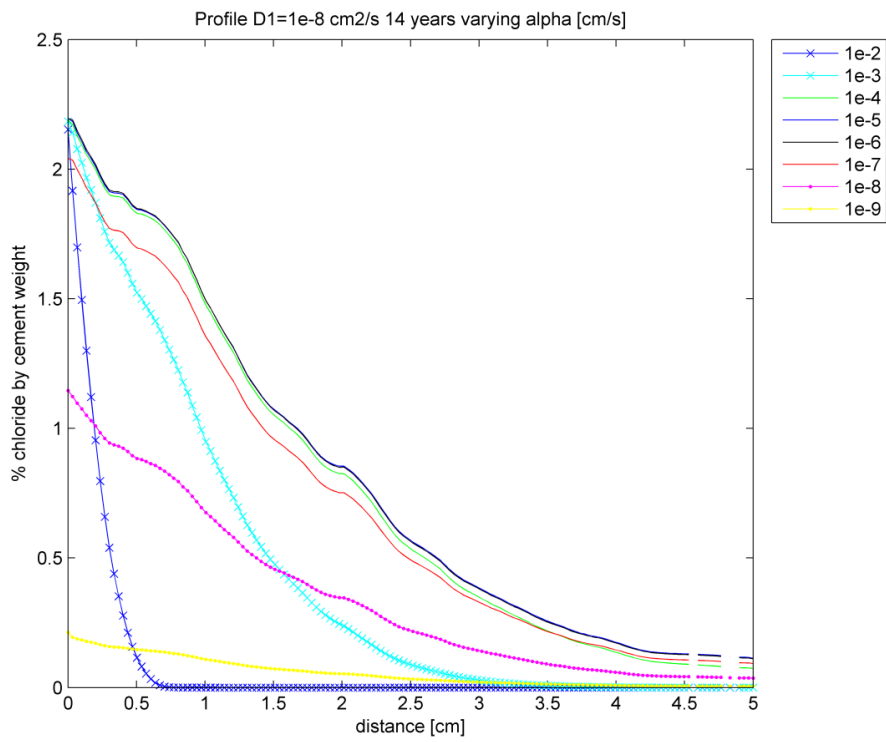
$$Cl(1\%, 15 \% \text{ porosity}) = \frac{23.63}{0.15} \frac{\text{g}}{\text{dm}^3} = 157.5 \frac{\text{g}}{\text{dm}^3}$$

# C. Measurement locations

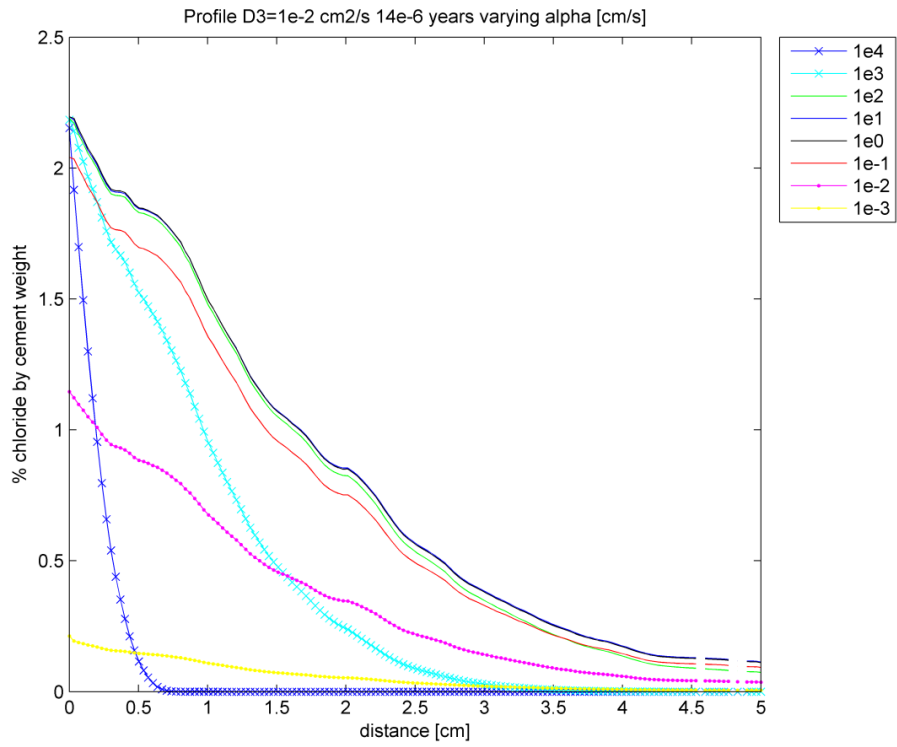




## D. Diagrams for the convective coefficient, Section 6.4.2



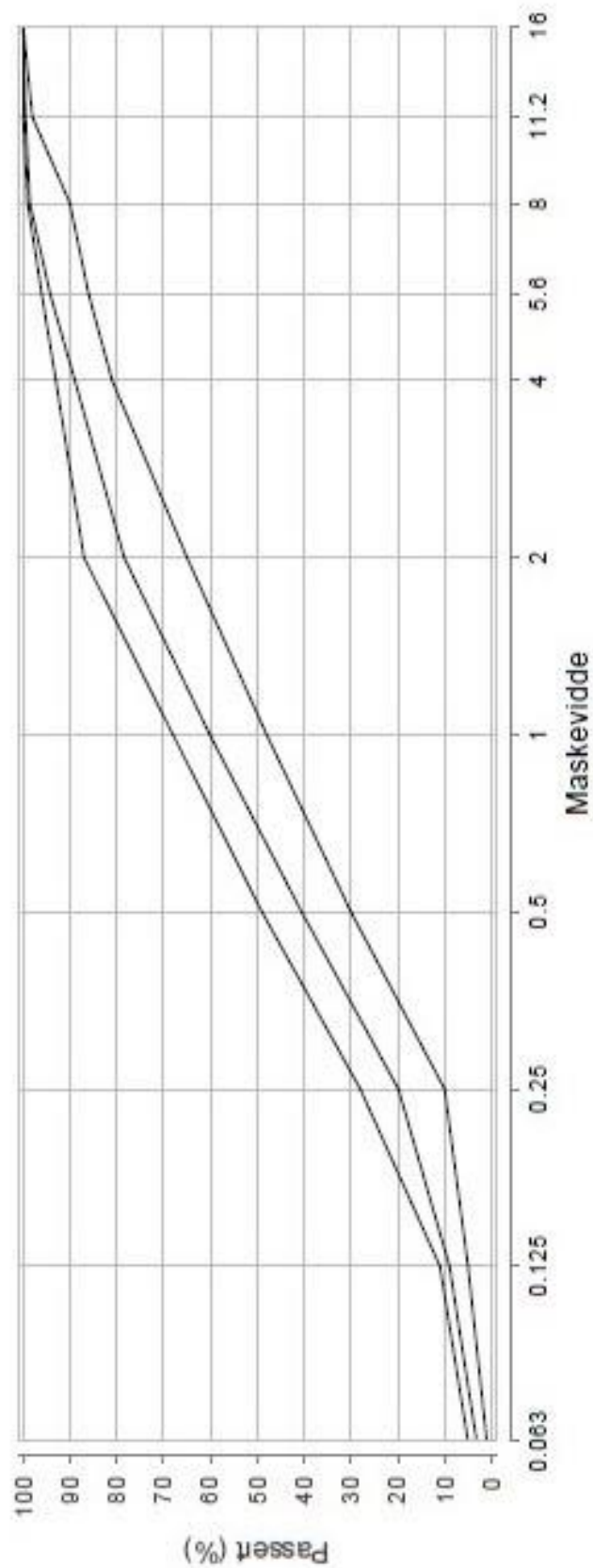




## **E. Sieve curves**

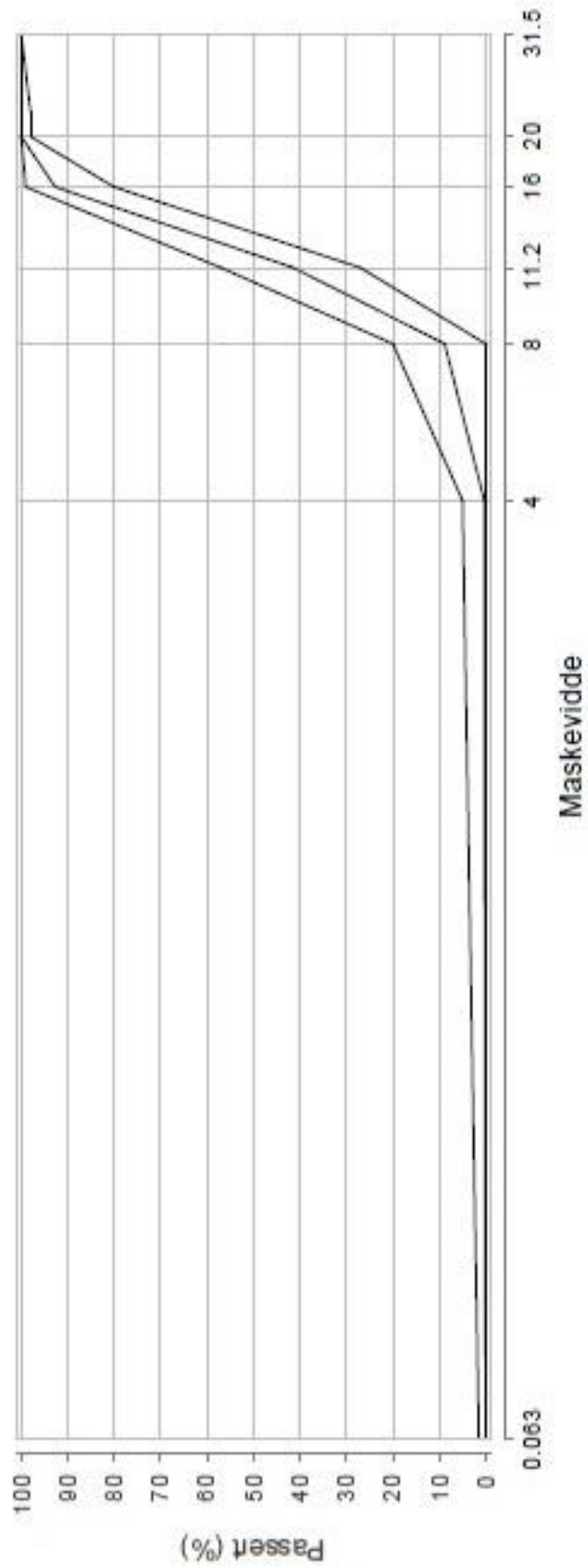
Pr.nr.	µm					mm						
	63	125	250	500		1	2	4	5.6	8	11.2	16
6	3.2	9.0	19.9	40.5	60.1	78.4	89.0	94.2	98.5	99.5	100.0	100.0

Sand			Grus		
Fin	Middels	Grov	Fin	Middels	Grov



	$\mu\text{m}$	mm						
Pr.nr.	63	4	8	11.2	16	20	22.4	31.5
7	0.0	0.3	8.8	41.4	92.7	100.0	100.0	100.0

Sand			Grus		
Fin	Middels	Grov	Fin	Middels	Grov



## F. Table for mesh size study

	DF1,5	Agg frac	Area	Flux , stat	Agg frac	Area	Flux, stat
	Aggfrac [%]	54	54		56	56	
	Aimed	48	48		48	48	
	Aggfrac [%]						
	Dmin [mm]	1,5	1,5		1,5	1,5	
Nel	50	0,4068	499,6007	5,71E-09	0,420793	510,8606	5,65E-09
		0,3996	503,5266	5,76E-09	0,425842	513,6163	5,58E-09
		0,4004	493,8283	5,79E-09	0,422676	508,5345	5,61E-09
		0,4171	488,1007	5,60E-09	0,401131	517,8065	5,85E-09
		0,3919	499,9339	5,86E-09	0,414415	502,3339	5,66E-09
		0,4195	494,3975	5,64E-09	0,412971	509,8404	5,69E-09
		0,3951	498,7515	5,81E-09	0,413671	508,4084	5,65E-09
		0,4107	487,6884	5,64E-09	0,417186	506,134	5,66E-09
		0,4012	497,5724	5,76E-09	0,408392	504,5916	5,77E-09
		0,3917	494,4201	5,85E-09	0,404379	516,5682	5,79E-09
<b>Average</b>		<b>0,4034</b>	<b>495,782</b>	<b>5,74E-09</b>	<b>0,414146</b>	<b>509,8694</b>	<b>5,69E-09</b>
std		0,00937	4,857163	8,64E-11	0,0075	4,747667	8,10E-11
Nel	100	0,4569	644,4895	5,68E-09	0,472212	669,3165	5,62E-09
		0,4508	645,0759	5,73E-09	0,478138	659,3632	5,55E-09
		0,4494	638,0863	5,75E-09	0,473749	658,1897	5,58E-09
		0,4651	628,8275	5,57E-09	0,454713	677,7034	5,82E-09
		0,4432	649,6371	5,82E-09	0,465721	659,4069	5,63E-09
		0,4675	639,5477	5,61E-09	0,463866	665,6331	5,66E-09
		0,4445	647,2042	5,78E-09	0,465841	654,1871	5,61E-09
		0,4599	630,4728	5,60E-09	0,468783	661,5527	5,63E-09
		0,4513	641,2811	5,73E-09	0,458968	663,5791	5,73E-09
		0,4417	644,9694	5,81E-09	0,459297	671,4347	5,76E-09
<b>Average</b>		<b>0,45303</b>	<b>640,9592</b>	<b>5,71E-09</b>	<b>0,466129</b>	<b>664,0366</b>	<b>5,66E-09</b>
std		0,00858	6,536743	8,50E-11	0,006928	6,72899	8,06E-11
Diff from prev.		0,123029	0,292825	-0,00645	0,125519	0,302366	-0,00571
Ratio A/V		2,380121			2,408932		
Nel	150	0,4676	672,046	5,64E-09	0,483294	699,3776	5,58E-09
		0,4614	672,8866	5,69E-09	0,488804	690,0854	5,51E-09
		0,4598	665,2113	5,71E-09	0,484475	687,6622	5,54E-09
		0,4752	655,7633	5,53E-09	0,466058	709,0044	5,77E-09
		0,4543	676,3296	5,78E-09	0,476778	689,073	5,59E-09
		0,4777	668,1381	5,57E-09	0,47487	694,969	5,62E-09
		0,4552	674,2127	5,73E-09	0,476683	683,195	5,57E-09
		0,4702	658,6795	5,56E-09	0,480011	689,6847	5,58E-09

		0,4618	669,1616	5,69E-09	0,469983	693,2609	5,69E-09
		0,4524	674,0245	5,77E-09	0,4707	701,581	5,72E-09
<b>Average</b>		<b>0,4636</b>	<b>668,6453</b>	<b>5,66E-09</b>	<b>0,4772</b>	<b>693,7893</b>	<b>5,62E-09</b>
std		0,008354	6,527732	8,43E-11	0,00676	7,264319	
Diff from prev.		0,023243	0,043195	-0,00742	0,023677	0,044806	-0,00742
Ratio A/V		1,858365			1,892371		
Nel	200	0,4713	682,1307		0,487232	709,9763	5,56E-09
		0,4651	683,4554		0,492653	700,3187	5,49E-09
		0,4634	675,4960		0,488258	698,3115	5,52E-09
		0,4788	665,8010		0,470037	720,6751	5,75E-09
		0,4581	686,7046		0,480684	699,7175	5,56E-09
		0,4814	677,9325		0,47874	705,7145	5,60E-09
		0,4589	684,6641		0,480467	694,1177	5,55E-09
		0,4739	669,0967		0,483885	700,7151	5,56E-09
		0,4655	678,8120		0,473873	704,0405	5,67E-09
		0,4562	684,5081		0,474647	712,9855	5,70E-09
<b>Average</b>		<b>0,4673</b>	<b>678,8601</b>		<b>0,4810</b>	<b>704,6572</b>	<b>5,60E-09</b>
std		0,008314	6,610453		0,006726	7,522211	
Diff from prev.		0,008006	0,015277	-1	0,008136	0,015665	-3,73E-03
Ratio A/V		1,908286			1,925436		-0,01677
Nel	300	0,473961	689,5807				
		0,467835	690,0646				
		0,46611	682,0657				
		0,481434	672,2952				
		0,460867	693,7725				
<b>Average</b>		<b>0,470041</b>	<b>685,5557</b>				
Diff from prev.		0,005929					

## G. Input data in analytical models

The input values used for the Simple error function model are shown in Table G-1 and the input values that were used in the DuraCrete model are presented in Table G-2.

Table G-1 Input values in the Simple error function model

<b>The Simple error function - input data</b>		
Diffusion coefficient	$D_0$	$1.6 \cdot 10^{-13} \text{ [m}^2/\text{s]}$
Chloride surface concentration	$C_s$	0.6 [% Cl <sup>-</sup> by concrete weight]
Time	t	14 years

Table G-2 Input values in the DuraCrete model

<b>The DuraCrete model - input data</b>			
Execution	1 day curing	$k_{c,cl}$	2.08
Environment and material	OPC, splash zone	$k_{e,cl}$	0.27
	OPC, atm. zone		0.68
Regression parameter	SF, splash zone	$A_{c,s,cl}$	8.96
	SF, atm. zone		3.23
Age factor	SF, splash zone	$n_{cl}$	0.39
	SF, atm. zone		0.79
Diffusion coefficient		$D_0$	$2.0 \cdot 10^{-12} \text{ [m}^2/\text{s]}$
Water binder ratio		w/b	0.4
Age of concrete		$t_0$	0.5 years
Time		t	14 years

For the regression parameter and the age factor, the material was chosen to silica fume (SF), this is because the concrete contains 5 % silica fume. For the environment and material, the material is chosen to OPC because for these factors, SF is not specified. The diffusion coefficient is the mean value from diffusion coefficient tests, Jensen

(2013). Values specified for the atmospheric zone were also considered, due to the fact that the profile according to these values fitted the measurements better than the profile according to the splash zone.

The input values that were used in the ClinConc model are presented in Table G-3.

Table G-3 values in the ClinConc model.

<b>The ClinConc model - input data</b>		
Duration of chloride exposure	$t$	14 years
Age of concrete at start of exposure	$t_{ex}$	1 day
Age of concrete at 6 months of exposure	$t_{6m}$	365/2 days
Chloride surface content	$c_s$	4 [g/l]
Water binder ratio	w/b	0.4
Gel content	$W_{gel6m}$	390 [kg/m <sup>3</sup> ]
Water accessible porosity	$\epsilon_{6m}$	0.11
Factor for chloride binding	$a_t$	0.36
Temperature laboratory conditions	$T_0$	296 K
Temperature environmental conditions	$T$	282 K
Activation energy of diffusion coefficients	$E_b, E_D$	40000 [J/mol], 42000 [J/mol]
Hydroxide concentration at 6 months	$OH_{6m}$	0.25 [mol/l]
Chloride binding coefficient	$f_b$	2.6
Chloride binding constant	$\beta_b$	0.38
Diffusion coefficient at an age $t_{6m}$	$D_{6m}$	$2.0 \cdot 10^{-12}$ [m <sup>2</sup> /s]
Cementitious binder content	$B_c$	420 [kg/m <sup>3</sup> ]
Extension coefficient	$k_D$	1.5

The input values used in this model were taken from the proposed values from tables in Tang (2008), which corresponds to this type of concrete. The water binder ratio is given from the concrete prescription. The age factor,  $a_t$ , is specified in the range 0.1-0.6, where 0.36 is the typical value from field exposure data and chosen. The environmental temperature is taken as the average temperature of one year at the



location of the bridge, which is approximate 9°C. The diffusion coefficient is the same as for the DuraCrete model and the other is a bit lower but with a higher chloride surface concentration. The extension coefficient should be taken as 1.5-2 for concrete containing silica fume. The chloride surface concentration is assumed to be an average constant over the 14 years and is adjusted so the chloride profile should fit the measurement data in the best way.

